Satellite Constellation Design for Mid-Course Ballistic Missile Intercept

by

Luke Michael Sauter

B.S. Astronautical Engineering
United States Air Force Academy, 2002

SUBMITTED TO THE DEPARTMENT OF AERONAUTICS AND ASTRONAUTICS
IN PARTIAL FULFILLMENT OF THE REQUIREMENTS FOR THE DEGREE OF

MASTER OF SCIENCE IN AERONAUTICS AND ASTRONAUTICS
AT THE
MASSACHUSETTS INSTITUTE OF TECHNOLOGY

JUNE 2004

Signature of Author: _____
Department of Aeronautics and Astronautics
May 7, 2004

Certified by: _____
Dr. Ronald J. Proulx
Charles Stark Draper Laboratory, Inc.
Thesis Supervisor

Certified by: _____
Dr. Richard H. Battin
Senior Lecturer, Department of Aeronautics and Astronautics
Thesis Advisor

Accepted by: _____
Edward M. Greitzer
H.N. Slater Professor of Aeronautics and Astronautics
Chair, Committee on Graduate Students

1
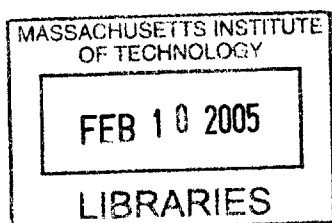
[This Page Intentionally Left Blank]

Satellite Constellation Design for Mid-Course Ballistic Missile Intercept

by

Luke M. Sauter

Submitted to the Department of Aeronautics and Astronautics on May 7, 2004 in
Partial Fulfillment of the Requirements for the Degree of
Master of Science in Aeronautics and Astronautics

ABSTRACT

This thesis will establish a conceptual approach to the design of constellations for satellite-based mid-course missile defense. The ballistic missile intercept problem leads to a new paradigm of coverage where interceptor "reachability" replaces line-of-sight coverage. Interceptors in this concept are limited in their time of flight and ΔV capabilities. Classical design approaches, based on ground coverage, are employed to provide a priori constellations for ballistic missile defense from a postulated North Korean attack. Both symmetric and asymmetric constellation types, designed for Earth coverage, provide bounds on the number of satellites required. A detailed parametric analysis is used to explore the constellation design space. Various constellation types are optimized to maximize missile defense coverage. Both genetic algorithms and gradient-based optimization techniques are employed. Satellite-based mid-course ballistic missile defense from a regional threat is achievable with as few as 21 satellites. Additional constellation intercept statistics, such as: the number of intercepts per missile, and interceptor closing velocities, are compiled to provide a lethality index. The effective capabilities of these constellations to defend CONUS, beyond the original regional threat, are also explored. It will be demonstrated that the constellations constructed in this work are capable of providing defense from an array of threatening states about the globe. This research illustrates how known design methods and astrodynamics techniques can be used to create new and viable methods of space-based missile defense.

Thesis Supervisor: Dr. Howard Musoff
Title: Principle Member of the Technical Staff, Charles Stark Draper Laboratory

Thesis Supervisor: Dr. Ronald J. Proulx
Title: Principle Member of the Technical Staff, Charles Stark Draper Laboratory

Thesis Supervisor: Dr. Richard H. Battin
Title: Senior Lecturer, Department of Aeronautics and Astronautics

[This Page Intentionally Left Blank]

ACKNOWLEDGEMENTS

Publication of this thesis does not constitute approval by Draper or the sponsoring agency of the findings or conclusions contained therein. It is published for the exchange and stimulation of ideas.

The views expressed in this thesis are those of the author and do not reflect the official policy or position of the United States Air Force, Department of Defense, or The U.S. Government.

Luke M. Sauter, 2 Lt., USAF   Date

Table of Contents

11

List of Figures

15

List of Tables

Chapter 1

Introduction

Concepts for space-based ballistic missile defense were first developed in the early 1980's through the Strategic Defense Initiative (SDI) also commonly known as "Star Wars". Space based interceptor concepts ranged from the Brilliant Pebbles system to high-power directed energy concepts. In the waning years of the Cold War, these concepts lost funding and support. Following the Rumsfield commission report, stating the increased risk of missile capable rogue nations there was again a renewed interest in missile defense[8]. Currently National Missile Defense (NMD) is experiencing a large infusion of interest and has developed potential technology gains in several key areas. One area of great importance to this thesis is satellite constellation design for ballistic missile defense. Past research has looked at the potential for satellite based boost-phase missile defense constellations which have over 300 satellites[42]. However, this research focuses on the development of satellite constellations for the purpose of mid-course missile defense from a specific threat against the continental United States. The simulated threat of interest in this paper is from North Korea. Although just a conceptual study, the results and methodology can be applied to any particular threat or region. A number of the constellations presented are capable of missile defense from a wider range of threats to the United States.

1.1 Motivation

Ballistic missile defense first made an appearance in the early 1960's through the Safeguard program. This program became a reality through the use of nuclear tipped interceptors based at a North Dakota site. However, this program's lifespan was brief. It wasn't until the early 1980's that a new version of a missile defense program would come to life[9]. The Strategic Defense Initiative developed the framework of the modern

National Missile Defense program. In the waning years of the Cold War, missile defense programs were pushed to an idle state[8]. With the Rumsfeld commission report, the National Missile Defense Agency is seeking a viable defensive force against the potential threat of ballistic missiles[43]. The Missile Defense Agency is currently pursuing the development, testing, and deployment of land, sea, air, and space based assets to engage any ballistic missile threat[38].

The ballistic missile defense concept is broken down into three possible intercept regions of the missile flight: the boost phase, the mid-course phase, and the terminal phase. A typical missile flight trajectory is illustrated in the Figure 1.1. Suites of accompanying land, sea, and space-based sensors have been developed to enhance the defense and tracking capabilities during each phase of flight. While the missile defense agency is exploring defensive programs against all possible missile threats, this project focuses on defense against intercontinental ballistic missiles (ICBMs)[38].
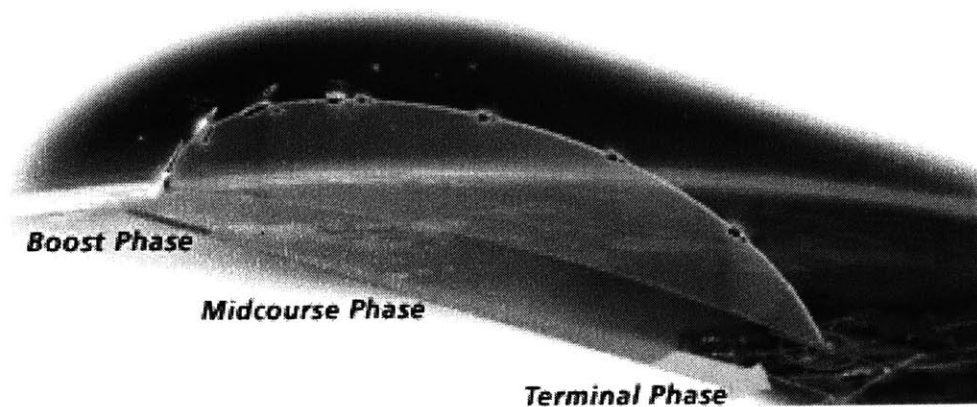
Figure 1.1: Phases of an ICBM Missile Flight[41]

Boost phase defense is the first intercept region of interest. During this phase, the missile is the easiest to identify and is traveling relatively slowly. In the case of an intercontinental ballistic missile, this phase lasts approximately 3-5 minutes[38]. Boost phase is potentially the easiest portion of the trajectory to intercept. However, problems arise in the need to have interceptor assets in close proximity at the time of launch. While this may be possible in theater defense scenarios, it is less feasible in global strategic-

defense scenarios. Strategic boost phase defense would require a number of assets in close vicinity to all possible threats.

After the ballistic missile has completed burning its propellant, it starts the longest part of its flight, the mid-course portion. Mid-course can last 20 to 30 minutes and is in a relative freefall towards its final destination[38]. During this portion of the flight, only a limited number of radar assets can track the trajectory. The two planned mid-course defensive interceptors are: the Space Based Laser (at the time of this thesis funding to this project has been cancelled) and sea/land-based long-range missiles[38]. These systems require significant launch capability to place an asset at the appropriate heights and thus are usually limited in availability.

The last 30 seconds of the missile flight is known as the terminal phase. In this phase the ballistic missile is traveling at extreme speeds and its trajectory can be very accurately determined[38]. A few of the well-known intercept assets for the terminal phase are the Patriot missile system, the Arrow system, and the Theater High Altitude Area Defense (THAAD) system for long-range defense. They attempt missile intercept in the last half of the mid-course flight through the transition into the terminal phase. In order for these systems to attempt a hit-to-kill interception, nearly head-on geometry with extreme closing velocities must be overcome between the missile and the interceptor.

While several assets exist for space-based surveillance of ballistic missiles, there is very little in development for space-based interceptors. Research done in a 2003 report entitled "Boost Phase Intercept Systems for National Missile Defense," by the American Physical Society concludes that spaced based interceptors for the purpose of boost phase intercept are not a realizable solution[42]. Space based terminal phase missile defense also does not lend itself towards realizable solutions. In these cases, a very large number of satellites in very low orbits would be required. Space based mid-course defense has been developed using the spaced based laser, but very little publicly available research has been done on this topic. Space-based platforms for missile defense would seem to be desirable due to the high altitudes and long flight times of ballistic missiles. Further

details and information on the current ballistic missile defense program are publicly accessible and easily obtained on the Internet and other sources[8],[9],[38],[42].

1.1.1 Current Interception Resources and Capabilities

Current mid-course and terminal phase defenses have some proven capability. At this time systems like the Arrow, THAAD, and Patriot have been battle proven for theater defense[38]. Strategic defense assets are still in development. Weapons such as the standard missile 3 (SM3) and other long range interceptors have the potential to serve as a defense shield against strategic attacks[41]. The limitation of these systems lay in the fact that they are fixed ground-based assets with a set intercept range. Only a small number of these systems can be deployed. Head-to-head intercept closing geometries create another challenge to some defense schemes.

Nearly all of these intercept assets are based on liquid or chemical rocket technology. Unless American made ICBMs are used for interceptors, this means that most interceptors have roughly equal or less thrust capability than the missile they are trying to intercept. The only advantage to these systems is their attack profile. Interceptor technology for mid-course defense will require a certain amount of advanced trajectory awareness. The Space Based Infrared System (SIBRS) and Defense Support Program (DSP) are current American space assets capable of identifying a missile launch and estimating its trajectory. Additional land-based and sea-based radar assets are available to obtain updated and refined trajectory awareness.

1.2 Defense Scenario

This thesis abstracts the notion of constellation coverage to produce a feasible near-term solution to space-based mid-course missile defense through the use of a constellation of satellite based interceptors. An ICBM will fly through low Earth orbiting altitudes during the mid-course portion of flight. Additionally, a missile's trajectory would likely have been determined during the boost phase of flight, or shortly after, by the assets previously mentioned. With trajectory awareness, a satellite based interceptor

20

will be fired so as to place the interceptor at the target location and time at which the ballistic missile threat will arrive. Satellite constellation design will be explored to ensure complete missile defense. A constellation of satellites serving as interceptor launch platforms could add enhanced capability to the currently envisioned ballistic missile defense scenarios. While potential ballistic missile threats could come from any part of the world, this research focuses on satellite constellations for missile defense from a specific threat. This research could be extended to cover further threats or modified as the threat nature changes. Results of this research have already shown defensive capabilities greatly beyond the intended threat.

1.2.1 Threat Capability

The specific threat considered for this research is a simulated ICBM attack from North Korea. Presently, the North Korean capability is largely unknown. Given the unstable and aggressive political nature of the North Korean state, it was chosen as the most likely threat requiring a ballistic missile defense for the United States. North Korea has not yet demonstrated the true capability of its latest Taepodong ICBM. The current belief is that it is capable of hitting Los Angeles (L.A.), some 9,500 km away.

The threatened region can be identified using the distance to L.A. as the maximum range and Anchorage as a minimum range and sweeping out a region over an azimuth from L.A. to Bismarck. This threat region encompasses every major population center that a North Korean missile would be capable of hitting within the Continental United States (CONUS). A missile corridor is created from a set of minimum-energy trajectories that can hit the threatened region emanating from a specified point in North Korea. For this work, the missile corridor is defined to be the exo-atmospheric portion of the trajectory, 100 km above the surface of the Earth. The mid-course portion of flight can last anywhere from 21 to 31 minutes, depending on the missile's target location. The missile corridor and threatened region used for this analysis are depicted in Figure 1.2. ICBM threats from additional launch sites or to other regions will have similar trajectory corridors. Constellation designs discussed in this paper can be adapted to individual corridors or multiple corridor regions as needed.

21
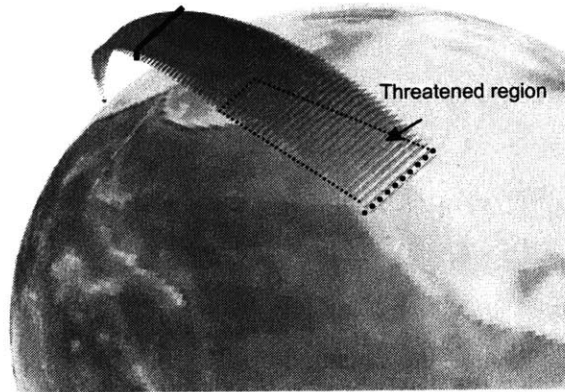
Figure 1.2: Simulated Taepodong Missile Corridor and Threatened Region

1.2.2 Threat Defense Concept

This thesis focuses on the concepts behind constellation design of satellite-based interceptors for mid-course ballistic missile defense. The notion of constellation coverage is abstracted from classical constellation design to produce a feasible near-term solution to space-based missile defense. Coverage, or reachability, is defined in this context as the ability for interceptors, based on a satellite in the constellation, to reach a particular location within a bounded amount of time. Coverage is often considered to be the visual acquisition of a fixed region on the Earth. The "acquisition" time is therefore frequently excluded from consideration of the satellite footprint. When the ability of the interceptor to reach a specified location is limited by speed and time, this problem becomes a complicated multi-dimensional dilemma.

Several designs for space-based missile interceptors have been conceived. These include the use of upper stage boosters, lasers, and even clouds of debris. This research will explore the use of a less dramatic, arguably more realistic, intercept vehicle. Currently available solid rockets used for air-to-air missiles, or upper stage "payload assist modules", are the foundation for the interceptor designs applied to this work. A satellite bus could potentially carry several of these weapons. These interceptors typically have a velocity change capability (ΔV) smaller than that of a larger upper stage rocket;

however, the ΔV of such an interceptor can be scaled from a small rocket to a large one as needed in further studies. The constellation design process considered in this work can be adapted to any interceptor chosen.

A conservative and practical interceptor choice was based on the AIM-120 AMRAAM Air-to-Air missile. Its initial velocity capability was assumed for the characteristics of the satellite-based interceptor*. This capability is approximated as a fixed 1.3 Km/sec instantaneous ΔV. This same ΔV can also be achieved with a staged pair of ATK Thiokol Star 12 upper-stage motors. The weight for a configuration like this would be approximately 150 lbs with a 30 lb terminal interceptor[†]. This study only focused on getting an interceptor to the target; the homing portion of interceptor flight for kinetic intercept was not considered. This portion of intercept has been demonstrated many times for current ballistic missile defense concepts. Following chapters of this work will further develop the intercept scheme needed for mid-course ICMB defense against a specific threat.

1.3 Thesis Outline

This paper uses the North Korean missile threat in union with the defense concept described above to produce methods for designing constellations of satellite-based interceptors for missile defense. Chapter 2 and Chapter 3 of this work introduce the fundamentals of astrodynamics and classical constellation design methods, respectively. Each of these chapters is necessary to explain space-based missile defense. Chapter 2 starts from a basic and historical description of orbital motion, ground tracks, and reference frames. A section of this chapter is also developed to the orbital element description of an orbit. This is followed by a development of orbital perturbations with

---

* Air Force, "Fact Sheet, AIM-120 AMRAAM,"
http://www.af.mil/news/factsheets/AIM_120_AMRAAM.html

† ATK Thiokol Star 12 information gathered from the Encyclopedia Astronautica website: http://www.astronautix.com. Calculations not discussed here were completed according to reference[58].

specific development around the J_2 perturbation. This chapter concludes with an analysis of orbital transfer using the hyperbolic locus of velocity vectors.

Classical methods of constellation design constitute the basis of Chapter 3. In this chapter several coverage methods are used to create several types of constellations. A constellation type defines a set of common orbital characteristics for an arrangement of satellites about the Earth. Some of these orbital characteristics include common orbital elements, combinatorial parameters (like the common number of satellites per plane), and other design conditions. An example of a defined set of orbital characteristics is the evenly placed arrangement of satellites into several planes of polar circular orbits. This general set of common satellite arrangement characteristics describes the star pattern constellation type. This chapter will look at constellation types ranging from symmetric circular patterns to eccentric ad-hoc placement designs. There are many different ways to arrange the satellites inside of this basic constellation type framework. Specific arrangements are known as constellation configurations. A specific constellation configuration defines a total number of satellites and number of orbital planes within a specific constellation type. The coverage method uses the definition of coverage to place satellites into a constellation type. For example, in the star pattern constellation type a coverage method, based on a string of sensor footprints, is used to determine how many satellites are needed in a plane, and how many planes are needed to achieve whole-Earth coverage. Whole-Earth coverage in this example is the desired intent of the constellation or the coverage definition.

Chapter 4 continues to develop the missile defense concept, and the potential missile threat region, as well as defining the coverage manifold created from the release of a satellite based interceptor. Coverage, or reachability, is defined in this context as the ability for interceptors, based on a satellite in the constellation, to reach a particular location at a fixed time. Coverage is often considered to be the visual acquisition of a set region on the Earth, the satellite footprint, and therefore "acquisition" time is frequently excluded from consideration. A multi-dimensional intercept problem is created when the desire to reach a specified location is limited by speed and time. This chapter will identify

the timing issues associated with that intercept problem. An algorithmic scheme for interceptor coverage based on the hyperbolic locus of velocity vectors is developed.

Chapter 5 of this paper will briefly describe modifications to classical constellation design approaches for missile defense applications. A new definition of coverage for missile defense is created around a two-dimensional fence barrier scheme. Several classical methods of constellation design are abstracted to design constellations capable of compete missile defense at the fence barrier. This design scheme has the effect of reducing the dimensionality of the intercept problem and providing a tractable method for constellation design. This chapter highlights the manner in which classical constellation design methods are abstracted for use with missile defense concepts. New constellation types will be developed through intuition gained from classical constellation design research. These methods will ultimately be applied to a simulated missile defense scenario to determine coverage. Additional constellation design ideas, such as constellation coverage gap filling, are also developed.

Chapter 6 provides a detailed analysis of the results of constellation design using the fence coverage method. Each constellation type, abstracted from the classical schemes, will be examined for its usefulness at missile defense. Abstractions of classical methods only provide an a priori estimate to the specific constellation configuration. Many additional configurations are explored around the a priori design estimates. Optimization tools are used at this point to tweak constellation design parameters per configuration to maximize missile defense coverage capability.

The notion of volumetric coverage is introduced in Chapter 7 in an effort to improve coverage results for constellations with fewer satellites. Volumetric coverage removes simplifications of fence coverage. It allows for additional intercept capability in ballistic missile defense constellations. Volumetric coverage is applied to previously generated fence coverage constellations. This coverage definition makes it possible to explore additional constellation coverage capabilities. An expansion of the missile threats against the whole CONUS is one such additional coverage capability explored in the volumetric analysis.

Chapter 8 presents the results of volumetric coverage. Constellation design is not easily abstracted for the volumetric coverage definition. The effectiveness of constellations, designed for fence coverage, is measured with respect to the new volumetric coverage definition. Greatly improved coverage results suggest that smaller constellations can provide 100% coverage. Full parametric coverage results for many constellation configurations are developed. This chapter concludes with an exploration into additional coverage capabilities of existing constellation including: multiple intercept capabilities, additional ΔV capabilities, and additional treat deniability capabilities.

The conclusions and future work of Chapter 9 reiterate the many important conclusions gained throughout this research. This chapter also discusses constellation design, maintenance, and stability issues important in the deployment of satellite constellations. Many avenues of future work are presented for readers interested in expanding the missile defense concepts presented throughout this thesis.

Appendix 1 is given to aid readers with concepts of optimization and its implementation. Some of the enabling concepts behind the optimization tools, used in this research, are also discussed. In particular, the nonlinear programming package SNOPT and a genetic algorithm optimization package will be examined.

Chapter 2

Astrodynamic Fundamentals

This thesis work is designed around the conceptual use of satellite-based interceptors for mid-course ballistic missile defense. The intercept scheme is developed around an orbital transfer vehicle with a limited time of flight and impulse-velocity capability. This chapter provides the enabling concepts needed to understand orbital motion, perturbations, and orbital transfers. While a full and comprehensive understanding of astrodynamics would take more than a chapter to describe, this chapter will provide an appropriate description for readers unfamiliar with the area of study. The concepts described here allow for an understanding of the orbital dynamics required to correctly transfer an intercept vehicle from a satellite in one orbit to target in another orbit.

2.1 Orbital Motion

Astrodynamics is a term referring to the study of the motion of objects in space. The motion of planets and stars has been a topic of interest for several thousand years. The formal study of astrodynamics did not take shape until the 16th and 17th centuries with the works of Copernicus, Brahe, Kepler, Galileo, and Newton[46]. Kepler, using Brahe's detailed observations of the motion of Mars, developed the first laws of Astrodynamics. These laws[‡] were revolutionary at the time for describing orbital motion. Newton later developed a more detailed mathematical representation to fully describe orbital motion. Newton's equations develop the first two-body mechanical representation of orbital motion. Only the gravity of the identified bodies is considered in this

---

[‡] Keplers Laws[46]:

    1. Planets move in ellipses with the Sun at one focal point.

    2. The line joining a planet to the Sun sweeps out equal areas in equal time.

    3. The square of the orbital period of a planet is directly proportional to the cube of the average distance to the Sun

representation. Since Newton's work, several individuals have further developed the mathematics of orbital motion. Such developments have led to an accurate understanding of orbital motion allowing humans to walk on the Moon and send probes in the far reaches of the Solar System.

In the beginning, Kepler identified that planets and other bodies follow set paths around larger bodies in space. These paths or orbits can be thought of as grooves in space in which one body travels while orbiting another. A key feature, implied by Kepler's laws, is that all orbital paths can be simply described by conic sections. Figure 2.1 shows how conic sections are represented by a two-dimensional slice through a set of right circular cones. All orbits described in this thesis are represented by either elliptical or circular conic sections. Parameters known as orbital elements describe the characteristics of the conic representation of an orbit as well as a satellite's position in that orbit. The Keplerian orbital elements will be discussed in more detail later in this chapter.
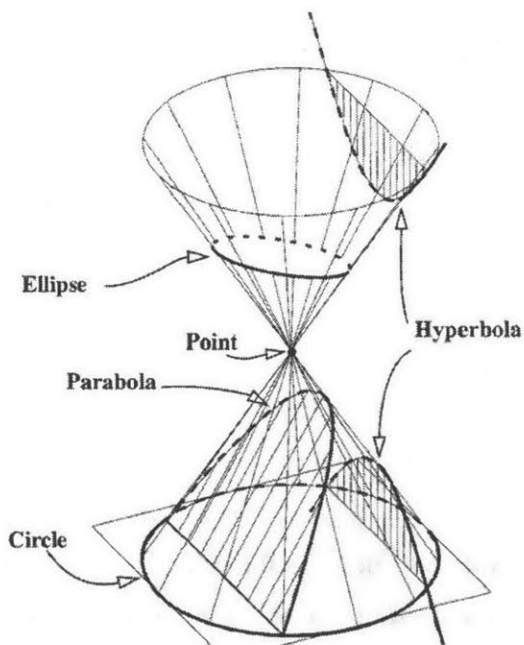
Figure 2.1: Conic Sections[48]

2.1.1 Two-Body Motion

Along with many other mathematical advances, Newton was the first to develop a mathematical representation of the influence of gravity on orbital motion. This representation stems from Newton's Three Laws of Motion as well his Universal Law of Gravitation. These laws were first published in Newton's famous *Principia* in 1687[46]. Newton's first law explains that an object in motion will tend to stay in motion until acted upon by another force. Newton's second law further develops the idea that a force is the change in momentum per change in time. In the absence of a loss of mass, this law is expressed in vector form by Equation (2.1). In Equation (2.1), the sum of the applied forces (F) is equal to the mass (m) of the body to which it is applied times the resulting acceleration (a) of that body, where $\overline{F}$ and $\overline{a}$ denote vectors. Further developing the characteristics of motion, Newton's third law states that for every force acting on a body there is an equal and opposite force that must exist. These laws describe the basis of motion for any object including those in an orbit.

$$\sum \overline{F} = m \cdot \overline{a} \qquad (2.1)$$

A satellite, which is any orbiting body, is always experiencing gravitational attraction force. Newton's laws of motion alone are not enough to fully describe orbital motion in the presence of this force. Newton's Universal Law of Gravitation completes the remaining mathematical description of orbital motion and is given by Equation (2.2). This equation describes the gravitational force of attraction between the mass of a satellite ($m_{satellite}$), and the mass of the central body (m_{center}) as a function of the distance between them (r). Combining Equations (2.1) and (2.2), the equation for two-body motion can be developed. By adding the gravitational forces of the satellite and central body with respect to an inertial origin, the vector representation of the resulting acceleration between the bodies is shown in Equation (2.3). Any perturbing accelerations that may affect orbital motion are lumped together into the a_{pert} term in this equation. Additionally, the Universal Gravitational Constant (G) is combined with the sum of the masses of the central body and the satellite to form the gravitational parameter (μ) as

shown. Equation (2.3) is given with reference to an inertial coordinate system. For two-body motion $a_{pert}=0$. Section 2.2.1 will explore the effects of perturbed orbital motion caused by non zero values of a_{pert}. This equation is the mathematical representation of Kepler's laws and can be used to describe the motion of planets, satellites, and nearly all celestial bodies.

$$\bar{F} = \frac{G \cdot m_{Center} \cdot m_{satellite}}{r^3} \bar{r} \tag{2.2}$$

$$\ddot{\bar{r}} + \frac{\mu}{r^3}\bar{r} = a_{pert} \tag{2.3}$$

Where $\mu = 398600.5$ km^3/s^2 for this research[58]

2.1.1.1 Coordinate Systems and Time

A coordinate frame serves as the fundamental basis for a mathematical description of an orbit. A coordinate frame is often described as an orthogonal axes set and a point of origin which serve as a reference frame for vectors and points in space. Two of these coordinate frames are directly related to orbital motion. The inertial and Earth fixed coordinate frames share a common point of origin at the center of the Earth. The plane of the equator and the rotation axis of Earth define the orthogonal vector set for both coordinate frames. The inertial coordinate frame is commonly known as the Geocentric Equatorial System, (ECI or IJK)[48]. This coordinate frame can be seen in Figure 2.2. The $\hat{I}$ axis of this frame points toward a defined stationary vernal equinox. This coordinate frame is fixed in space while the Earth fixed frame rotates with the motion of Earth, as its name implies. All of the orbital dynamics and calculations in this thesis are completed in an inertial fame. While the Earth fixed frame, commonly known as ECF, is not used for calculations, this frame has obvious benefits for understanding missile defense over a specific region on the Earth.

30
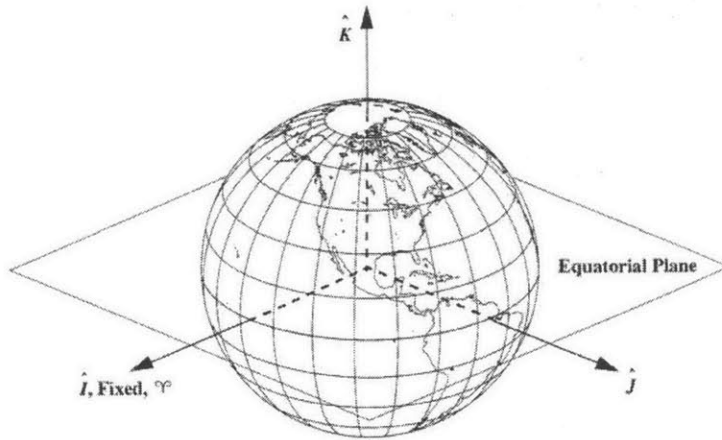
Figure 2.2: Geocentric-Equatorial Coordinate System, ECI[48]

In a simplistic sense, the prime meridian over Greenwich, UK serves as a common alignment of both coordinate systems at zero Greenwich Sidereal Time, GST, angle (θ_{GST}). As the Earth rotates, the angular difference between the inertial frame and the Earth fixed frame changes. By measuring the passage of time, one can easily compute the angular difference in coordinate frames. The angle to a specific ground location, Local Sidereal Time angle (θ_{LST}), is found by simply adding the East longitude of the ground location to the GST. This geometric relationship can be seen in Figure 2.3.
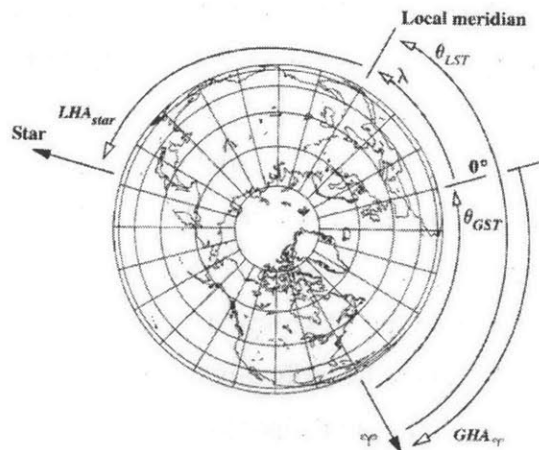
Figure 2.3: Geometry of Time Conventions[48]

31

2.1.2 Orbital Elements

A satellite "state" determines specifically where a satellite is and where it is going. There are several different conventions for describing the "state" of a satellite. At a minimum six parameters must be used to describe the trajectory of a satellite. The specific position and velocity vectors, with reference to an inertial coordinate frame, are one such example. These parameters make it hard to conceptualize where a satellite is and what path it will follow. Another example of determining the location and path of a satellite is the use of orbital elements. The classical Keplerian elements describe the conic section of the satellite orbit and where in that orbit the satellite is located. These parameters make it simpler to conceptualize a satellite's orbit; additionally they often make it easier to propagate the satellite's state forward in time when few perturbations are considered.

The six Keplerian orbital elements are: semi-major axis (a), eccentricity (e), inclination (i), right ascension of the ascending node (Ω), argument of perigee (ω), and true anomaly (v). Additionally the mean anomaly (M) and the orbital parameter (p), also known as the semi-latus rectum, are alternate forms of elements that will be discussed here. Mean anomaly can be substituted for true anomaly and is often used in its place for calculations. Each of the orbital elements is described as follows:

- The semi-major axis (a) is a physical distance measure of the size of the orbit. In an elliptical orbit, this parameter represents the physical distance from the center of the ellipse to farthest point in the orbit. A representation of a is shown in Figure 2.4. The line connecting the occupied focus (F), the location of the central mass, and the vacant focus (F^*) bisects an ellipse. The distance from the center of Earth to the point in the orbit of closest approach is the radius of perigee (R_p). Additionally, the distance to the farthest point in an orbit from Earth is the radius of apogee (R_a). These points are defined as perigee and apogee respectively. The sum of R_p and R_a is equal to twice the semi-major axis. The geometry of this relationship can be seen in Figure 2.4.
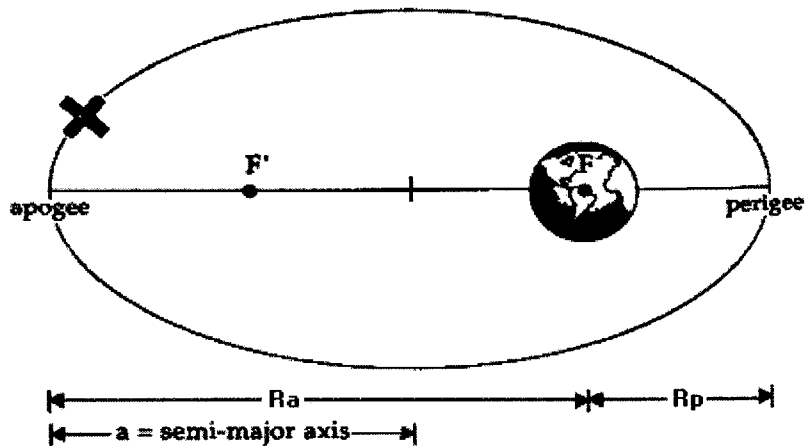
Figure 2.4: Geometry of an Elliptical Orbit[46]

- Eccentricity (e) describes the shape of an orbit. Eccentricity is roughly equivalent to the angle at which a right circular cone would be cut to form a conic section. An eccentricity of zero means that the orbit is circular. An eccentricity ranging from zero to one represents an elliptical orbit; one and greater represent parabolic and hyperbolic orbits, which will not be explored. An example of the manner in which orbital shape is determined by eccentricity can be seen in Figure 2.5.
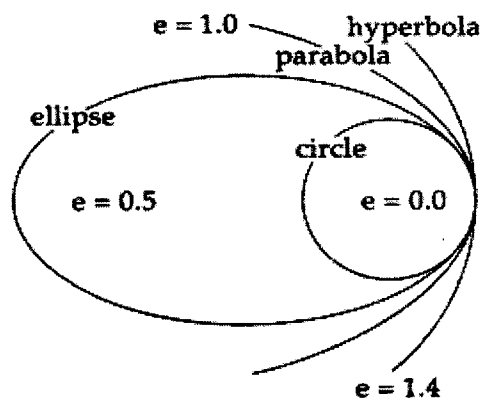
Figure 2.5: Orbital Eccentricity[46]

The elements a and e describe the shape of an orbit. Often another element, known as the parameter (p), is used to define an orbit. The parameter

was established as a mathematical simplification of a common term in orbital dynamics. The relationship of p to a and e is expressed in Equation (2.4). The distance from the occupied focus to the orbit, traveling in a straight line, perpendicular to the semi-major axis, is the physical representation of the parameter.

$$p = a(1 - e^2) \qquad (2.4)$$

- Inclination (i) determines the "tilt" of an orbit. This angle is measured from the $\hat{K}$ axis of the inertial coordinate frame to the momentum vector, $\overline{h}$. The momentum vector of an orbit is defined as the vector orthogonal to the plane formed by the position and velocity vectors. This vector is perpendicular to the orbital plane. Inclinations from 0 to 90 degrees refer to posi-grade orbits, meaning the satellite travels in the same direction as the Earth rotates. Inclinations from 90 to 180 degrees represent retrograde orbits where a satellite would travel opposite direction of the Earth's rotation. This and the following elements are illustrated in Figure 2.6.

- Longitude/Right ascension of the ascending node (Ω) is the parameter that describes "swivel" of an orbit about the equator. This element is defined by the angle between the principal axis of the inertial frame, $\hat{I}$, and the ascending node. The ascending node is defined as the location where the satellite crosses from the Southern Hemisphere into the Northern Hemisphere. A vector pointing to this location is defined by the cross product between the $\hat{K}$ and $\overline{h}$ vectors.

- The argument of perigee (ω) describes the orientation of the orbit in the orbital plane. This parameter is the angular distance from the ascending node to perigee in the plane of the orbit. For circular orbits, with no defined perigee, this parameter is undefined. For circular orbits the location of the satellite can be depicted as an angle from the ascending node directly to the satellite in the orbital plane.

- True anomaly (ν) is used to identify the location of a satellite in its orbit. It is defined as the angle from perigee to the position vector. Another element often

34

used for the same purpose is Mean anomaly (M). Mean anomaly has no physical interpretation. It is defined as the angle from perigee to the satellite location along a hypothetical average angular motion orbit. Mean anomaly for any orbit is defined by Equation (2.5), where the mean motion (n) is constant given the semi-major axis of the orbit, and (t-τ) is the time since perigee passage.

$$M = n(t - \tau)$$

$$n = \sqrt{\frac{\mu}{a^3}}$$ (2.5)

The orbital elements are a very convenient way to understand and describe an orbit. Figure 2.6 below is a basic representation of an orbit. The elements: i, Ω, ω, and v can all be seen in this figure in their relative geometry. True anomaly, and also mean anomaly, are the only elements of the six that change with time in the absence of perturbations. For this reason, propagating the state of a satellite in time is a simple problem of updating v by means of Kepler's equation given some time of flight. Equation (2.6) is Kepler's equation in terms of the mean anomaly and thus time of flight. E in this equation represents the Eccentric anomaly. This angle is a representation of the satellite position on a circular orbit with the same semi-major axis. This mathematical relationship can be found in Equation (2.7) and the geometric relationship is shown in Figure 2.7. In this figure, the satellite is located at P, and the line from Q to P to R is perpendicular to the line connecting the center of the ellipse (c) with the focus (F). As can be seen throughout this section, orbital elements are an easy way to obtain a simple geometric understanding of orbital motion.

$$M = E - e \sin E$$ (2.6)

$$\tan \frac{1}{2} v = \sqrt{\frac{1+e}{1-e}} \tan \frac{1}{2} E$$ (2.7)

35
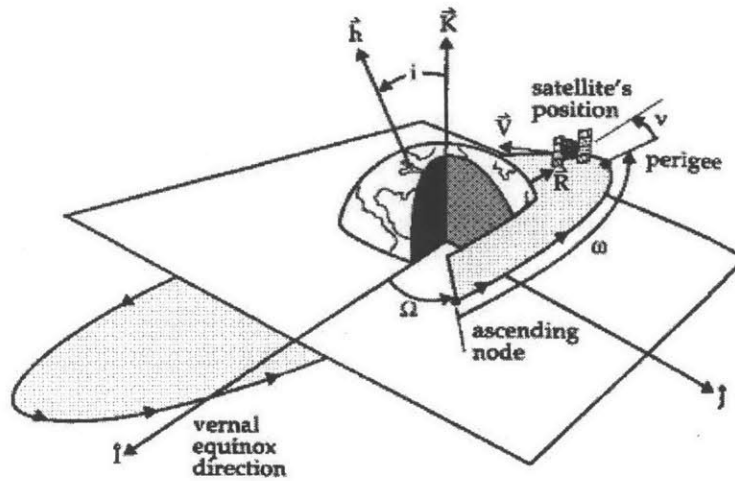
Figure 2.6: Example Orbit Defined by Keplerian Elements[46]
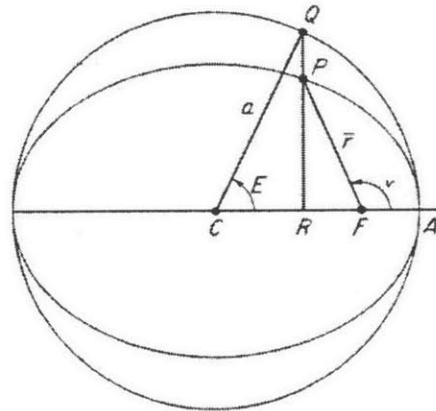
Figure 2.7: Geometry of the Eccentric Anomaly[1]

2.2 General Orbit Perturbations

As described earlier, the path of a satellite is defined by its orbit. Assuming a spherical Earth earlier allowed for the simple conic section description of an orbit in the two-body analysis. However, the Earth is not a perfect sphere. Continents, oceans, mountains and other features create varying gravitational forces within Earth that effect satellite motion. Other celestial bodies have a third-body gravitational effect on a satellite's motion. Perturbations to the gravitational field are often large enough to move

36

the orbit of the satellite dramatically over time. Other perturbations like atmospheric drag and solar radiation pressure can also perturb an orbit.

While perturbations cause irregularities to the motion of the satellite based on the simple conic section description of an orbit, they can also be used to benefit satellite mission planning. With an understanding of perturbations a satellite orbit can be created taking advantage of these effects. One example of this type of orbit design is the repeat ground track orbit. This type of orbit will be discussed in later in this chapter. The satellites of interest to this paper reside in low Earth orbit (LEO), where the largest perturbations come from atmospheric drag and the J_2 oblateness. The strength of the drag perturbation decreases dramatically with altitude. At roughly 1000 km altitude, which is the approximated altitude of the satellites in this research, drag will have a negligible effect on the satellite motion[57].

2.2.1 Orbit Perturbation Theories

Three mathematical methods have been developed to describe and understand perturbation effects on an orbit. These methods are: Special perturbation techniques, General perturbation techniques, and Semi-analytic techniques[48]. Each method has its own benefits and drawbacks for representing orbital motion in the presence of perturbations.

Special perturbation techniques numerically integrate the orbital motion by adding together all perturbation accelerations, a_{pert}. Equation (2.3) must therefore be numerically integrated. This method is usually computationally expensive and prone to growing errors in numerical rounding over time. However, special perturbation techniques are very accurate for predicting the motion of a satellite in the near term.

The General perturbation techniques develop analytic representations for the rate of change in orbital elements. These rates are derived from the original perturbation accelerations. Unlike special perturbation methods, general methods produce less accurate prediction of satellite position very quickly. This method has the advantage that individual perturbation effects can be added as needed once the underlying dynamic

37

effects have been derived. This method is used throughout the remainder of the research and will be explored in more detail in the following section.

Lastly, the semi-analytic method separates perturbation effects into categories based on their effect on orbital motion. Secular and long periodic effects are propagated numerically with large step sizes, i.e. 1-day. Short periodic effects are added analytically. This method is very accurate and is moderately computationally expensive. Constellation design in this research does not require this level of orbit propagation accuracy.

2.2.1.1 Potential Function

As mentioned in the previous section, general perturbation techniques will be used to determine satellite motion in this thesis. One advantage to the general perturbation theory is the ability to select which perturbations to include in orbit propagation. Due to the concept development nature of this research only the largest perturbation effect will be considered. The largest perturbation comes from the gravitational irregularity of the oblate Earth. As the Earth spins, mass around the equator is pulled outward creating an extra bulge near the equator, or oblateness. This extra mass causes added torque on the satellite's orbit. This torque causes both the longitude of the ascending node and the argument of perigee to drift depending on the inclination. Because of this motion the epoch mean anomaly will also experience a drifting motion. These effects are better understood through the mathematical derivation of irregular mass distribution on an orbit.

The perturbing acceleration of non-uniform mass distribution over the Earth is found in Equation (2.8)[5]. The potential function, R, is a sum of all of the zonal harmonics of mass distribution. The position vector of the satellite in ECI is denoted by $\bar{r}$. P_k represents a Legendre polynomial of the kth order. The co-latitude angle ϕ is the angle between a unit vector pointing along the $\hat{K}$ axis of the coordinate system ($\mathbf{i}_k$) and a unit vector pointing along the position vector to the satellite ($\mathbf{i}_r$). The J_k coefficient in the potential function represents a scaling factor, based on empirical data, of the kth order zonal harmonic. The magnitude of the J_2 perturbation is roughly three orders of

38

magnitude greater than any of the other zonal geo-potential coefficients[48]. For this reason the perturbation effects from J_2 have the greatest effect on the orbit and subsequently are often the only perturbation explored for initial mission planning purposes.

$$\bar{a}_{pert} = \frac{d}{d\bar{r}}R = \frac{d}{d\bar{r}}\left[\frac{\mu}{r}\sum_{k=2}^{\infty}J_k\left(\frac{R_{\oplus}}{r}\right)^k P_k\left[\cos(\phi)\right]\right] \qquad (2.8)$$

Where Earth's radius, $R_{\oplus}$ = 6378.137 km, and J_2 = 0.00108263

2.2.2 Variation of Parameters

General perturbation techniques rely on an understanding of how perturbations affect the orbital elements. To understand the effects of the potential function, Equation (2.8), on orbital motion, it is necessary to determine the rate of change in R with respect to the orbital elements. This process is known as variation of parameters. The purpose of this technique is to describe the complex perturbations affecting an orbit as simpler rates of change to the orbital elements. This method was originally developed by Euler and then later improved upon by Lagrange and Gauss[48].

2.2.2.1 Lagrange Planetary Equations

Lagrange's contribution to the variation of parameters is a set of equations carrying his name: The Lagrange Planetary Equations. These equations result from a derivation of the potential function with respect to each of the orbital elements. This derivation can be easily followed in the noted references[5],[48]. Shown in Equation (2.9), the Lagrange Planetary Equations provide the rate of change in each orbital element with respect to time as functions of the rate of change in the potential function with respect to the other orbital elements[5]. Many of these orbital element rates will change over an orbit. Also included in this list of element rates is the rate of the epoch mean anomaly, M_o. The relationship of the epoch mean anomaly to the standard mean anomaly is given in Equation (2.10).

39

$$\frac{da}{dt} = \frac{2}{na}\frac{\partial R}{\partial \lambda}$$

$$\frac{de}{dt} = -\frac{b}{na^3 e}\frac{\partial R}{\partial \omega} + \frac{b^2}{na^4 e}\frac{\partial R}{\partial \lambda}$$

$$\frac{di}{dt} = -\frac{1}{nab\sin(i)}\frac{\partial R}{\partial \Omega} + \frac{\cos(i)}{nab\sin(i)}\frac{\partial R}{\partial \omega}$$

$$\frac{d\Omega}{dt} = \frac{1}{nab\sin(i)}\frac{\partial R}{\partial i} \qquad\qquad\qquad (2.9)$$

$$\frac{d\omega}{dt} = -\frac{\cos(i)}{nab\sin(i)}\frac{\partial R}{\partial i} + \frac{b}{na^3 e}\frac{\partial R}{\partial e}$$

$$\frac{dM_o}{dt} = -\frac{1-e^2}{na^2 e}\frac{\partial R}{\partial e} - \frac{2}{na}\frac{\partial R}{\partial a}$$

$$\text{Where,} \quad b = a\sqrt{1-e^2}$$

$$M_o = M - n(t - \tau) \qquad\qquad (2.10)$$

2.2.3 J_2 Perturbation Effects

To gain a useful understanding of the perturbation effects on orbits, one additional derivation is needed. Since the J_2 perturbation will have the largest effect on the orbits of this research, the effects of that zonal geo-potential perturbation must be examined. To get an approximate understanding of the average rate of change, the potential function must be averaged. The averaged potential function (R_{ave}) for the J_2 perturbation is shown in Equation (2.11)[5]. Applying Equation (2.11) to the Lagrange Planetary Equations, Equation (2.9) establishes the pertinent rates of change in orbital elements for the J_2 zonal perturbation. Only three of the rates have any numerical value: $\dot{\omega}$, $\dot{\Omega}$, $\dot{M}_o$. The perigee drift rate, $\dot{\omega}$, is given by Equation (2.12)[48]. This drift rate will cause the location of perigee, thus the orientation of an orbit to Earth, to precess within the orbital plane. A critical inclination of 63.42 degrees will cause this rate to decrease to zero. The drift rate in the longitude of the ascending node, $\dot{\Omega}$, is developed in Equation (2.13)[48]. This rate will cause the node location of the orbit to rotate about the Earth. This has the effect of swiveling the orbital plane around the rotation axis of the Earth. Lastly, the drift rate in

40

the epoch mean anomaly, $\dot{M}_o$, is given in Equation (2.14)[48]§. This effect causes an additional rate of change to the mean motion. Each of these perturbation rates are shown in differential form. The effects of these rates on the epoch orbital elements over time can be approximated using a first order Taylor series. These rates are fundamentally only dependent on the orbital elements a, e, and i, remembering that n and p also depend only on these elements. All orbital dynamics included in this research include these perturbation effects except for the interceptor flight dynamics.

$$R_{avc} = \frac{n^2 J_2 R_{\oplus}^2}{4(1-e^2)^{\frac{3}{2}}}(2 - 3\sin^2(i)) \qquad (2.11)$$

$$\frac{d\omega}{dt} = \frac{3}{2}J_2 \left(\frac{R_{\oplus}}{p}\right)^2 n\left[4 - 5\sin^2(i)\right] \qquad (2.12)$$

$$\frac{d\Omega}{dt} = -\frac{3}{2}J_2 \left(\frac{R_{\oplus}}{p}\right)^2 n\cos(i) \qquad (2.13)$$

$$\frac{dM_o}{dt} = -\frac{3}{4}J_2 \left(\frac{R_{\oplus}}{p}\right)^2 n\sqrt{1-e^2}\left[3\sin^2(i) - 2\right] \qquad (2.14)$$

2.2.4 Ground Tracks

An important aspect of an orbit with great significance to constellation design is the concept of an orbital ground track. Orbital elements allow one to visualize an orbit from a space perspective. However, it will also be of great importance to understand what an orbit looks like over the surface of Earth. A ground track is the path on the Earth a satellite will travel in its orbit. If a line from the satellite were extended in the nadir direction, pointing to the center of the Earth, this line would trace the ground track.

---

§ This equation in the reference has a sign error.

41

Since the Earth is approximately spherical, a Mercator projection of the entire surface is one method for representing a two-dimensional map of the satellite ground track about the Earth, as shown in Figure 2.8. Ground traces have a distinctive sinusoidal pattern as the satellite moves from west to east. The orbit in the sample figure is a low altitude circular, inclined orbit which circles the Earth 27 times in two days. The ascending node of the orbit can be identified as the point where the ground track crosses the equator from south to north. The orbit in the figure starts on an ascending node noted by a circle on the figure. Additionally, the inclination of the orbit is identified as the highest latitude reached at the apex of a cycle. The Keplerian period of an orbit is the time it takes for a satellite to complete one full revolution. The Keplerian orbital period can be easily visualized in the figure as portion of the orbit that makes one complete pass from ascending node to ascending node. This orbital period (P) can be calculated by using Equation (2.15) below.
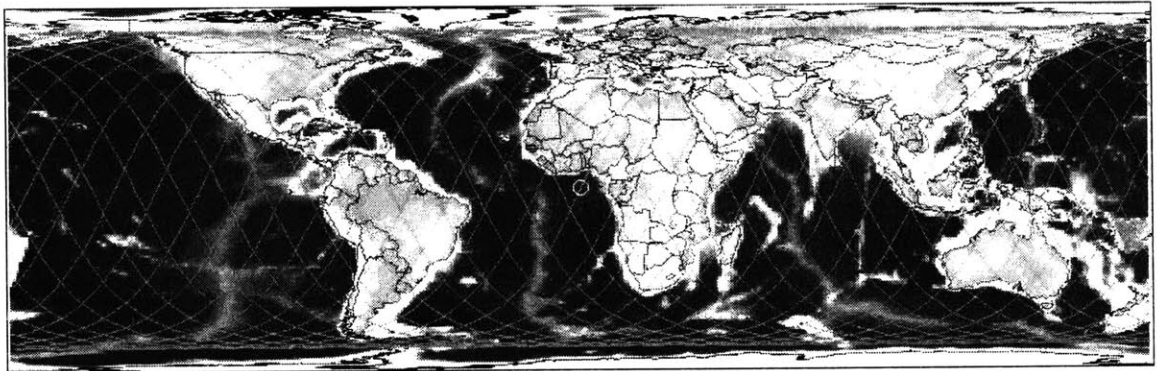
Figure 2.8: Satellite Ground Track of a 27/2-Repeat Ground Track Orbit

$$P = 2\pi \sqrt{\frac{a^3}{\mu}} = \frac{2\pi}{n} \qquad (2.15)$$

2.2.4.1 Repeat Ground Track Orbits

A special type of ground track of interest to this research is a repeat ground track. Since the Earth is rotating underneath the orbit, the ground track's ending point will not usually connect with the starting point. Perturbations will also cause deviations in the

ground track over time. A repeat ground track, however, forms a continuous trace about the Earth. This has the effect of the satellite observing the same ground points day after day. Repeat ground tracks, taking perturbations into account, are highly dependent on the right combinations of the semi-major axis, eccentricity, and inclination. In order to repeat the same path, the orbital period needs to be commensurable with the rotation time of the Earth, i.e. one Earth revolution. This rate combination is identified as a ratio of the number of orbits completed by a satellite to the number of Earth revolutions to complete those orbits. Figure 2.8 from above is an example of a 27/2 repeat ground track. A satellite in this orbit will make 27 orbits every two Earth revolutions and end up over the exact same starting location. The start and ending points to this orbit exactly match inside the circle drawn around the first ascending node.

The key feature to designing a repeat ground track orbit is ensuring that the nodal period (P_Ω), the time it takes a satellite to go from one node back to that same node, be some rational fraction of the Earth's rotation rate[48]. The nodal period, shown in Equation (2.16)[48], is very similar to the Keplerian orbital period of Equation (2.15). In order to make sure the ascending nodes always line up, it is necessary to include perigee drift rate ($\dot{\omega}$) and the epoch mean anomaly rate ($\dot{M}_o$). These rates are determined by the effect of the J_2 perturbation experienced by an orbit. The period of the Earth's rotation with respect to the ascending node of the orbit is known as the nodal period of Greenwich ($P_{\theta g}$). This period is directly related to the Earth's rotation rate ($\omega_\oplus$) and the nodal drift rate of the orbit ($\dot{\Omega}$) due to the J_2 perturbation and is expressed in Equation (2.17)[48]. These rates must be equal, based on the ratio of satellite orbits over the desired number of Earth revolutions. To determine a repeat ground track one must iterate on the semi-major axis given inclination and eccentricity; these elements are imbedded in the development of the perturbation drift equations.

$$P_\Omega = \frac{2\pi}{n + \dot{M}_o + \dot{\omega}} \tag{2.16}$$

$$P_{\theta g} = \frac{2\pi}{\omega_\oplus - \dot\Omega}$$

(2.17)

Where $\omega_\oplus$ for this research is 6.300388809866574 radians/day[58]

2.3 Orbital Transfer

The flight of an interceptor is based on a two-body orbital transfer problem. In general, there is an infinite combination of possible transfer orbits and flight times that will take a vehicle from one point in space to another. Determining the orbit capable of transferring a satellite from one point to another in a fixed transfer time is known as the Lambert problem. The methods and concepts described in this section focus on a method of orbital transfer identified as the orbital boundary value problem using the hyperbolic locus of velocity vectors. The algorithmic solutions developed here are used to define the intercept capability of a satellite-based intercept vehicle after firing.

2.3.1 Fixed Impulse ΔV

In order to intercept a missile threat, it is necessary for an interceptor to transfer from the initial satellite orbit to the future location of that missile. The interceptor must arrive at the same time as the missile in order to make interception possible. To do this, an interceptor must change its orbit to a transfer orbit capable of interception. To change orbit, the interceptor must provide a change in its velocity state from that of the initial satellite state. The change in velocity is denoted as a ΔV.

As stated the preceding chapter, the interceptor will only be capable of a single burn from its chemical rocket motor. Chemical rockets are only capable of providing a fixed ΔV. The burn duration of the interceptor is very short. In the case of both the upper stage motors and the AIM-120 AMRAAM interceptor examples, burn durations last roughly eight seconds[58]. When compared to the flight times in a transfer orbit ranging anywhere from roughly 5 to 25 minutes, this burn can be approximated as instantaneous.

Thus the interceptor is assumed to have an impulsive ΔV. Such an assumption allows for a simplification to the problem of orbital transfer.

2.3.2 Lambert Problem Geometry

The Lambert problem is best understood as selecting the best available transfer orbit from one point in space to another. This problem was originally developed from the desire to determine an orbit given only two position measurements and time of flight. There are an infinite number of possible orbits that cross through any two points in space. To identify a particular transfer orbit of interest will require some additional knowledge about the transfer problem.

Determining where a satellite will be after some time on a transfer orbit usually requires a solution to Kepler's problem. An alternative method of determining the state of a satellite at any point in an orbit is through the use of the f and g functions[5]. Given the initial position ($\bar{r}_o$) and velocity ($\bar{v}_o$) vectors at one point in an orbit, the final position ($\bar{r}_f$) and velocity ($\bar{v}_f$) vectors can be found using the matrix in Equation (2.18) [5]. In this equation, the f and g functions form a state transition matrix for the position and velocity of a satellite developed around the orbital elements of the transfer orbit. These equations also require the angular separation between the initial and final position vectors (θ). The f and g functions shown as part of Equation (2.18) are for elliptical and circular orbits, the corresponding functions for other orbit types can be found in the noted reference[5]**. Note that these equations apply to a particular transfer orbit given its p.

** *These functions are also limited to orbital transfers with θ not equal to 180 degrees*

$$\begin{bmatrix} \bar{r}_f \\ \bar{v}_f \end{bmatrix} = \begin{bmatrix} F & G \\ F_t & G_t \end{bmatrix} \begin{bmatrix} \bar{r}_o \\ \bar{v}_o \end{bmatrix}$$

Where,

$$F = 1 - \frac{r_f}{p}(1 - \cos(\theta))$$

$$F_t = \frac{\sqrt{\mu}}{r_o p}\left[\sigma_o(1 - \cos(\theta)) - \sqrt{p}\sin(\theta)\right] \qquad (2.18)$$

$$\sigma_o = \frac{\bar{r}_o \bar{v}_o}{\sqrt{\mu}}$$

$$G = \frac{r_o r_f}{\sqrt{\mu p}}\sin(\theta)$$

$$G_t = 1 - \frac{r_o}{p}(1 - \cos(\theta))$$

The geometry for an orbital transfer from one point (P_o) to another point (P_f), described with the equation above, is given in Figure 2.9. In this figure, the vector connecting the initial and final position vectors is known as the cord vector ($\overline{C}$). The magnitude of this vector is given by Equation (2.19). The angle θ is also apparent in the figure.
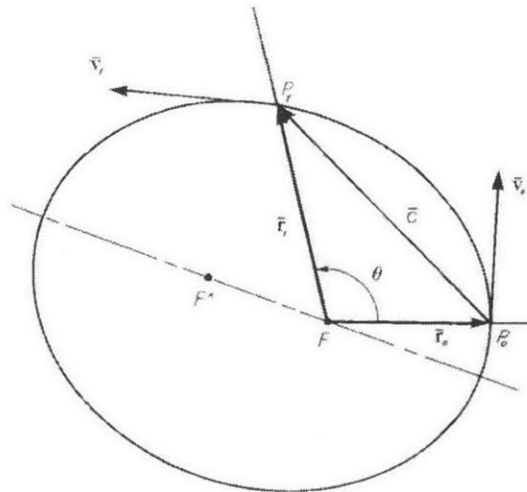
Figure 2.9: Orbital Transfer Geometry[5]

46

$$\overline{C} = \left| \overline{r}_f - \overline{r}_o \right| \qquad\qquad (2.19)$$

A non-orthogonal reference frame can be defined by the unit vectors of the $\overline{C}$ and $\overline{r}_o$ vectors (A unit vector points in the same direction as the vector in its subscript but it has a magnitude of one.) The $\overline{i}_C$ and $\overline{i}_{r_o}$ unit vectors as a basis will be used to find solutions to the Lambert transfer problem. Given any particular transfer orbit, the velocity vectors can be directly resolved onto this non-orthogonal basis. This resolution for the initial and final velocities is shown in Figure 2.10. The angle between the initial or final position vectors and the cord is defined by ϕ_o or ϕ_f respectively. The magnitude of the velocity component along the initial position vector, v_ρ, is given by Equation (2.20). The magnitude of the velocity component along the cord, v_c, is given by Equation (2.21). Note that each magnitude is known once the initial transfer geometry and orbit are given. In this manner, a simple relationship arises between the initial and the final velocity vectors and the magnitude of their components along the skewed axes. This relationship is given by Equation (2.22), were $\overline{i}$ indicates the unit vector of the vector defined in the subscript. The relationship between these equations is only possible by the velocity resolutions on the non-orthogonal basis formed by $\overline{i}_C$ and $\overline{i}_{r_o}$.
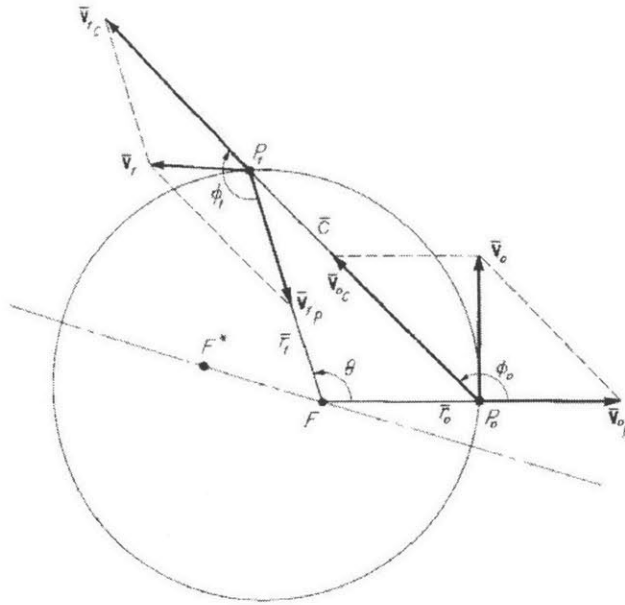
Figure 2.10: Skewed Axis Resolution of Transfer Orbit Velocities[5]

$$v_\rho = \sqrt{\frac{\mu}{p}} \frac{1-\cos(\theta)}{\sin(\theta)} \qquad (2.20)$$

$$v_c = \frac{C\sqrt{\mu p}}{r_o r_f \sin(\theta)} \qquad (2.21)$$

$$\begin{bmatrix} \bar{v}_o \\ \bar{v}_f \end{bmatrix} = \begin{bmatrix} v_c \bar{i}_C & v_\rho \bar{i}_{r_o} \\ v_c \bar{i}_C & -v_\rho \bar{i}_{r_f} \end{bmatrix} \qquad (2.22)$$

2.3.3 Terminal Locus of Velocity Vectors

The orbital transfer geometry described in the section above provides an insight into an interesting phenomenon of orbital transfer. When the Lambert problem is displayed in this manner, the infinite set of orbits capable of transferring from P_o to P_f can be encapsulated in a one-dimensional locus of allowable initial velocities, $\bar{v}_o$. This locus of possible velocity vectors forms one-half of a hyperbola, with the non-orthogonal reference axes as its asymptotes. This hyperbolic locus of velocity vectors can be seen in

48

Figure 2.11. The equation of the hyperbolic locus is based on the magnitudes of the resolved vector components. This equation for the hyperbola is given in Equation (2.23). Note that: ξ, in this equation, is a constant given only the transfer geometry, and is independent of a particular transfer orbit.

Figure 2.11: Hyperbolic Locus of Initial Velocity Vectors[5]

$$\xi = v_c v_\rho = \frac{\mu C}{r_o r_f} \sec^2(\frac{1}{2}\theta) \tag{2.23}$$

The entire range of transfer orbit possibilities, from some initial velocity, is depicted in Figure 2.11. The dashed region of the hyperbola represents the velocity vectors of a hyperbolic transfer orbit. The subscript p represents the velocity vectors capable of a parabolic transfer orbit. All other velocity vectors correspond to elliptical or circular orbits. The velocity vectors with a wavy bar represent the conjugate velocity vectors needed to travel from P_f to P_o. These vectors do not contribute to the intended transfer scheme. The subscript m represents the minimum energy transfer orbit velocity.

2.3.4 Orbital Transfer Using the Locus of Velocity Vectors

The satellite based interceptor problem employs the hyperbolic locus of transfer velocities to determine if an intercept is possible. A satellite will be traveling in an orbit

that does not necessarily take it to the desired target point. In this case, the initial velocity does not lie on the hyperbolic locus needed to reach the desired target point. For this reason, a ΔV is needed to allow the tip of the interceptor velocity vector to lie on the hyperbolic locus. For an interceptor with a fixed ΔV, there is an entire sphere of launch angles available to allow the interceptor velocity to lie on the hyperbolic locus.

2.3.4.1 Minimum Energy Transfer

The minimum energy transfer orbit velocity described in the previous section is the foundation of the transfer problem. Several interesting relationships arise from the minimum energy orbit and the desired transfer orbit. At the minimum energy velocity: v_c = v_p [5]. The parameter of this transfer orbit (p_m) is defined only by the transfer geometry, and is given in Equation (2.24)[5]. The semi-major axis for the minimum energy transfer orbit is given in Equation (2.25)[5]. This equation is also given as a function of the semi-perimeter of a triangle, s. The ratio of any transfer orbit parameter to the minimum energy parameter is equivalent to the ratio of that orbit's velocity vector components[5]. The relationship of the semi-major axis of any transfer orbit can be found as a function of the ratio of that transfer orbit's parameter to the minimum energy orbit parameter. This relationship is given in Equation (2.26)[5]. Once a particular orbit's a and p have been calculated, many of the orbital characteristics for describing an orbit, described earlier, are easily developed.

$$p_m = \frac{r_o r_f}{C}(1 - \cos(\theta)) \tag{2.24}$$

$$a_m = \frac{1}{2}s = \frac{1}{4}(r_o + r_f + C) \tag{2.25}$$

$$a = \left[\left(\frac{r_o + r_f}{C}\right) - \frac{1}{2}\left(\frac{p_m}{p} + \frac{p}{p_m}\right)\right]^{-1} \frac{r_o r_f \cos^2(\frac{1}{2}\theta)}{C} \tag{2.26}$$

2.3.5 Time of Flight

The time of flight necessary for an interceptor to travel between two points must be computed. There are an infinite number of orbits between any two points each with a particular time of flight. For this reason, the transfer time of a vehicle is also an integral part of the Lambert problem. Once an available transfer orbit has been chosen from the hyperbolic locus, it is necessary to determine the time of flight equal to the desired intercept time. Johann Lambert was one of the first individuals to study the relationship for the time of flight (TOF) as a function of the semi-major axis of the transfer orbit, the distance to the starting and end points, and the cord length between them. Lagrange's analytic solution form of Lambert's theorem is given in Equation (2.27). The equations for the angles $\alpha_\angle$ and $\beta_\angle$ are given in Equations (2.28) and (2.29) respectively. From these angles, the transfer time is expressed in terms of semi-major axis and the transfer geometry as Lambert theorized.

$$TOF = \sqrt{\frac{a^3}{\mu}} \left[(\alpha_\angle - \sin \alpha_\angle) - (\beta_\angle - \sin \beta_\angle) \right] \qquad (2.27)$$

$$\alpha_\angle = 2\sin^{-1}\left(\sqrt{\frac{s}{2a}} \right) \qquad (2.28)$$

$$\beta_\angle = 2\sin^{-1}\left(\sqrt{\frac{s-C}{2a}} \right) \qquad (2.29)$$

The introduction to orbital dynamics presented in this chapter is sufficient to understand missile defense via space-based interceptors. Orbital perturbations, transfer velocities, and time of flight techniques have been developed around a basic understanding of orbital motion. The intercept timing necessary to place an interceptor and target missile in the same place at the same time is a complex issue, which will be revisited in Chapter 4. Additional sources of understanding in astrodynamics topics can be found in the noted references of this chapter.

51

[This Page Intentionally Left Blank]

Chapter 3

Classical Approaches to Constellation Design

Since the first satellites were put into orbit, engineers and scientists have been pondering ways in which a group of satellites can be used to accomplish some common purpose. A group of satellites working in unison towards a common purpose is called a satellite constellation. If the satellites in the constellation travel in close proximity to one another to accomplish a purpose, the constellation is known as a formation. Classical constellation design, applied to ballistic missile defense, and not formation design, is the focus of this research. The common purpose of the satellites in a constellation is often the line of site acquisition of a region on Earth. Satellite coverage requires some unknown integer number of satellites, each of which requires six orbital parameters to establish location and motion within the constellation. Thus to establish a constellation $6*T$ variables must be known, where T is the total number of satellites in a constellation. This problem is complicated by imposing constraints on the motion of all satellites such that the minimum required coverage of the constellation always is maintained. In this context, constellation design is a nonlinear mixed integer problem.

Some of the first serious work in constellation design was done to study the feasibility of arrays of satellites for communication purposes. Both Louis Vargo and David Lüders developed the some of the first documented approaches for constellation design[50],[34]. Another of the key pioneers of satellite constellation design was J.G. Walker. Walker laid down another, more geometrical, approach towards constellation design in the early 1970's[56]. Several more pioneers in constellation design helped to further develop these concepts creating approaches of their own, which now serve as the modern basis for constellation design[tt]. Much of the early work in constellation design

---

[tt] Several alternated design methods can be found in the following references: [11],[39],[47],[50][55].

focused on Earth coverage from nadir pointing sensors. Often the design goal, or metric, for the coverage of a constellation is to establish the minimum number of satellites necessary for continuous coverage. With fewer than the minimum number of satellites, coverage becomes discontinuous. In this case, the coverage definition evolves to the maximum (or average) revisit time. Many of the more recent constellation design studies have explored this new coverage scheme[27],[28],[33],[59].

Coverage, in a classical context, is usually defined as the region on the Earth's surface that is in direct line of site to a satellite. The geometric arrangement of satellite coverage footprints forms the coverage geometry. Nearly all classical design methods focus on a coverage geometry involving nadir pointing surface coverage with sensors that have the ability to instantly see their coverage area. This assumption, which is accurate for electromagnetic sensing or imaging, allows for the common coverage geometry shown in Figure 3.1. All of the parameters for this type of coverage geometry can be obtained analytically from planar and spherical geometry calculations. The basic analytic relationship for this coverage geometry is shown in Equation (3.1). This equation is derived directly from the geometry of Figure 3.1 using the Law of Sines, where ε is the elevation angle, r_e is the radius of the Earth, h is the orbital altitude, and θ is the Earth central angle of the coverage footprint. The analytic representation allows coverage to be completely determined with respect to the arrangement of the satellites. Multi-fold coverage is obtained when multiple satellites can achieve coverage of the same point on Earth[53]. Ensuring good coverage geometry over time for a particular set of target locations creates a coverage definition. Classical constellation designs are typically constrained to the following coverage definitions: whole-Earth, latitude-bounded, and area-specific location coverage. Coverage performance can also be numerically computed using a set of grid points arranged around the surface of Earth[29]. This method is often substituted for pure analytic coverage determination. In these cases, the grid of points and the time step for analysis must be carefully defined. However, determination of coverage at any point often uses the relationship given in this figure.

sat

h

Sub-Satellite Point

ε

θ

r_e

Earth's Center
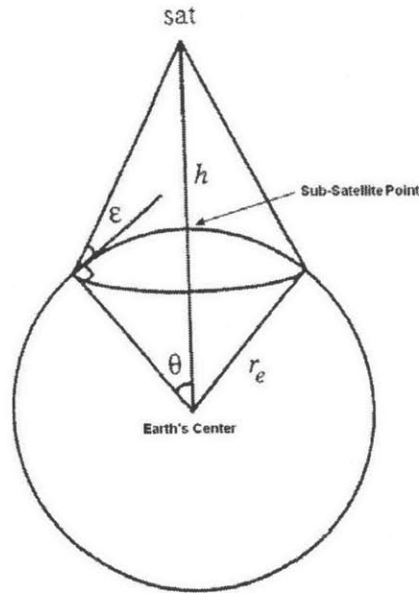
Figure 3.1: Earth Central Angle Coverage Geometry

$$Cos(\theta + \varepsilon) = \frac{Cos(\varepsilon)}{1 + h/r_e} \qquad (3.1)$$

Many arrangements of satellites have been named constellations by classical designers. All of these constellations share a coverage geometry and meet some coverage definition. This research attempts to classify classical constellation arrangements into a specific structure. Starting with sensor coverage geometry and desired targeting goals, a coverage definition is created. Satellites can be placed in numerous arrangements which meet the desired coverage geometry. When satellites are arranged with common orbital characteristics such as elements, combinatorial parameters (like the common number of satellites per plane), and other design conditions (like a common ground track), that arrangement becomes a constellation type. A constellation type defines the basic structure and layout of a satellite arrangement. There are numerous sub-variations within a constellation type each resulting in a unique constellation configuration. Sub-variations arise from free design parameters like the choice in inclination, or the total number of planes and satellites to use. Constellation designers use specific methods for arranging

55

the free design parameters to meet the desired coverage definition. These methods for arranging satellites, within a constellation type's framework, are known as coverage methods. Multiple coverage methods are capable of designing configurations within any set constellation type's framework.

The coverage method forces a satellite constellation to meet a coverage definition, i.e. whole-Earth coverage. Satellite placement polygons, sub-satellite separation distances, streets of coverage, Earth central angle, enclosing polygon, overlapping polygon areas, coverage timeline optimization, and ad-hoc genetic algorithm design approaches are the most common coverage methods with respect to constellation design. Each method can be used for designing a constellation that achieves the desired coverage definition, whether it is partial, regional, or whole-Earth coverage. Each approach has varying degrees of success and each has its own limitations. This chapter will discuss each coverage method, and the type of coverage definition for which each method is used.

3.1 Earth Coverage with Circular Orbit Constellations (Star and Delta Patterns)

Whole-Earth coverage is the first coverage definition that was explored for constellation design. The first constellation design methods of Vargo, Lüders, Gobetz, Walker, Bestè, Ballard, and others, focused on using common inclination and altitude circular orbits about a spherical Earth to achieve coverage[2],[7],[21],[29],[34],[44],[50],[51],[56]. These methods are distinguished by the great deal of symmetry in the placement of satellites within the constellation. Symmetrical patterns of satellites are easier to work with because they limit the number of unknown parameters in a design to a handful of common parameters. J_2 perturbation effects on the orbital cohesion of symmetric constellations can be ignored by assuming the whole pattern will drift in unison. Also analysis of the coverage over time becomes an easier problem as well. All satellites follow the same pattern and thus only a short time span of an orbit needs to be analyzed to ensure that coverage is maintained indefinitely. This time span is an important

simulation parameter and will be explored per constellation type. Once complete coverage is established according to some definition, the symmetry of the pattern ensures that the coverage will remain constant as the Earth rotates underneath.

In common altitude and inclination circular orbits, little more than a good understanding of spherical geometry is needed to develop a working constellation. Polygon enclosure, sub-satellite separation distance, streets of coverage, and Earth central angle formulations were the first approaches to constellation design based on symmetrical patterns of satellites. While each formulation is slightly different, they all focus on establishing Earth coverage using only commonly inclined circular orbits without regard for relative motion of the Earth underneath. Satellites are placed symmetrically in such a way that coverage will always be maintained. While these assumptions and simplifications restrict the design space, the coverage of the resulting constellations can be quite good. Each of these design approaches will be discussed in further detail below with respect to the whole-Earth definition of coverage. In whole-Earth coverage all points on the surface of the Earth must have direct satellite coverage based on the coverage geometry illustrated in Figure 3.1.

3.1.1 Polygon Formulation

One of the first approaches to designing a constellation of satellites was to establish a polygon(s) enclosing Earth at some inclination. The Easton and Berescia's paper illustrates the use of four satellites spaced into a regular tetrahedron about the Earth[15]. An alternative use of a four-satellite polygon enclosing the Earth can be seen in Figure 3.2[13]. While the polygon used in this figure ensures coverage with eccentric orbits, the Easton and Berescia's regular polygon will have coverage gaps due to the motion of the satellites in circular orbits. It is intuitive, that one satellite will be able to view, at most, less than half of Earth even from extreme altitudes. This can be imagined by allowing a sphere to be placed inside of a cone. The cone will touch the sphere tangentially forming a circle that encloses less than half of the sphere. For this reason, two satellites equally spaced in one plane will create at most one-fold coverage over all parts of the Earth except for a small region at each pole. Another set of satellites is

57

needed to provide sufficient coverage of this region at all times. The idea is to use the geometry of equally spaced satellites, forming a polygon in one plane, in conjunction with another plane to ensure that all parts of the Earth are continuously visible by at least one satellite.
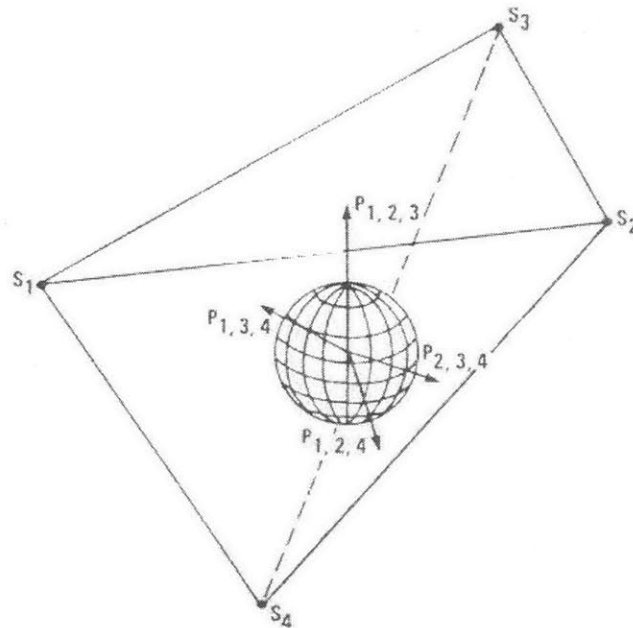
Figure 3.2: Polyhedral Enclosure Constellation with Eccentric Orbits[13]

The idea of enclosing the Earth with satellites at the vertexes of a regular shape was first referenced in a paper by Frank Gobetz on satellite networks for coverage[21]. Gobetz further explores the use of satellite patterns in planes mimicking polyhedrons about the Earth like tetrahedrons, cubes and so forth. Polyhedron constellations of this fashion have problems maintaining coverage as the satellites move in their orbits. While this is not a practical constellation design using circular orbits, it has been shown that this approach can be successfully applied to highly elliptical orbits[12]. The process of using elliptic orbits to form polyhedrons about the Earth will be discussed in greater detail later in this chapter.

3.1.2 "Streets of Coverage" Formulation

If low altitude orbits are required, the complexities of the polygons needed to cover the Earth increases dramatically. For this reason, another method for determining coverage from a series of satellites in an orbital plane was developed. The coverage of a satellite is greatly dependent on its orbital altitude as recognized by Equation (3.1). This realization led a coverage method called "streets of coverage" or SOC[44]. The SOC method uses the same cone and sphere analogy as before. The coverage footprint from the cone will enclose a circle upon the sphere. By lining up several satellites in an orbital plane, a dense set of overlapping coverage circles are created. This series of coverage circles can be seen in Figure 3.3[44]. The continuous coverage "street" width (2C), for this orbital plane, is two times the distance from the orbital plane trace to the minimum overlapping coverage footprint as shown in Figure 3.3. The value of C is directly related to the coverage footprint radius, θ, and the number of satellites in a plane, S. This relationship is given in the figure itself. As this figure illustrates, one street of coverage will provide continuous coverage under the orbit trace, but is insufficient to provide complete Earth coverage. Using multiple streets of coverage from satellites in several planes, continuous whole-Earth coverage can be achieved.
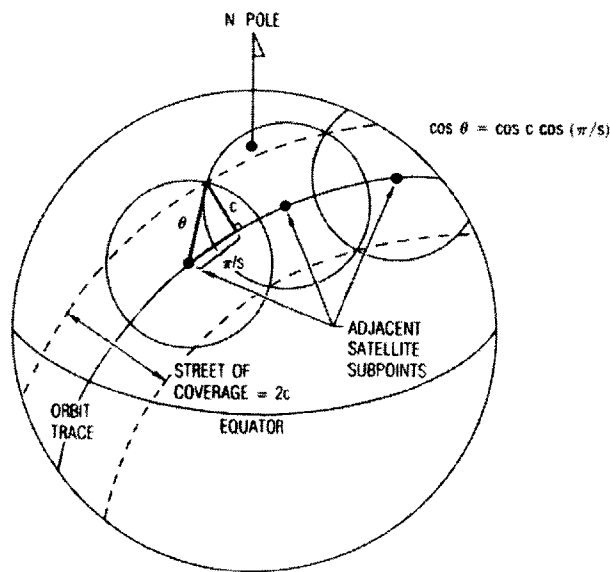
Figure 3.3: Street of Coverage for One Orbital Plane[44]

Once a given number of satellites are assigned to a plane, the dimensions of street of coverage can be identified. A constellation designer now needs to establish what the orbit trace of this street, and streets created by additional orbital planes, will look like over a complete orbit. Arranging the streets of coverage, thus the orbital planes, to produce the desired coverage results is somewhat of an art form. Initially both Vargo and Lüders used this approach with commonly inclined orbital planes[34],[50]. The process for inclined orbital planes requires that the inclination be sufficient to provide coverage to the polar region. The number of planes required for complete coverage is then dependent on the coverage width at the equator, where the streets are the farthest apart. Given a desired altitude and inclination, a minimum number of satellites required for whole-Earth coverage can be readily obtained by geometry. The following sections explore some of the ways in which streets of coverage method can be used to create specific constellation types.

3.1.2.1 Polar Streets of Coverage Constellations

Two basic constellation types arise from the streets of coverage design method. The first type was introduced by Lüders and then more fully developed by D.C. Beste and L. Rider several years later[45]. This type of constellation requires that all orbits have a common inclination of 90 degrees. All of these polar orbits will provide continuous coverage over the poles with the coverage gaps arising at lower altitudes as the streets are spread farther apart. The number of planes in a constellation is directly related to the latitude, from the pole, in which continuous coverage is desired. This idea can be seen in Figure 3.4. More orbital planes are required in order to decrease the latitude of the continuous coverage region. Thus more planes make the separation angle between planes at the equator, or some specified latitude (λ), smaller. For whole-Earth coverage, the street of coverage from each orbital plane needs to be evenly spaced about one half of the equator so that each coverage street is touching its neighbor. This type of constellation was given the name of a star pattern by Walker in his research and will be known as such in this paper.
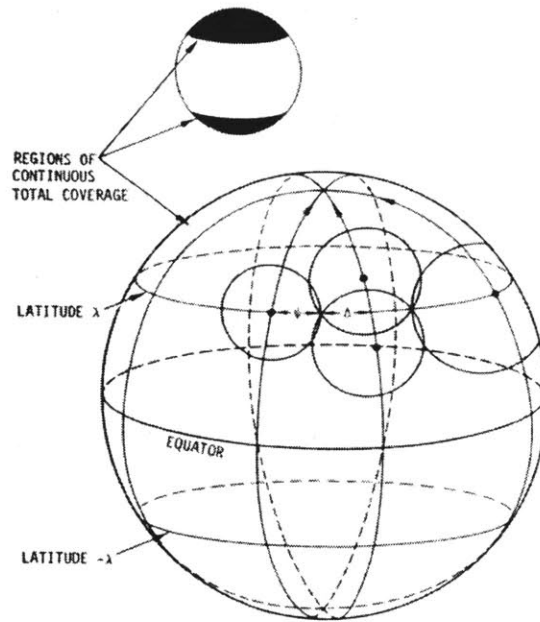
Figure 3.4: Polar Streets of Coverage Geometry[7]

Star patterns can also be created efficiently, as noted by Beste, by taking into account the relative motion of the satellites in adjacent planes[7]. The excess coverage area outside width of one street of coverage can be exploited by imposing the rule that all satellites in one hemisphere travel in a common direction. Relaxing a symmetric longitude of the ascending node placement, a large common coverage area can be created with these excess coverage areas from adjacent streets. Satellites need only be phased appropriately, from one orbital plane to another, to exploit this additional coverage capability between adjacent streets of coverage. Satellites in the two orbital planes at the extremes of the hemisphere will travel in opposite directions to each other. The coverage from these streets will not be able to take advantage of the excess coverage gain and must be placed so that their common streets widths touch. Placement of a constellation in this case becomes a matter of how best to arrange the longitude of the ascending nodes over one side of the Earth. Latitudes close to the equator will create the largest separation in orbital planes. Ensuring complete coverage at a specified latitude will guarantee coverage for all higher latitudes up to the pole. This is the idea expressed in Figure 3.4 from above. The equation for the number of planes (P) required for coverage to some latitude (λ)

61

given the coverage radius (Ψ) and the street of coverage width (Δ) is shown below in Equation (3.2).

$$(P-1)\Psi + (P+1)\Delta = \pi \cos(\lambda)$$ (3.2)

In a star pattern, all of the satellites move from one pole of the Earth to the other in sets of polar orbits. By following the above equation for establishing coverage, a complete constellation can easily be created. Satellites must then be placed in orbits to ensure that the coverage variables, Ψ and Δ, are properly established. The constellation design variables needed to define such a constellation are the common orbital altitude, the number of planes, and the total number of satellites. Three design variables is a dramatic reduction in the number of unknowns needed to create a working constellation. However, the limitations of the star pattern structure can be quite great. Star patterns often require significantly more satellites than other constellation types for whole-Earth coverage. This is due in part to the common crossing point which all satellites must spend time covering. The next constellation type explored by the use of the streets of coverage method eliminates the single crossing point for multiple crossover points from inclined orbits.

3.1.2.2 Inclined Streets of Coverage Constellations

Another fundamental constellation type that is developed from the streets of coverage approach is the delta pattern constellation. Much like a star pattern, this constellation type requires that all the orbital planes share a common inclination and be equally spaced about the equator. The orbit traces from each of the orbits, on a Mercator projection, look similar to a series of sine waves phased some common distance apart. While initially developed from the work of Vargo and Lüders, the most in-depth analysis of this approach was done by L. Rider[35],[44]. Rider used the streets of coverage method, and the idea of orbit traces approximating sine waves, to mesh a constellation together. Extending out from each orbit trace, the maximum street of coverage half-width is (C). Overlaying the streets from each orbit trace, one can identify portions of the Earth without coverage. The relationship between six orbital traces, and their corresponding coverage streets, denoted as dotted lines on either side of the solid orbit trace, is

illustrated in Figure 3.5. The streets of coverage are only shown on the top fourth of this graph. Circled numbers on the Equator denote each orbital plane.
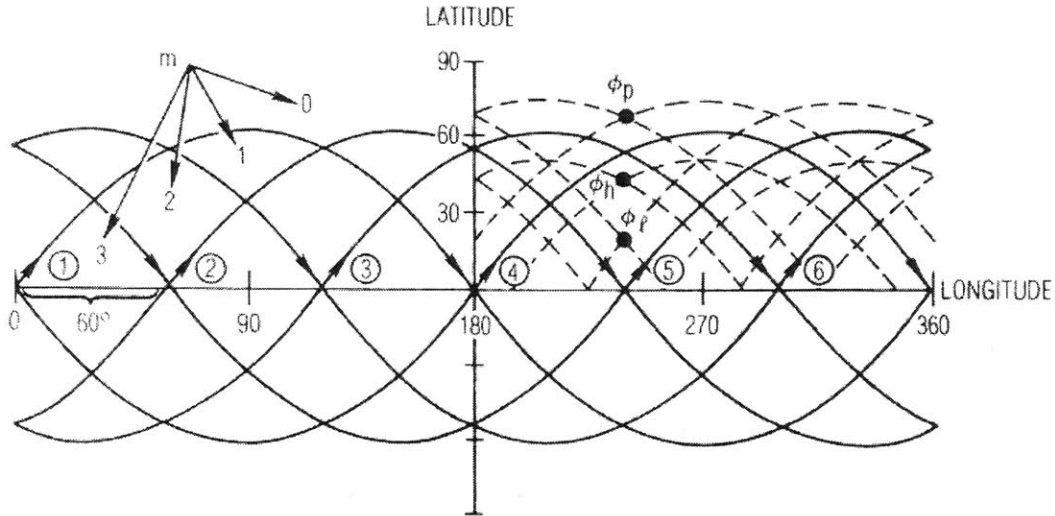
Figure 3.5: Streets of Coverage Meshes for Inclined Orbit Traces[44]

In order to calculate the number of planes necessary for complete coverage, one need only look at the orbit trace meshes. Meshes, as seen in the figure above, are the areas associated with the region inside the intersection of orbit traces. A mesh number (m) also designates each area. Using this framework, Rider developed a set of equations to relate the latitudes of the streets of coverage crossing points in terms of a few design parameters. The design parameters are the inclination (i), C, and the number of planes necessary (P) at a particular mesh (m). The more planes in a constellation the more meshes that are created. The upper and lower latitude points where the streets of coverage cross, are the highest and lowest latitudes of dual coverage area surrounding the crossing orbits. The upper latitude of coverage from the crossing point of two streets of coverage is defined by the parameter ϕ_l. In a similar manner, the lowest point of coverage from the crossing point of two streets of coverage is given by ϕ_h. The relationships for these latitudes with respect to the constellation design parameters are expressed in Equations (3.3) and (3.4) respectively. Ensuring that $\phi_l = \phi_h$ for a given mesh, one can calculate the P and C parameters needed to ensure at least one fold of coverage within the mesh.

63

$$\sin(C) = \sin(\phi_l)\cos(i) - \cos(\phi_l)\sin(i)\cos([m+1]\pi / P) \qquad (3.3)$$

$$\sin(C) = \cos(\phi_h)\sin(i)\cos([m-1]\pi / P) - \sin(\phi_h)\cos(i) \qquad (3.4)$$

This method of establishing mesh coverage can be applied to create a constellation for partial Earth coverage. It is possible, as shown through the equations above, to establish upper latitude bounds of continuous or even multi-fold coverage. The upper bound of coverage is defined by ϕ_p at the zero mesh, as seen in Figure 3.5 above. Partial Earth coverage can require fewer satellites, lower orbital altitudes, or fewer orbital planes. Extrapolating from the equations listed above, it is even possible to establish a latitude zone of continuous coverage. This is done by specifying a range of lower and upper latitudes to cover and ensuring each mesh within that zone has continuous coverage.

For some purposes, it may be desirable to have multi-fold coverage over a region. Both the star and delta pattern constellations have specific regions that are better suited for multi-fold coverage, due to manner in which streets of coverage overlap. Star patterns, as mentioned earlier will have multi-fold coverage at the pole and decreasing capability with decreasing latitudes. When increased coverage over polar-regions is desirable, star patterns are the preferable option. On the other hand, inclined orbits tend to have better multi-fold coverage capability over the mid-latitude and equatorial-regions[31],[44]. These features are exploited to create constellations that cover a bounded latitude range. Additionally, each constellation type can be constructed to achieve multi-fold whole-Earth coverage, at a cost of many additional satellites.

3.1.3 Walker's Sub-Satellite Separation Formulation

Not long after the streets of coverage approach was first applied to constellation design, J.G. Walker developed and published a series of reports on constellation design that approached the geometry of coverage in an innovative way[56]. Applying the same analogy used in the previous formulation, a sphere inside of a cone will have a distinctive circular footprint of coverage on a sphere. The sub-satellite point of this footprint depicts

the center of the coverage region. Many satellites, in common altitude circular orbits, will create many of these circular foot prints all over the sphere. Walker's coverage method uses the geometry of the sub-satellite points and associated circular coverage footprints to find the maximum sub-satellite distance that is allowable for complete coverage of a spherical Earth. An example of this geometry can be seen in Figure 3.6. In this figure, an S denotes the sub-satellite points and the coverage footprint extends an angle Ψ from the satellite. A.H. Ballard was another pioneer who explored Walker's method of satellite separation geometries to build satellite constellations[2]. Figure 3.6 illustrates how a separation distance can be found for any three satellites whose convex hull of sub-satellite points does not include another sub-satellite point. The maximum separation distance from all three satellites R_{max} is calculated with use of spherical geometry for a spherical triangle. By positioning satellites so R_{max} is less than or equal to Ψ for all sets of satellites over the Earth, whole-Earth coverage can be established.
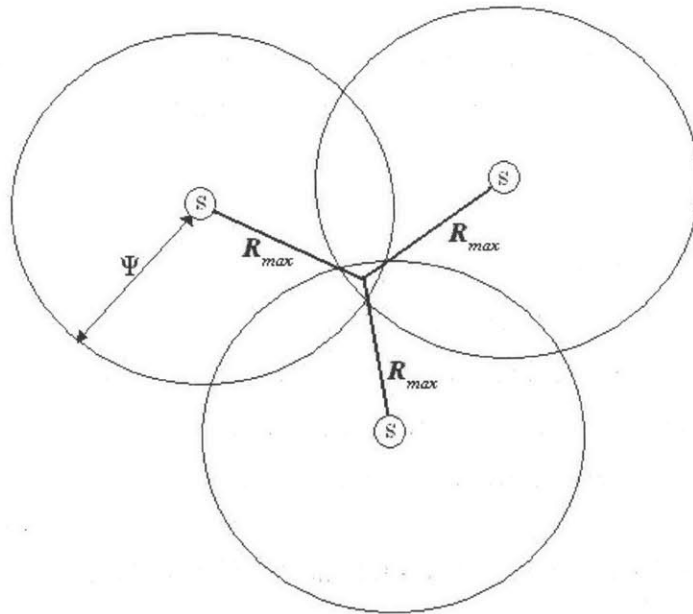
Figure 3.6: Spherical Geometry for Sub-Satellite Separation Distance

In the same manner as the streets of coverage method, two constellation types were explored through this coverage method. The first constellation type results from common polar orbits symmetrically spaced about the equator. As noted earlier, Walker

designates this type of constellation a star pattern. The other constellation type is called the delta pattern. This type of constellation is sometimes called a Walker, or Walker delta pattern in recognition of J.G. Walker's research.

3.1.3.1 Walker Delta Pattern Parameters (T, P, & F)

With either the star or delta pattern, once coverage has been calculated, the coverage must be maintained throughout pattern changes due to satellite motion. To ensure that the delta pattern coverage would repeat itself, Walker imposed a set of basic rules for the design of a delta pattern constellation. These rules specify that the constellation be composed of some number of planes (P) separated equally about the Earth's equator. A common number of satellites must be equally spaced within each orbital plane. The total number of satellites is designated by (T) and must be divisible by P. All satellites are in commonly inclined circular orbits at the same altitude. The satellites from one plane to the next plane are relatively phased from one another by an angle multiplication factor (F), where F takes an integer value from one to P-1. F is a multiplication factor for the pattern unit angle given by PU=360/T degrees. If a satellite is at its ascending note, the next most easterly satellite will be $F*PU$ degrees in its orbit past its own ascending node. With these rules and a given inclination and orbital altitude, a constellation of this fashion can be completely created from only three parameters: T, P, and F[52],[57]. With this method the number of variables needed to completely define a constellation is five. To define the location of every satellite in a random constellation configuration would require 6*T variables, as stated earlier. While this method introduces a lot of symmetry to a constellation while removing some design freedom, it does so at a significant drop in the variability of the design space. This makes delta patterns very attractive from a coverage analysis standpoint. The symmetric nature means that delta patterns are repetitive on a definable time scale.

As a final aid to determining coverage for a delta pattern constellation, it is helpful to look at the sub-satellite points and orbital traces on a pseudo Earth. The pseudo Earth to be used is a reference sphere, of the same dimensions as Earth, which spins with a period equal to the orbital period of the satellites. In this fashion, each of the orbital

traces draw out figure 8's on the sphere. Sub-satellite separation distances are calculated relatively easily for one full orbit without the complicated hassle of determining coverage of crossing orbit traces. The relationship of the satellites within figure 8 patterns will quickly identify where and when the pattern will be strained to maintain coverage. A typical delta pattern (5,1,1), created as an example in Walker's 1971 paper, is shown in Figure 3.7. The location of each satellite, A through E, is denoted by an arrow depicting its motion two positions, $1/20^{th}$ of a period apart. The orbit traces shown in this figure, are shown from a downward looking perspective over the North Pole. The figure depicts both the portions of the traces that can be seen directly (shown as a solid line) and the portions hidden behind the Earth (shown as a dotted line.) The longitude of the ascending node for each orbital plane is also identified. It should be noted now for later use, that the orbital traces of a delta pattern will create spherical polygon around the poles. These polygons will have the same number of edges as orbital planes. A pentagon can be seen in top down view of the orbital traces of the five plane delta pattern shown in Figure 3.7. The associated orbital traces of the same constellation on the pseudo sphere can be seen in Figure 3.8. This figure is a Mercator projection of the orbit traces on the pseudo Earth.
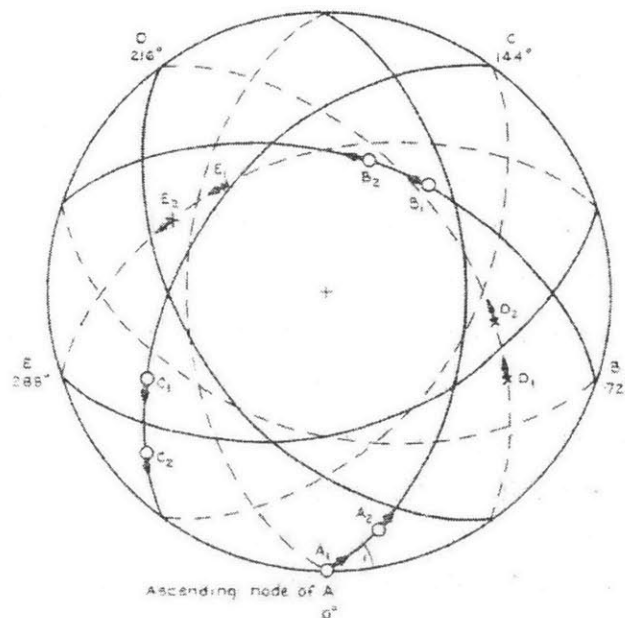
Figure 3.7: Five Satellite Walker-Delta Pattern Constellation[56]
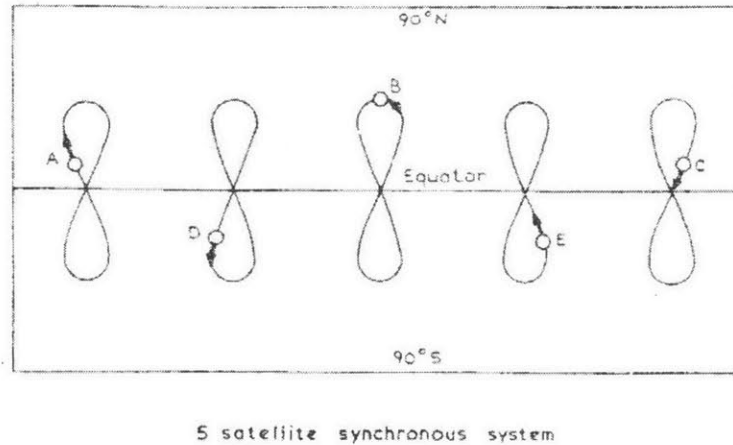
Figure 3.8: Five Satellite Walker-Delta Patterns on Pseudo Sphere[56]

Both delta and star patterns can provide multi-fold Earth coverage[54]. Multi-fold coverage algorithms that require less effort than finding the maximum sub-satellite separation distance for any group of satellites have been developed[24],[25],[26]. These algorithms can also be applied to constellations with eccentric orbits. The goal is to measure the area of union from all the coverage footprints. If this union includes the entire surface of the Earth, then whole-Earth coverage is established. The inclusion-exclusion principle of set theory can then be used to quickly determine the intersection areas and thus the levels of coverage at any point on the surface.

3.2 Earth Coverage with Eccentric Orbit Constellations

The methods of coverage determination discussed to this point have traded freedom in constellation design for a reduction in the variables needed for constellation design. By eliminating or constraining individual parameters like eccentricity, some potential for successful coverage constellations with fewer numbers of satellites is lost. As discussed earlier, one goal in constellation design is to reduce the required number of satellites to perform a specific coverage definition. Thus, the gain in coverage due to eccentric orbits may be worth the added design complexity. Recognizing this potential advantage, the evolution of constellation design has grown towards using eccentric orbits. Initially the polygon enclosure method, using circular orbit, the minimum number of

satellites needed for whole-Earth coverage was determined to be six[15]. Using Walker's innovative methods for coverage and constellation design, it was determined that whole-Earth coverage could be obtained with five satellites[56]. Several years later, J. Draim applied the method of polygon enclosure to construct a four-satellite constellation for whole-Earth coverage[13]. This constellation was unique in the fact that it used a set of highly elliptic orbits to maintain coverage with the motion of the satellites. The layout of this constellation is illustrated in the polygon enclosure constellation of Figure 3.2. These examples show the potential benefit of eccentric orbits for the design of constellations.

3.2.1 Polygon Approach

Vargo first presented the idea of a tetrahedron of satellites enclosing the Earth. However, it wasn't until Draim's use of elliptic orbits that a viable constellation was developed[12]. The idea behind this approach is simple, and not much different from the approach developed earlier. The goal is to place satellites in orbits such that the plane connecting any three satellites does not capture the surface of the Earth. Each polyhedron requires some set number of satellites to compose the vertices connecting each face. This polyhedron is not constrained to be regular, i.e. when all the edges connecting the vertices are of equal length. This allows the polyhedron flexibility to move as needed with satellite motion and still enclose the Earth. Draim showed that high altitude satellites in eccentric orbits could rotate about the Earth and maintain the polyhedron enclosure of the Earth[14]. Additional folds of coverage can also be achieved in this manner at the price of even higher altitude and more eccentric orbits. One such constellation, a 10-satellite pentagonal polyhedron developed by Draim for continuous four-fold whole-Earth coverage, can be seen in Figure 3.9.

69

Isometric View

Three-View Drawing
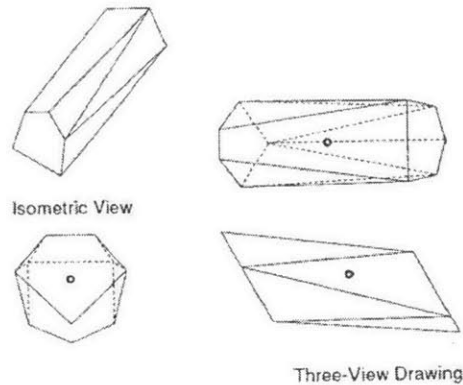
Figure 3.9: **10-Satellite Pentagonal Polyhedron for Continuous Quadruple Coverage**

3.2.2 Other Uses for Eccentric Orbits Constellations

While eccentric orbit constellations may be a bit hard to fully implement, there are other coverage benefits that could be worth the trouble. Eccentric orbits can be used for a number of applications other than whole-Earth coverage. The analogy of the cone and the sphere changes slightly when discussing elliptical orbits. With eccentricity the coverage footprint of a single satellite changes throughout the orbit. The footprint size will be a function of the orbital altitude, as shown in the relationship for the Earth central angle illustrated in Figure 3.1. Satellites placed symmetrically by mean anomaly in an eccentric orbital plane will tend to congregate at the apogee of the orbit and become sparse near perigee. This effect allows for focused coverage in the vicinity of apogee with larger coverage footprints, and smaller coverage footprints with sparse coverage near perigee. Both of these effects have been exploited to develop constellations for area specific coverage, i.e. molniya, tundra, and cobra orbits[40],[46],[3]. Eccentric orbits have the ability to focus on specific areas. In fact, such area specific constellations often require only one orbital plane. However, circular orbit constellations for area specific coverage require more satellites (since they don't loiter at apogee.) This makes eccentric orbits very desirable for certain applications.

70

3.3 Area Specific Earth Coverage with Circular Orbit Constellations

Recent work has considered the development of eccentric and asymmetric constellations for area specific coverage. As noted in the previous section, eccentric orbits are better suited for this problem. Working with eccentric orbits adds a level of complexity to constellation design. For this reason many constellation designers prefer to work with circular orbits and relax other constraints like the symmetrical placement of satellites. One such relaxation allows for variable orbital inclinations. Constellations are developed by organizing the coverage timelines of each potential orbit inclination. J. Hanson, M Evans, and R. Turner first proposed this idea in a paper on maximum revisit time of a specific area[23]. Some of the previous constellation types, such as delta and star patterns, can be adapted to provide localized coverage of a latitude bounded region. Unfortunately, no other analytical constellation design approach for specific area coverage has been created for circular orbits. The only other approach to area specific coverage constellations relies on the use of genetic algorithms. This method is generally leads to an ad-hoc constellation arrangement.

3.3.1 Coverage Timeline Optimization Approach

One way to limit the number of variables in constellation design, and thus its complexity, is to transform the problem into one that is better understood. The times of favorable coverage geometry for a particular orbit can be expressed as a coverage timeline. Using several pre-computed timelines, particular orbits can be selected to meet the coverage definition requirements. Thus, the design method becomes an optimization problem for best arranging coverage timelines rather than a strict satellite placement problem as discussed in previous methods.

The coverage timeline of a specific orbit is the amount of time a satellite in that orbit can view a specific region in one repeat cycle. One benefit to this method is that coverage timelines only need to be computed once and results can be reused for the placement of multiple satellites. The two key orbital parameters when computing

71

coverage timelines are the initial right ascension of the ascending node and the inclination. To limit the design space only repeat ground track circular orbits are explored. The only variable remaining to be specified per satellite in the constellation is the initial mean anomaly. This variable is chosen as a function of where in the repeat cycle a particular satellite timeline is started. This notion of a common repeat cycle, relating to the repeat ground track cycle, is important to show that a constellation will have commensurable coverage for all time. Constellations developed in this fashion fall into the timeline optimized constellation type. An example of the timelines generated for a one-day repeat ground track over a series of inclinations is shown below in Figure 3.10. This figure was generated as part of the work done by D. Ma in the analytic creation of area specific constellations[37]. Given an inclination, the coverage timeline is the vertical slice of the graph at that inclination. It is apparent from the discrete nature of each timeline in the graph, that multiple satellites will be needed to fill in the gaps from any other satellite's timeline. Hanson and DiDomenico also noted from this type of analysis that some satellites will have better "lobes", lengths of time for continuous coverage (view periods), at certain inclinations[11],[23]. Inclinations close to the site of interest will provide fewer but longer view periods of a site, higher inclinations will provide more frequent observations but with less duration, and finally inclinations with coverage footprints lower than the site will never provide coverage of that site. The later set of inclinations can be discarded from the design analysis. As stated earlier, the trick is now to determine which timelines to use and how best to arrange the set.
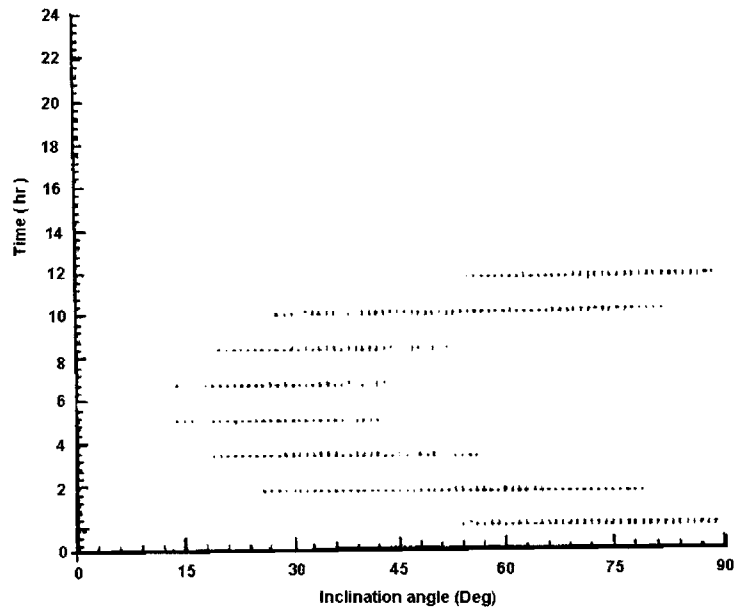
Figure 3.10: Coverage Timelines per Inclination[37]

Constellation design from this point becomes a fixed schedule optimization problem. This type of problem however is still not easy; in fact it is NP-hard meaning that a solution cannot usually be found in polynomial time. While this method may be exceedingly difficult to solve outright, there are methods that can be implemented to find locally optimal solutions. One such method, which is also explained in greater detail for the reader in Appendix 1, is the greedy algorithm. A greedy algorithm seeks to improve an objective function by taking the next best step. While implementing this approach will not necessarily find the optimal answer, it will find a reasonably good solution. Hanson, and later Ma, developed their own types of greedy algorithms for determining how best to arrange the satellite timelines. Another optimization method that can be used for this purpose is a genetic algorithm (GA.) The genetic algorithm process is discussed in greater detail in Appendix 1. The complicated nature of this problem approaches the limit of analytical constellation design. To develop constellations that allow additional design freedom, evolutionary optimization algorithms (such as GA) must be employed.

3.3.2 Maximum Revisit Time

If continuous coverage cannot be provided over a specific region, within the orbital constraints placed on a satellite, a useful cost function is the maximum revisit time. The maximum revisit time is the amount of time a specific area or site spends not covered by a satellite. This metric can then be weighed against the cost of additional satellites. Additionally, one can specify the metric to minimize the average revisit time over a site to get a more evenly distributed coverage profile. If the mission can handle gaps in coverage, any constellation types developed above can be modified for either of these new coverage definitions. Initially, constellations are designed using the methods described earlier for bounded regional coverage and then some satellites are removed. With fewer satellites the issue is how best to reorganize the constellation so that the revisit time is minimized. As mentioned earlier, the task of reorganizing a constellation is often left to the hands of a genetic algorithm or some other optimization scheme. Several authors have done considerable work in this area. The most notable work with genetic algorithms for constellation design was done by T. Lang[30].

3.4   Genetic Algorithm Optimized Constellations

Recently, constellation design has gained an interesting asset for optimally arranging satellites in the form of the genetic algorithm. Genetic algorithms use a randomized search procedure to place satellites in an effort to achieve an optimal objective function. In general, genetic algorithms allow designers to randomly search, within specified bounds, for the best method of arranging satellites in the constellation, with respect to a cost function. Because this is a random search algorithm the resulting placement of satellites in a constellation will usually appear to be ad-hoc. As shown earlier, the placement of satellite timelines is an extremely difficult optimization problem. General constellation design, without simplifying constraints, is even more difficult problem.   Genetic algorithms only require information on the objective function, i.e. coverage, and do not need any gradient information. These algorithms handle integer problems as easily as non-integer problems. For these reasons, genetic algorithms are very useful in solving the nonlinear mixed-integer problem of constellation design.

74

While genetic algorithms can provide solutions to problems, their use benefits from the application of engineering insight. Genetic algorithms are notoriously slow at converging to an optimal answer. Intelligent creation and bounding of variables inside a genetic algorithm helps to improve the speed and reliability of results. The results themselves depend on the nature of the constellation design problem. Many recent constellation designs have focused on the use and results of genetic algorithms for satellite placement[16],[17],[19]. One method of speeding up the convergence of a genetic algorithm process is to explore smaller problems with limited numbers of variables[19]. If whole-Earth coverage is desired, asymmetric genetic algorithm constellations are often as good or better than symmetric constellations[59]. For area specific problems, asymmetric genetic algorithm constellations often provide better coverage results than symmetric constellations[32]. Genetic algorithm results allow for the exploration and design of satellite constellations that may not be analytically graspable. While genetic algorithms can provide very interesting and asymmetric results when creating constellations they do not provide nearly as much insight into the inner workings of good satellite placement for constellation design.

This chapter has presented the key approaches developed in classical constellation design. Constellation design is founded around an understanding of a coverage geometry and definition, i.e. nadir-pointing satellite coverage footprints. In the past, this definition has been nearly common for all constellations. This research will venture away from the classical approach to coverage. The coverage methods used to place satellites in a constellation type will also be applied to create missile defense constellations. Constellation types ranging from the rigidly symmetric star and delta patterns to eccentric ad-hoc asymmetrical designs will be examined to determine relative effectiveness of each type. While classical constellation designs have created many approaches for nadir-pointing Earth coverage, very few designs have considered alternative coverage definitions like ballistic missile defense.

[This Page Intentionally Left Blank]

Chapter 4

Interceptor Coverage Development

Constellation design for satellite-based missile defense breaks away from classical design methods due to a new and complex definition of coverage. As previously mentioned, the space-based missile intercept problem is multi-dimensional. The first section of this chapter examines ICBM trajectories and the threatened region discussed in the defense scenario of Chapter 1. The intercept timing issues and the capability of space-based interceptors are developed into a mathematical definition of interceptor coverage from tools formed in Chapter 2. This definition, when combined with coverage methods abstracted from Chapter 3, becomes the basis for space-based missile defense.

4.1 Intercept Tractability Constraints

For the purpose of intercepting a ballistic missile in mid-course flight there are some realistic missile-tracking assumptions that must be made. The first of these is that the trajectory of any ICBM can be identified at launch or soon after by ICBM tracking assets. There are several assets, as mentioned in Chapter 1, currently capable of meeting this assumption. To account for the transmission and uplink of an ICBM trajectory to the appropriate satellite-based interceptors, two-minutes are allowed to pass after the missile is exo-atmospheric (100 km altitude.) It is assumed that the missile may be intercepted at any point thereafter until reentry. For this work, an interceptor is postulated to have a fixed impulsive ΔV. This leads to a constrained multi-dimensional intercept problem. The interceptor ignition timing will be developed in the following sections. The goal is to develop the means to put an interceptor in the right place, at the right time, to allow intercept of a single ICBM, launched at any time. To defend against multiple missile launches, each satellite may require additional interceptors. It is assumed that the interceptor will have the homing capabilities to complete the terminal moments of

77

intercept. Any small missile trajectory errors are assumed to be compensated for by the interceptor during this homing phase. However, the homing phase of the intercept will not be explored as part of this thesis.

4.2 Ballistic Missile Flight Determination

The specific threat of interest to this research is the postulated capability of the North Korean Taepodong ICBM. It was noted in Chapter 1, that at a maximum range, this ICBM was capable of hitting Los Angeles, roughly 9,500 km away. A line connecting Anchorage, AK to L.A., CA was swept out over an azimuth to Bismarck, ND. This area represents the threatened region from a North Korea missile launch. The minimum range considered is roughly 5,800 km. The area enclosed by sweeping the line over an angle of roughly 15.5 degrees represents the major population centers within the reach of a postulated Taepodong attack. The threatened region is represented in Figure 1.2. While this missile can hit important U.S. targets outside of this region, such as Hawaii, the potential for an attack on these isolated areas is slim.

4.2.1 Minimum Energy Trajectories

Trajectories of the Taepodong ICBM capable of hitting the threat region must now be established. For this study, a single launch point was defined from Pyongyang, North Korea. Additional trajectories from other launch location inside of North Korea will not vary substantially from the Pyongyang launch site. Minimum energy ICBM trajectories were generated to obtain a reasonably accurate assessment of the ballistic missile flight profiles. Determining the potential flight path of a missile is a complex Lambert problem involving the launch location and the target location.

The initial maximum flight-path angle (γ_{max}), and initial minimum flight-path angle (γ_{min}) for an ICBM, can be determined from Equations (4.1) and (4.2)[60]. The initial minimum-energy flight-path angle (γ) lies between these values. A common approximation for the initial minimum-energy flight-path angle is the average of the two extremes[60]. In these equations, θ represents the Earth Central Angle of the desired

78

ICBM range (measured inertially). In the case of this study, this range was varied from 5,800 to 9,600 km. Only the portions of flight that are exo-atmospheric, i.e. an altitude of 100 km or greater, were used in determining the mid-course portion of flight. The initial and final positions of the mid-course are represented by: r_o and r_f, respectively. The burn-out velocity magnitude (V) needed to travel a desired range along the minimum energy flight path angle is given by Equation (4.3)[60]. All possible minimum energy trajectories capable of reaching the threatened region can be calculated using this velocity calculation for all desired ranges and azimuths. The trajectories were then propagated in inertial space and translated into ECF coordinates to account for the rotation of the Earth during flight[4].

$$\gamma_{max} = \tan^{-1}\left\{\left[\sin(\theta) + \sqrt{\frac{2r_o}{r_f}(1-\cos(\theta))}\right]\bigg/(1-\cos(\theta))\right\} \tag{4.1}$$

$$\gamma_{min} = \tan^{-1}\left\{\left[\sin(\theta) - \sqrt{\frac{2r_o}{r_f}(1-\cos(\theta))}\right]\bigg/(1-\cos(\theta))\right\} \tag{4.2}$$

$$V = \sqrt{\frac{\mu(1-\cos(\theta))}{r_o\cos(\gamma)\left[\left(r_o\cos\gamma/r_f\right)-\cos(\theta+\gamma)\right]}} \tag{4.3}$$

The entire three-dimensional volume encompassed by all of these trajectories, from exo-atmospheric point to their re-entry point, is defined as the missile corridor. The three-dimensional side view representation of this corridor can be seen in Figure 4.1. A two-dimensional Mercator projection of this corridor can be seen in Figure 4.2. This figure also portrays the full range capability of a postulated Taepodong ICBM, identified as the lighter shaded portion of the Earth. The missile corridors created for this specific threat are fixed in the ECF frame. This means that the entire corridor will rotate with the motion of the Earth during a simulated analysis. All trajectories emanate from the common North Korean launch location. Another view of the missile corridor is shown in Figure 1.2. Trajectories emanating from other North Korean sites, or targeted at other locations in the United States, will slightly deviate from this corridor. The estimates on

range and azimuth were slightly enlarged to create a conservative missile corridor approximation, by accounting for some of these possible trajectories. Ensuring that any potential missile is intercepted before that missile traverses through the corridor is the goal of mid-course missile defense.
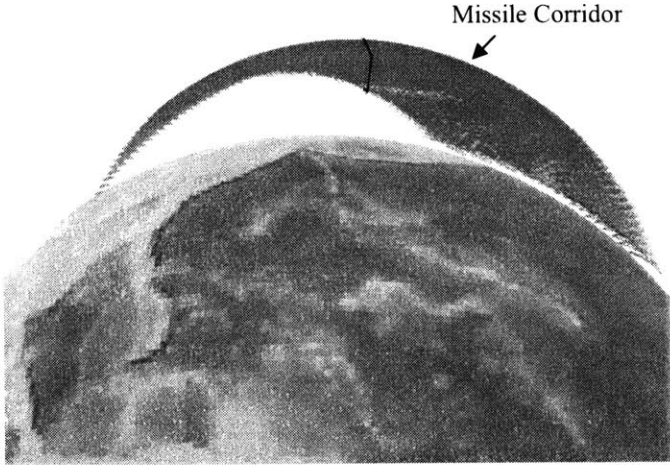
Figure 4.1: Side View of Missile Corridor
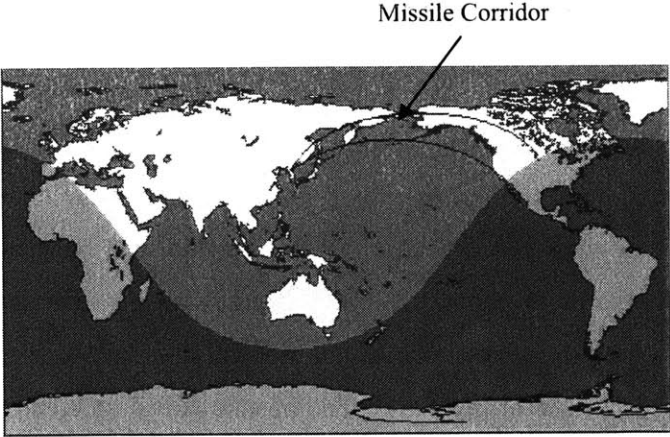
Figure 4.2: Mercator Projection of Missile Corridor

4.3 Interceptor Timing Problem

Coverage in the context of this work requires that a satellite-based interceptor can reach a target location at the appropriate time. The intercept timing issue is one of the most important aspects in determining coverage. An analogy of this problem can be drawn to a football pass from the quarterback to the receiver. The quarterback is the satellite bus, the ball is the interceptor, and the ICBM is the receiver. In order to complete a pass, or missile interception, the quarterback must ensure that his throw arrives at some point and at the same time as the receiver arrives at the intercept point. The quarterback must lead his target and time everything so that the receiver can complete the pass as planned. This analogy gives an idea of the timing issues involved, however the dynamics of orbital motion are far more complex than a receivers play route.

In the case of the space-based intercept problem, the time a missile trajectory has been identified and relayed to the appropriate satellites signifies the ICBM identification time (T_{ID}). In this research, it is assumed that T_{ID} is two minutes after the exo-atmospheric point. After this point the satellite has the option of loitering in its orbit or firing its interceptor. The interceptor ignition time, T_{ignite} is the time the interceptor is fired from the satellite. The time from T_{ID} to T_{ignite} is the satellite-loiter time (SLT). After some time of flight, based on orbital dynamics, the interceptor captures the ICBM in its trajectory at a nominal intercept time ($T_{intercept}$). A simple illustration of this timing geometry is shown in Figure 4.3. The trajectories of a satellite, the ICBM threat and the interceptor are displayed to achieve a sense of the timing. As identified in the figure, the capture time is the sum of the SLT and interceptor time of flight (Int_{TOF}). Capture time is also the missile flight time along the ICBM trajectory, after T_{ID}, where the intercept will take place. The ignition time and the intercept time are free parameters for timing an intercept. As this diagram suggests there are a wide range of possible intercept timing combinations. These combinations are bounded by the physical limitations imposed by orbital motion and the final reentry time constraint. Interceptor capability is the focus of the following sections.
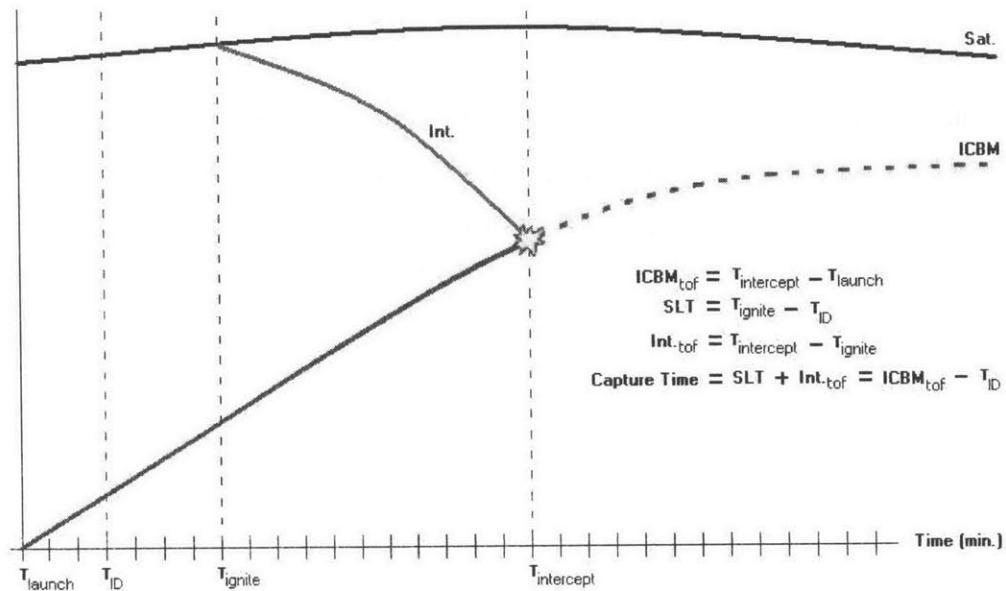
Figure 4.3: ICBM Intercept Timeline

In the figure:

$$ICBM_{tof} = T_{intercept} - T_{launch}$$
$$SLT = T_{ignite} - T_{ID}$$
$$Int._{tof} = T_{intercept} - T_{ignite}$$
$$Capture\ Time = SLT + Int._{tof} = ICBM_{tof} - T_{ID}$$

Axis labels: T_{launch}, T_{ID}, T_{ignite}, $T_{intercept}$, Time (min.)

One important timing issue associated with the intercept problem is the relative speed of all the actors. Note that the interceptor, satellite, and missile all have different characteristic velocities. The trajectory of each vehicle is determined by orbital motion. It should not be inferred from the diagram above that this is a 1-dimensional timing problem. In this case, the satellite, the interceptor, and the missile are all moving at different speeds and in different directions. These differences cause a distribution of terminal intercept geometries and relative closing speeds. Typically satellites in this research travel in circular orbits with a speed around 7 km/sec. An interceptor, as defined earlier, has a maximum ΔV of only 1.3 km/sec from the satellite. The average ICBM velocity magnitude will change dramatically over an orbit its trajectory from 4.8 to 6.9 km/sec. This large velocity separation is exploited when computing intercept solutions. In a 21-satellite constellation example taken from this thesis, a histogram of the number of intercepts for various closing speeds is shown in Figure 4.4. Most interceptors arrive with closing velocities between 3 to 9.5 km/sec. This fact illustrates that the relative approach speed of a satellite bus, as viewed from an ICBM, is large. Large closing speeds are

82

necessary for kinetic intercepts. A histogram of the number of intercepts for various terminal intercept angles is shown in Figure 4.5. This histogram illustrates that a majority of the interceptors approach the ICBM from rear to the side, i.e. 5 to 85 degrees from directly behind the ICBM. This is due in great part to the 63 degree inclination of the 21-satellite constellation. These terminal characteristics are not included in the design process, but are presented to provide an understanding of the relative speeds and approach angles at intercept.
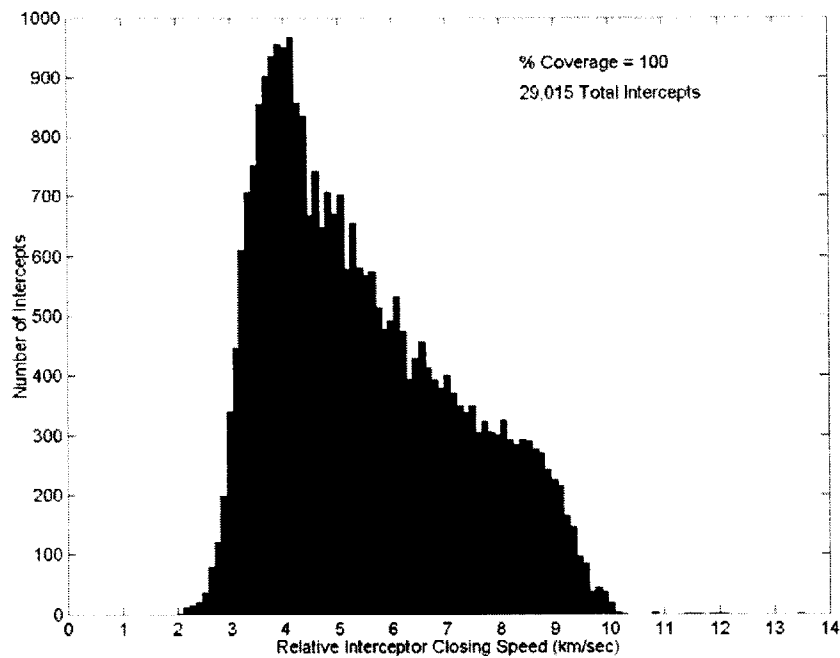
Figure 4.4: Histogram of Intercepts per Interceptor Closing Velocity

% Coverage = 100
29,015 Total Intercepts
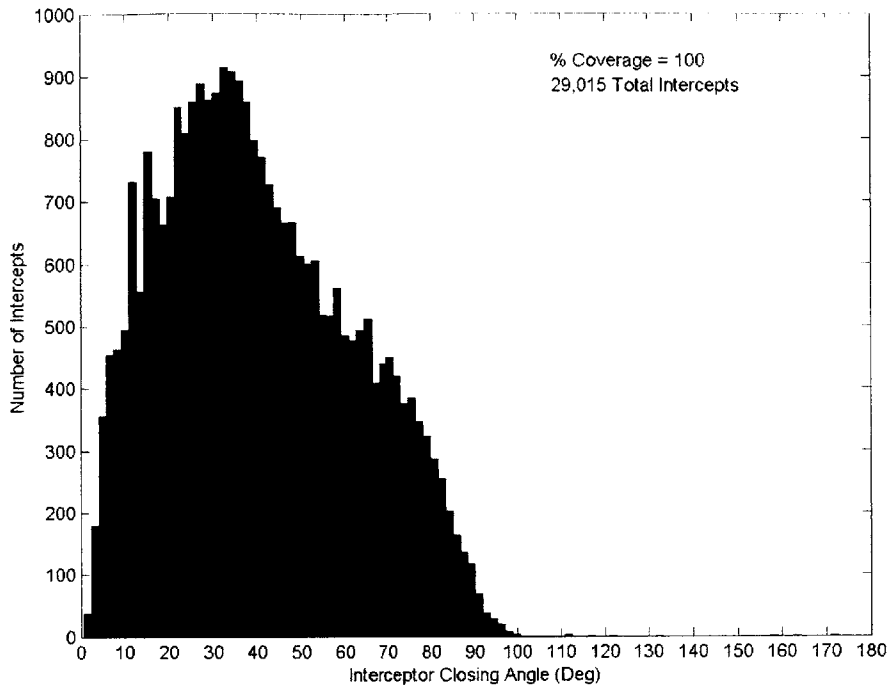
Figure 4.5: Histogram of Intercepts per Terminal Approach Angle

4.3.1 Coverage Development

Coverage in the context of this thesis is the ability of a satellite-based asset to intercept an ICBM within the threat corridor. This metric is a true-false condition for each interceptor at a particular instant in time. The interceptor either will or will-not be capable of intercepting a particular target location at the allotted capture time, from an initial orbital state. The capability of the interceptor is also limited by its ΔV. The ICBM threat corridor, where all intercepts take place, is a three dimensional volume. For these reasons, classical definitions of constellation coverage are not directly applicable for missile defense.

4.3.1.1 Multi-Dimensional Reachability Envelope

The interceptor reachability envelope is the region where an interceptor, fired at some time, could strike an ICBM given a set capture time. To gain an understanding of

84

the inertial interceptor capability, it is helpful to examine it from the geometric point of view. Firing an interceptor in every possible direction at a particular instant will create a sphere of reachability. This intercept region will seem to grow like a wave front emanating from the satellite over time. A simple illustration of this effect can be seen in Figure 4.6. The size of this manifold is largely related to the available capture time, which translates into allowable interceptor flight time. Figure 4.7 is a simple demonstration of the multi-dimensional timing issues involved within the intercept problem. A target can be intercepted, at a specific capture time, from a series of different combinations of flight times and satellite loiter times. Note that if a satellite loiters too long there is the possibility of entirely missing the ICBM. The work in this thesis will primarily focus on the first opportunity of intercept. Figure 4.8 indicates the influence of two-body dynamics on the reachability manifold, which begins to look like a cornucopia stretched about the Earth. This figure displays the spherical wave-front of inertial interceptor positions (in kilometers) at time intervals to the desired capture time. All of these positions represent an envelope of interceptor reachability (12-minute capture time in this case.) To be intercepted, a missile must be inside of the reachability envelope of an interceptor. This condition is not a guarantee of capture, but it is a requirement for intercept. The cut-off near the end of the manifold represents those trajectories that pierce the atmosphere. Intuitively, the satellite bus "pushes" its interceptor reachability manifold forward as it orbits the Earth.
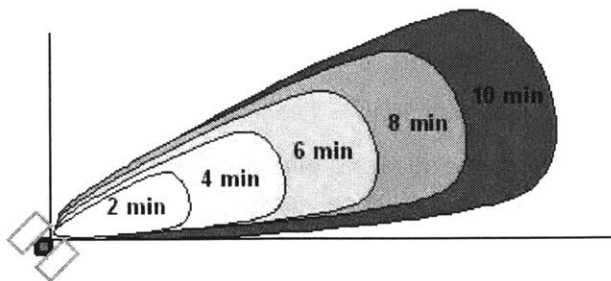
Figure 4.6: Interceptor Reachability with Increasing Time of Flight
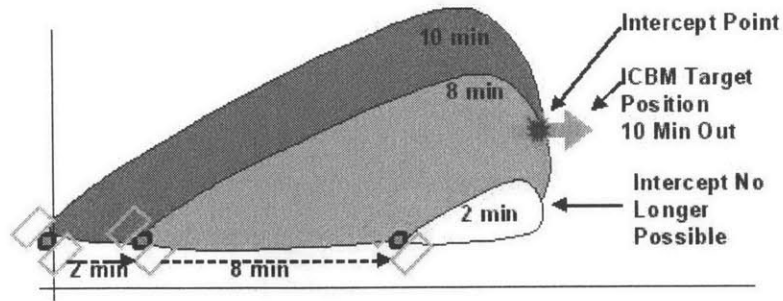
Figure 4.7: Interceptor Ignition Timing
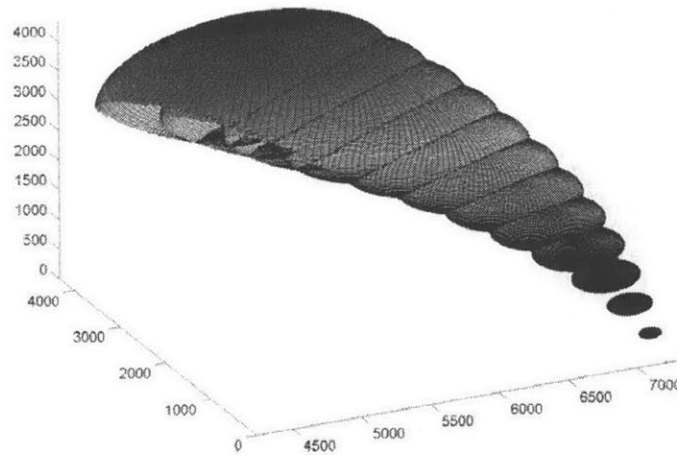
Figure 4.8: 12-Minute Interceptor Reachability Envelope

The reachability envelopes of an interceptor at 6, 12, 21, and 31 minutes are displayed in Figure 4.9. These graphics were generated by plotting the actual orbital path of many interceptors over time in Matlab®. The reachability envelopes represented in this figure are from a specific launch location and shown in an inertially fixed view. The geometric representation of interceptor reachability is helpful for understanding coverage, but alone, is insufficient for a complete intercept solution.
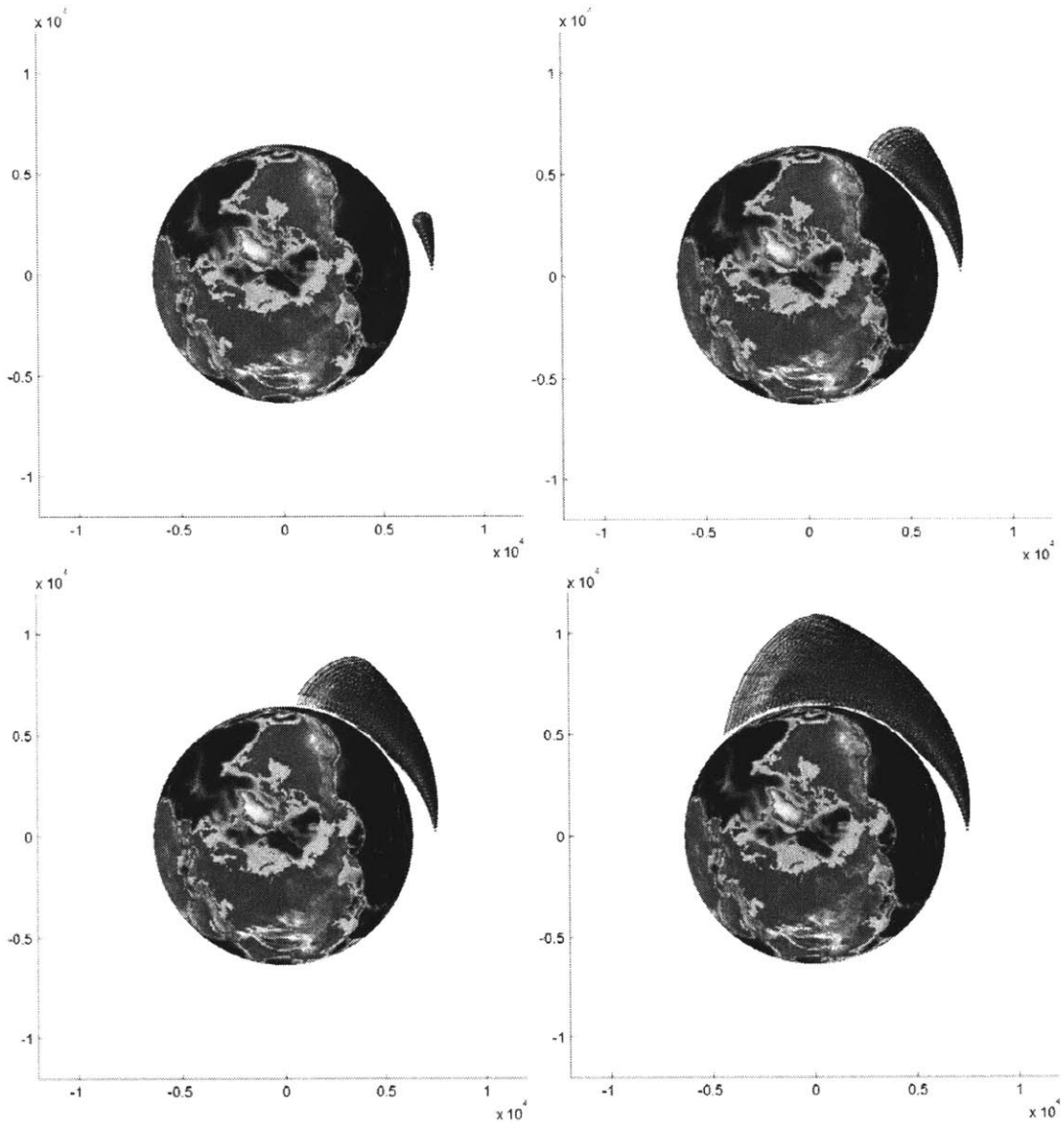
Figure 4.9: 6, 12, 21, and 31-Minute Interceptor Reachability Envelopes

4.4 Algorithmic Coverage Development

The geometric representation of interceptor reachability is effective for understanding satellite coverage for the purpose of missile defense. The mechanics of orbital transfer serve as a mathematically sound approach for intercept coverage analysis. Given a desired capture time, and inertial target location, an ignition time solution to the ΔV fixed Lambert problem must be computed. Figure 4.10 represents the flow diagram

of the interceptor coverage determination function. This figure embodies the algorithm described in this section. Functional inputs include: the satellite position and velocity, the desired ICBM target/intercept locations, and the available capture times. This function uses three nested loops to determine if a satellite in the constellation, with an available capture time, is capable of intercepting an ICMB target location. This function iterates to determine the timing sequenced needed to intercept a target location as the missile arrives. The function outputs the percent coverage over a given simulation time.
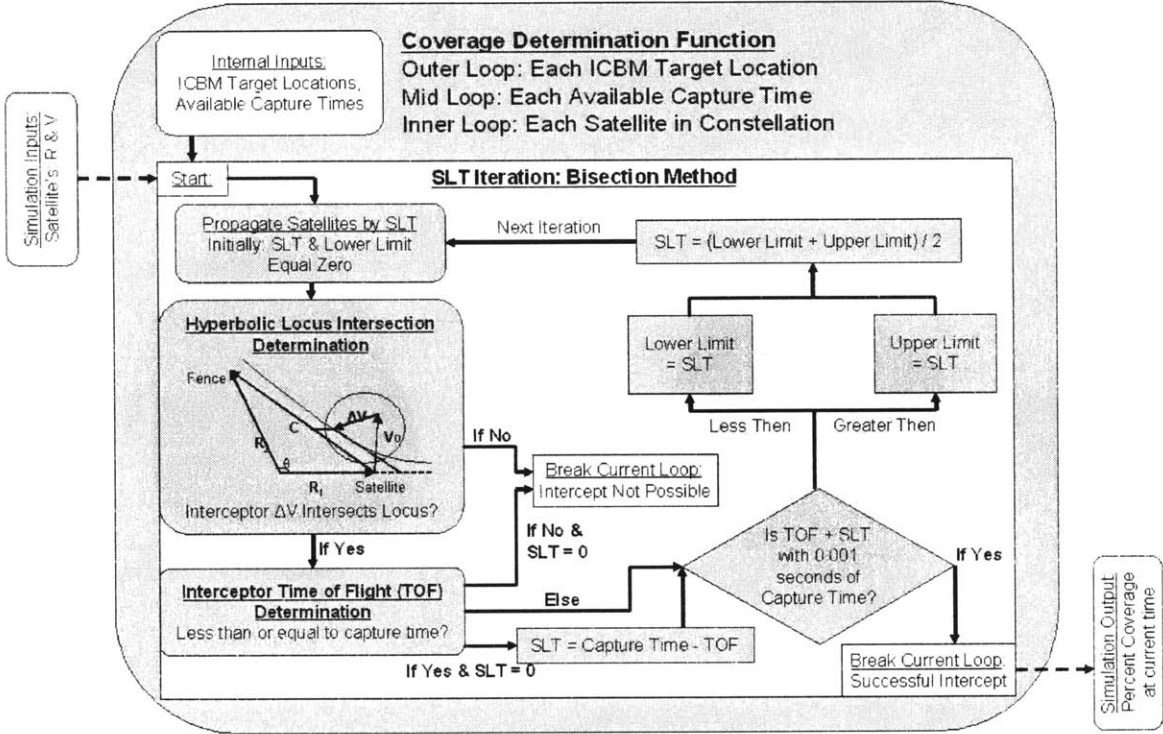
Figure 4.10: Algorithm for Coverage Determination Function

4.4.1 Intersecting the Hyperbolic Locus

The hyperbolic locus of transfer velocities is useful in finding a solution to the fixed ΔV and fixed time of flight intercept problem. As developed in Chapter 2, the hyperbolic locus of velocity vectors represents the complete set of velocities that will transfer an object from one point to another in some orbit. This hyperbolic locus exists in only two dimensions defined by the unit vector of the cord ($\overline{i}_c$) and the unit vector of the

88

initial position ($\overline{i}_{r_o}$). Therefore, the hyperbolic locus lies in the plane connecting the initial firing point with the desired target point. In most cases, a satellite bus will not be traveling in this plane. If the interceptor is allowed to fire in any direction, this creates a sphere of possible velocity changes emanating from the initial satellite bus velocity. The radius of this sphere is the magnitude of the fixed ΔV. If the sphere of possible velocity vectors intersects the hyperbolic locus then the interceptor can hit the chosen target with the interceptor velocity, V_f. This intercept concept is depicted in Figure 4.11 in the plane of the hyperbolic locus.
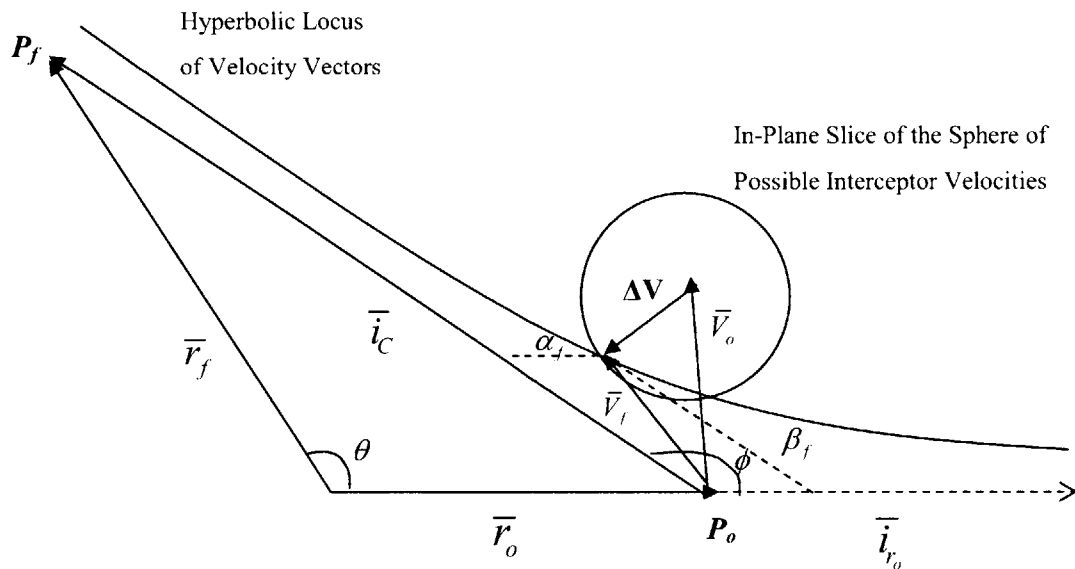
Figure 4.11: Orbital Transfer using the Hyperbolic Locus of Velocity Vectors

The roots of Equation (4.4), below, are used to determine if the sphere of possible intercept velocities will allow the final velocity to lie along the hyperbolic locus. In this equation, θ, ϕ, V_o, and ξ are given in the transfer orbit development of Chapter 2, many of these variables are also identified in the figure above. The variables: α and β represent the components of the velocity vector resolved in the non-orthogonal reference frame. These parameters were represented in Chapter 2 by v_ρ and v_c respectively. The α parameter denotes the velocity component along the initial position vector, and β parameter represents the component along the cord vector. The change in notation is necessary to simplify the identification process for multiple vector component

resolutions. The subscripts to these variables refer to either the initial or final velocity vectors. The roots of this fourth order equation, given in Equation (4.4), will always have two imaginary parts. The two remaining roots may be real, repeated, or imaginary. If the roots are real, the largest β_f will result in shortest interceptor time of flight. This is due to the fact that velocities with larger β_f will result in orbits approaching hyperbolic transfers, which have the shortest times of flight between two points. The semi-major axis of the interceptor's transfer orbit is obtained from Equation (2.26). The time of flight for transfer is then given by Equation (2.27). If the interceptor time of flight is equal to the capture time then an intercept solution is found. If the flight time is less than the capture time, the procedure must be iterated to compute the exact ignition time and SLT. The iteration process will be discussed in the following sections. This analysis of the hyperbolic locus intersection represents the physical intercept availability in the coverage determination function shown above in Figure 4.10.

$$
\begin{aligned}
&\beta_f^4 - \beta_f^3 (2\beta_0 + 2\alpha_0 \cos\phi) + \beta_f^2 (V_0^2 + 2\xi \cos\phi - \Delta V^2) \\
&- \beta_f (2\alpha_0 \xi + 2\beta_0 \xi \cos\phi) + \xi^2 = 0
\end{aligned}
\tag{4.4}
$$

4.4.2 Time of Flight Limitations

Interception must occur at a target location, exactly when the ICBM reaches that location. There may be multiple satellites capable of hitting a target location. However, some of the interceptors may require significant flight times. The time of flight of the interceptor must therefore be limited to within the available capture time. These calculations rely on a specific inertial location of the target. This location must be chosen once the ICBM has been identified. The amount of capture time to intercept an identified missile is variable up to a maximum value. The maximum capture time is equal to the remaining flight time of the ICBM until reentry. For this thesis, all of the timing analysis was completed on a discrete one-minute timeline. However, solutions to the intercept timing problem were iterated to a tolerance of less than ten-thousandths of a second to ensure nearly exact timing. The interceptor time of flight can be found from the analysis

90

in Chapter 2. The time of flight evaluation is the next step in the coverage determination function given in Figure 4.10.

4.4.3 Satellite Loiter Time Iteration

The hyperbolic locus allows for a transfer to a specific target location, which is identified as the point an ICBM will occupy at $T_{intercept}$. Although this point and intercept time is fixed, the interceptor time of flight needed to get there is not. If the interceptor reaches the target earlier than $T_{intercept}$, the satellite must loiter for some length of time before firing to make up the difference. The satellite will loiter in its own orbit while it is waiting to fire. During this loiter time, the satellite may float in or out of the preferred intercept environment that was previously intended. In this case, intercept availability and flight time must still be within the constraints for a feasible solution. If the interceptor continues to approach the target location more quickly than the missile, then more loiter time is required. However, if the intercept geometry becomes un-feasible or the time of flight too long, the given loiter time must be reduced. This problem lends itself nicely to a bisection approach to determining the correct satellite loiter time[‡‡]. The algorithm's solution finds the SLT needed to allow an interceptor to arrive at the same time as the ICBM. In this manner, an iterative solution to interceptor coverage is developed. The functional flow of this algorithm is represented in the coverage determination function of Figure 4.10.

Throughout many intercept simulations, the algorithm for satellite loiter time often converged very rapidly to a solution. The histogram for the number of algorithm iterations per number of intercept attempts is displayed in Figure 4.12. This figure demonstrates the quick nature of convergence for most intercept attempts. The difference between the interceptor flight time and the allowable capture time was used as an initial guess at the needed satellite loiter time. The bisection algorithm was allowed a maximum of 20 iterations. The average loiter times needed for each intercept attempt can be seen in the histogram of Figure 4.13. This figure shows that satellites often require very little

---

[‡‡] An understanding of a simple bisection approach is found in the appendix

loiter time. But, there are cases where satellites loiter for a long some time and are still able to intercept the ICBM. Note that in these scenarios the available capture time was allowed to increase up to the entire ICBM flight time. Both of these figures examined the same number of example intercept attempts, some 36,450 intercepts over six hours.
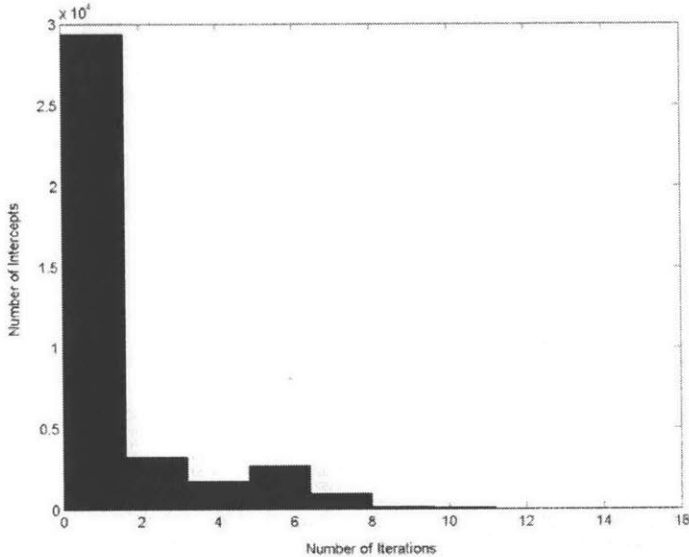
Figure 4.12: Histogram of Intercepts per Required Convergence Iterations
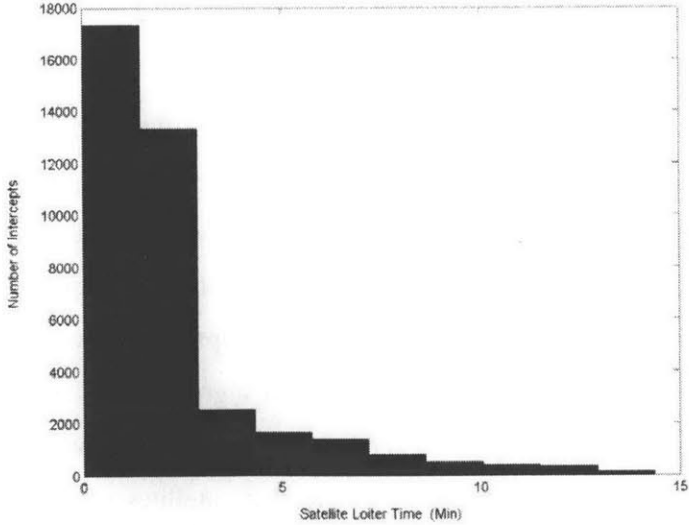
Figure 4.13: Histogram of Intercepts per Required Satellite Loiter Time

92

A continuity argument can be made for the intercept geometry during this timing problem iteration. To illustrate this geometry, it is helpful to think of a reference frame fixed to the moving satellite. A simple two-dimensional illustration is of the intercept problem from this perspective is provided in Figure 4.14. In this satellite-fixed frame, interceptor flight paths appear to emanate like a wave fronts from the satellite. These wave fronts represent the interceptor capability for a specified time of flight. An ICBM's path would follow some unknown continuous path through the intercept region. If an interceptor can reach a desired target point on the ICBM path before the interceptor would reach that same point, the satellite must loiter away some of its available capture time. The effect of loitering would be manifested as a change in the flight path of the ICBM. However, as the desired target point moves it will eventually cross an interceptor capability envelope corresponding to the remaining capture time available. Thus an interceptor could then be launched to intercept an ICBM at the precise time and location. One could make the argument that if an interceptor can initially reach the target location in less than or equal to the allotted amount of capture time, then by continuity, it is capable of intercepting the ICBM. No iteration of the exact SLT would be necessary. Implementing this course of action produced the exact same interceptor coverage results. However, this is a complicated continuity argument to justify because of the high level of dimensionality in the intercept timing problem. In any respect, the iterative method of intercept analysis provides a computationally efficient and precise method for determining the coverage capability of a satellite-based interceptor.
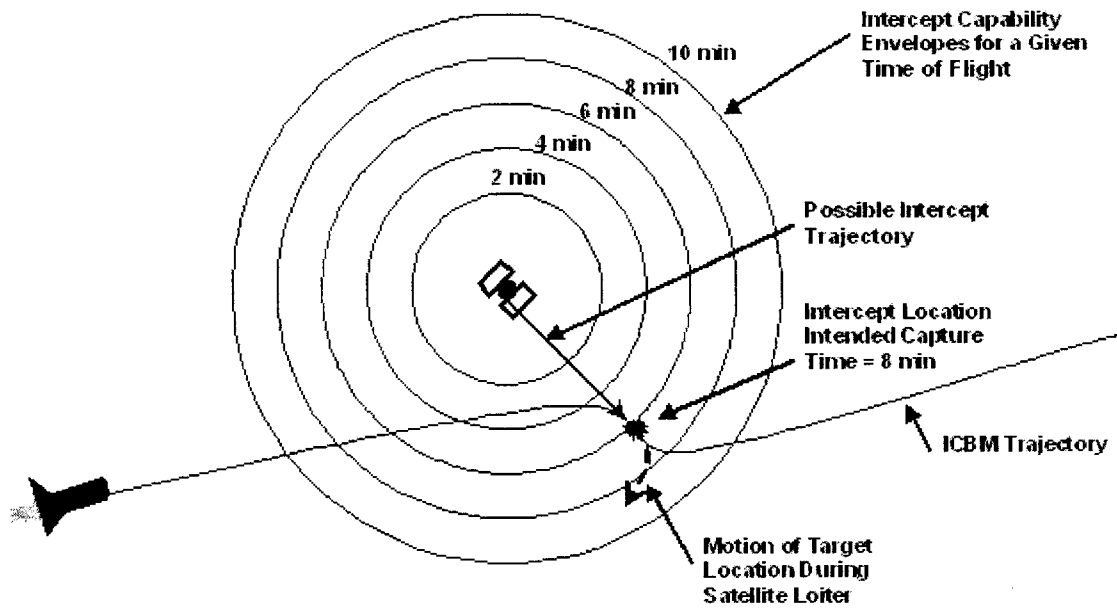
Figure 4.14: Satellite Perspective Illustration of Intercept Problem

Chapter 5

Fence Coverage Constellation Design

Pursuit of an adequate ballistic missile defense coverage definition led to a complex multi-dimensional intercept problem. The focus of this chapter is to develop satellite constellation design methods using this new coverage definition. Discussion of the coverage definition demonstrated the large range of possible intercept timing combinations. This chapter simplifies the intercept timing problem in an effort do develop constellation design methods similar to those used in classical approaches. The stated goal of this research is to develop constellations to defend the United States from a specific threat. The missile corridor encompasses the available region for intercepting ICBMs. To simplify coverage from within this corridor, the concept of a fence barrier is created. This barrier will serve as a defense shield by ensuring that all ICBMs will be intercepted, as discussed in Chapter 4, at the barrier location. The two-dimensional slice of the threat corridor creates a tractable approach to constellation design based on abstracted classical coverage methods. Many of the classical constellation design approaches, discussed throughout Chapter 3, are abstracted for missile defense purposes within this chapter. New constellation types and design methods are also created from the fence barrier approach to ballistic missile defense.

5.1 Missile Corridor Barrier

As described in detail within Chapter 4, all potential missile trajectories capable of threatening the CONUS are encapsulated in the missile corridor. To provide coverage, i.e. missile defense, a satellite-based interceptor may hit an ICBM at any point in its corridor. Dimensionality of this problem is reduced by creating an artificial barrier, or vertical slice, through the missile corridor. Specifying a desired target location in this manner fixes the capture time for each trajectory and eliminates the variability of $T_{intercept}$.

To ensure complete missile defense, satellite-based interceptors must be capable of hitting every point on the two-dimensional surface of the fence at all times. This capability ensures that no missile could sneak past the defense fence. Designing a satellite constellation with this capability is the focus of this chapter. The reduction, in the allowable intercept region within the missile corridor, means giving up opportunities to intercept at other locations in the corridor. The benefits of adding back this degree of freedom will be discussed in future chapters with reference to the volumetric coverage definition.

5.1.1 Timing and Location

The fence location was chosen to be roughly half way through the missile corridor. This location corresponds to a twelve-minute capture time for the arrival of the fist ICBM in the corridor, and a twelve-minute ICBM flight time from T_{ID}. Other ICBM trajectories will have time of flights to the fence barrier that are greater than or equal to twelve minutes. Each of these flight times relates to a unique capture time per trajectory. The orientation of the fence, at a mid-point location within the corridor, is vertical to the Earth's surface. It is fixed over one location on Earth in the ECF coordinate frame, implying that it rotates with the motion of the Earth. The location of this barrier is represented as the solid dark line in Figure 1.2 and Figure 4.1. The location of the fence was chosen for several reasons. This region of the missile corridor has the smallest cross-sectional area and is near the highest average ICBM altitude. Smaller cross-sectional areas exist at earlier points in the corridor, but these points allows less capture time. There is a design trade off on where best to position the fence for best coverage with the fewest number of satellites. This thesis is focused more on the development of a particular design methodology rather than a complete analysis of this design trade space.

The fence location was chosen at the furthest point an ICBM could traverse the corridor in twelve minutes. The convex hull of all of the trajectories at this location serves as the actual size of the coverage area. This cross-sectional area, also known as the fence, can be seen in Figure 5.1. Each point on this area represents a unique arrival time for a particular trajectory. A general feel for the size of the fence can be obtained

96

from the dimensions given on the figure. The fence is roughly rectangular being approximately 700 km tall by 1300 km wide. The figure demonstrates the relative position of the fence over the surface of Earth. As the figure also demonstrates, the fence defines the two-dimensional coverage area for missile defense from ICBMs traveling through the corridor. Unlike classical coverage areas, this area is vertical, and at an altitude of 1092 km above the surface of the Earth. The fence is located between 65.34 and 55.38 degrees North latitude and at 177.66 degrees East longitude. This places the fence at orbital altitudes and roughly over the Bering Strait.
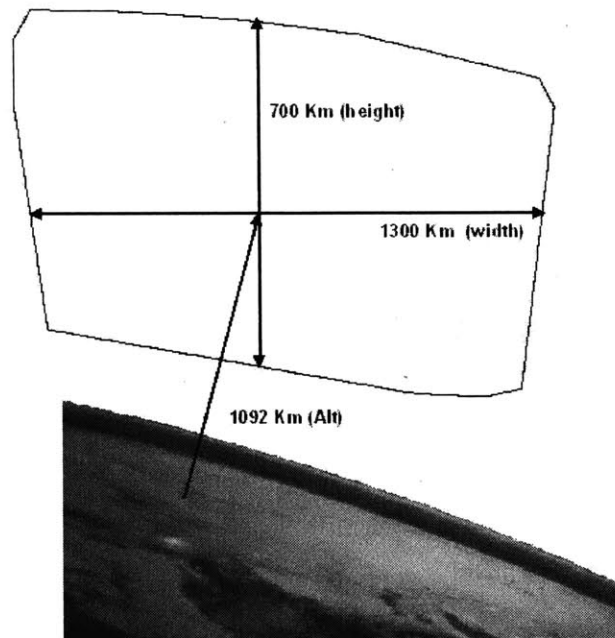
Figure 5.1: Cross-Sectional View of Vertical Fence Barrier

Guaranteed ICBM interception at this two-dimensional wall ensures 100% ballistic missile defense of CONUS from the specific (North Korean) threat. Note that every point on the fence area must be covered at every instant in time to ensure no missiles get through. This scheme allows the coverage problem to become more tractable for constellation design. It is conceptually easier to apply classical constellation design methods to the missile defense problem using this fence defense scheme. However, fence coverage does not take into account other missile interception opportunities.

5.1.2 Coverage Considerations

In the mathematical algorithm for the interceptor timing, a bisection method is used to compute the actual satellite loiter time and interceptor time of flight needed to hit the ICBM. This algorithm does not change with fence coverage. However, the outer loop for exploring all possible capture times per trajectory can be removed. The complexity of the intercept problem has been reduced to coverage of a specified set of target locations on the fence. These locations relate to a set capture time for each trajectory. Through iteration the necessary combinations of satellite loiter time and interceptor time of flight are found to ensure capture at the fence location.

5.1.2.1 Coverage Implementation

Geometrically, fence coverage can be obtained using coverage footprints similar to those of classical coverage geometries. The interceptor reachability envelope is pushed about the Earth in the direction of motion of the satellite. The intersection of the reachability envelope with the two-dimensional fence represents the interceptor coverage footprint. As the satellite moves in time, its coverage footprint on the fence will grow and shrink. One interesting aspect of coverage on the two-dimensional fence is the convex nature of the problem. At any instant when the reachability envelope intercepts the fence area a convex coverage footprint is created on the fence. Additionally, each of these convex footprints lie at the roughly the same location in the mid-point of the fence (note that this feature was built into the design of the constellation and will be discussed below.) To ensure complete coverage, every point on the fence must be covered at all times. Populating the fence area with numerous discrete points slows computation time for coverage analysis. A simplifying approximation can be made based on the geometric notion of convex sets. If only the exterior outline of the fence, since it is also a convex set, is populated with points the interior can be ignored. Due to convexity, coverage gaps in the interior of the fence, if they exist, will be apparent on the edge of the fence. On average these footprints are much larger than the fence region, and the center of the footprints is always at the mid-altitudes of the fence. This geometric understanding of satellite coverage is helpful, but geometric insight alone does not solve the problem. A

98

complete mathematical analysis is necessary to establish the precise intercept timing combination to ensure accurate coverage.

Populating the fence boundary provides a very good approximation of coverage. To test this, the coverage from several constellations was computed over both: a set of points along the exterior of the fence, and a denser set of points scattered over the entire fence area. Several constellation types were tested through the same scenario at one-minute time increments. In the test with only the exterior points, 16 points were used spread about the fence perimeter. In the denser testing analysis, 1000 points were placed randomly throughout the fence area. Several constellations were considered, all with very nearly 100% coverage using the exterior points. Of the constellations tested, only four instances in all of the constellations tested showed any discrepancies with coverage outages predicted from the exterior point's analysis. These four discrepancies each lasted one minute or less. All were outages that could have been predicted with a denser set of exterior points. An example is shown in Figure 5.2 below. In this figure, the random test points that are not covered appear as dots in the fence area. The estimated coverage loss in this example delta pattern constellation, at this instant, was 22%. The area not covered by the reachability footprint has been outlined on this figure by tracing the exterior of the not covered points. This area is a gap in coverage and was detected by the exterior point analysis. It is apparent from the figure, that the coverage gaps are the areas where the convex reachability footprints do not completely cover the fence area. Testing results demonstrate that exterior point analysis is an appropriate approximation.
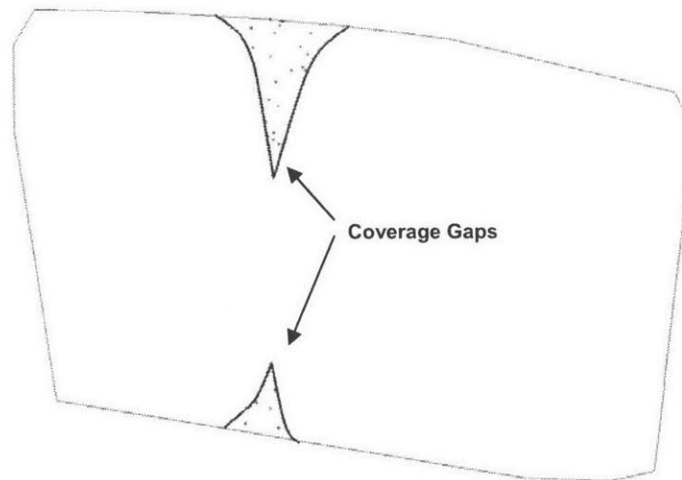
Figure 5.2: Coverage Gaps from Inadequate Reachability Footprint Overlapping

100% coverage of all the points on the fence at each instant in a simulation defines complete missile defense using the fence definition of coverage. During a simulation the satellites in a constellation configuration are propagated at some discrete time interval, usually one-minute for these research purposes. At each minute the intercept capability of each satellite is determined against each point of the fence. The number of points intercepted divided by the total number of exterior points represents the percent coverage at that instant. This percentage is stored at each time step and the simulation is progressed forward. The coverage process is repeated throughout the duration of the simulation. This whole coverage analysis and simulation process defines the complicated non-linear "function" that is constellation coverage. The general algorithmic process for fence coverage simulations, using the constellation designs developed here, will be further described in the following results chapter.

5.2 Adaptation of Classical Constellation Designs

A specific coverage location is identified with the use of the fence barrier approach to missile defense. Unlike classical constellation designs, this target area is a vertical strip suspended above a fixed geographic location. It is possible to abstract several methods of constellation design to support this coverage concept. This section

100

outlines several coverage methods classically used to create various constellation types. These coverage methods will be used to create a priori estimates of constellation configurations capable of 100% missile defense at the fence. Individual configurations, of each constellation type, are created from modified parameters of the a priori constellation designs. The methods described here are based on abstracted methods of classical two-dimensional Earth-surface coverage. A priori constellation configurations, designed in this analysis, must be modified and tweaked to obtain better actual fence coverage results from the coverage estimates of the abstracted methods. The following portions of this chapter will describe the design results of each method of constellation design.

This section explores the use of abstracted classical methods of constellation design as well as the development of new derivations to constellation designs. Most of the constellation types described here are similar to the classical constellation types with the same name. Constellations developed around the fence coverage definition will be slightly different from their classical counterparts.

Many of the first classical constellations were developed using circular orbits in highly symmetrical patterns. Later constellation designs allow for asymmetrical constellation placement and the use of eccentric orbits. The constellation development in this work will follow a similar path. Highly symmetric circular orbit constellations are developed first. These constellations are followed by other methods of constellations design focused around area specific coverage. Later, the use of genetic algorithms to construct ad-hoc constellations with very little symmetry will be explored. The use of constellations with eccentric orbits will be discussed briefly.

5.2.1 Pseudo Spherical Earth Approach

Some of the first successful classical constellation designs were developed through the use of symmetric patterns of circular orbits. As discussed in Chapter 3, these constellations were developed around circular orbit footprints on the surface of the Earth. Unlike the classical coverage definition, interceptor reachability does not leave a discernable footprint on the surface of Earth. The interceptor coverage capability is a

time-varying manifold. In order to develop constellations similar to classical designs, a pseudo spherical Earth is created. The reachability manifold from each satellite is mapped to this pseudo Earth creating a satellite footprint similar to that of classical coverage footprints. Using these pseudo footprints, constellations similar to classical constructions can be readily developed.

The shape of a reachability envelope from a satellite is similar to a cornucopia as described throughout Chapter 4. Using the notion of a fence barrier twelve minutes down range in the missile corridor, the twelve minute capture envelopes from each satellite will all share a common size and shape. The reader is directed to Figure 4.8 for a geometric view of a twelve minute reachability envelope. The pointing direction of the envelope is based on the altitude of the satellite and the direction of its motion. If all the satellites in constellation are at a common orbital altitude in circular orbits, all of the reachability envelopes will be identical and point in the direction of motion for each satellite. This feature can be exploited to develop coverage footprints on a pseudo spherical Earth at the orbital altitude. The term pseudo spherical Earth refers to an imaginary sphere with a radius identical to the orbital radius of each satellite. Therefore each satellite travels on this sphere over its entire orbit. In this manner, a two-dimensional "coverage footprint" can be traced on the sphere around each of the reachability envelopes. The effective coverage on the pseudo sphere, doted with coverage footprints, is now similar to the classical representation of coverage on the Earth's surface. For this reason the sphere at the common orbital altitude is known as the pseudo spherical Earth. The coverage footprints from each satellite and the satellite traces on this sphere are used to define an abstracted SOC method.

Coverage footprints on the pseudo spherical Earth represent only a two-dimensional portion of the reachability envelope. The interceptor capability above or below this sphere is not taken into account with the coverage footprint. Using the idea of a coverage footprint, an a priori constellation can be generated. Unfortunately, the desired coverage area of the fence is perpendicular to this pseudo sphere. For this reason, a priori constellation designs will need to be modified to ensure compete fence coverage outside of the pseudo sphere approximation. Additionally, several constellation configurations

102

will be developed and explored around the a priori constellation design. These configurations will have different numbers of orbital planes and total numbers of satellites but follow the rules for construction based on the desired constellation type. In this manner, an entire design space will be explored around each constellation type to provide a collection of configurations capable of complete missile defense.

5.2.1.1 Modified Streets of Coverage

The streets of coverage design approach allowed classical constellation designers to develop constellations based on strings of coverage footprints in an orbital trace. Classically, designers used a string of satellites in an orbital plane with connecting coverage footprints to create a common coverage area around the Earth. This idea can be seen in Figure 3.3. Using coverage footprints on the pseudo sphere, this method can also be applied to constellation design under the new coverage definition. In a similar fashion to the classical street of coverage approach, a coverage swath is laid about the pseudo-sphere with a half-width distance, C, extending on either side from the orbit trace. This represents the continuous coverage region per orbital plane. Several of these streets from additional orbital planes can by overlaid on the Earth until the desired coverage results and a constellation are developed.

The intersection of the interceptor reachability envelopes with this pseudo sphere is a two-dimensional surface. This surface, or "coverage footprint", looks very much like an ice cream cone (as apposed to the classical circular coverage footprint.) The approximate dimension for the Earth central angle along the length of the cone is 40.34 degrees, with a width at the widest point of 13.14 degrees (for a twelve minute reachability envelope.) Placing several satellite coverage footprints in one orbital plane, an abstracted street of coverage can be created. This abstracted street of coverage, depicted in Figure 5.3, allows for an a priori constellation design using some of the same methods as classical designs.

103
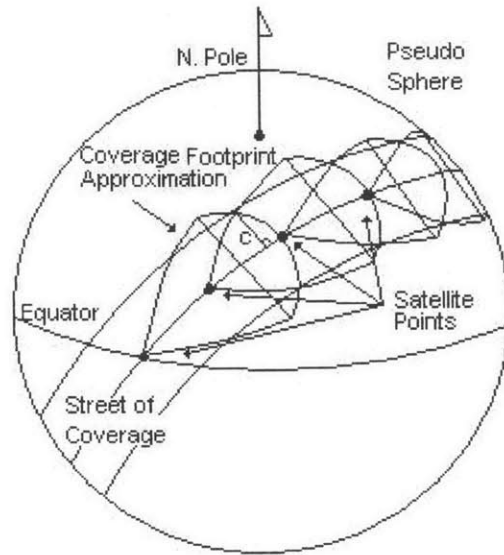
Figure 5.3: Pseudo Streets of Coverage Approach

5.2.1.2 Star Pattern Approach

The star pattern is a simple constellation to construct and a good starting point for the abstracted streets of coverage approach to constellation design. Star pattern constellations only need a set number of parameters to completely describe the arrangement of satellites. The number of parameters is independent of the total number of satellites actually in the pattern. A benefit to the star pattern constellation type is that it will provide 100% coverage from either pole to a specific latitude. Generally fewer numbers of satellites are needed in star patterns to provide coverage above a specified latitude. Since the fence coverage area is in the upper northern latitudes, this research only seeks coverage over these latitudes.

The star pattern is created by arranging a fixed number of planes, each having an identical number of satellites, semi-symmetrically about the equator. This results in all the orbital planes having a common intersection point at either pole. An example of a star pattern was depicted in Figure 3.4. To develop a constellation with the new coverage definition, circular coverage footprints are replaced with the ice-cream cone shaped footprints on a pseudo sphere. The Δ parameter serves as the common street of coverage

104

half-width, depicted as C in Figure 5.3. Ψ is the maximum half with of a cone, roughly 6.57 degrees for a twelve minute envelope. The number of planes (P) necessary to extend coverage from the pole to some specified latitude (λ) can be found from Equation (3.2)[7]. In this abstraction, the Δ and Ψ parameters of the new reachability footprint are simply applied to the same classical equation. The desired latitude of coverage in this case only needs to extend down far enough to cover the fence latitude. The lower latitude of the fence, as mentioned previously, is 55.38 degrees. With these parameters and Equation (3.2), an a priori constellation configuration was generated using thirteen planes with eleven satellites per plane, or 143 total satellites, for complete fence coverage on the pseudo sphere.

The a priori constellation from Equation (3.2) assumes that all the satellites in one hemisphere are traveling in the same direction, i.e. north to south. In this way, there are only two orbital planes that will see satellites traveling in opposite directions. Adjacent orbits traveling in the same direction can be partially phased with one another. Walker's inter-plane phasing parameter, F, is not used in the classical streets of coverage approach. However, it is useful with the new coverage paradigm. Adjusting the parameter F allows the coverage lobes for each street to mesh like gears, filling coverage gaps in three dimensions. The F parameter affects the amount of Δ available in the design of star patterns for a given number of planes. While not originally used in the streets of coverage formulations, this parameter will be used in both the star and delta pattern constellation designs to find the best phasing for better coverage results.

A constellation configuration for a star pattern is given by a set number of planes and satellites per plane. The a priori constellation configuration developed is based on the two-dimensional pseudo sphere coverage abstraction. The parameters F and Δ are both adjustable measures for ensuring that orbital planes are close enough together to provide coverage to the desired latitude. Both of these parameters directly affect the spacing of the orbital planes about the Equator. The parameters: F, Δ, and common orbital altitude (h) must be adjusted to provide the optimal coverage results for each configuration. Additional configurations with varying numbers of planes and satellites per plane must be explored around this estimate to find constellations actually capable of 100% fence

105

coverage. Note that optimizing about the design parameters F, and Δ, and not constraining the integrality of the results, will cause constellations to slightly lose some of their original symmetry.

By running simulations for a little over twelve hours in simulation time, the Earth will rotate underneath half of the constellation. This will allow the fence coverage area to see all parts of the constellation, and not allow the optimization to drive to constellation away from continuous coverage configurations. Because of the nature of the coverage function, the nonlinear optimization package SNOPT was used to tweak the allowable constellation parameters to maximize the percent coverage during the simulation. SNOPT allows a user to input partial derivatives to a nonlinear function when they are available[20]. However, the coverage function is not a simple function for which partial derivatives can be easily obtained. For this reason, the finite-differencing capability of SNOPT is employed to compute partial derivatives of the simulation coverage function. The potential for the optimizer to fall into a local minimum was always apparent. For this reason, the optimization was run for several test cases with differing initial starting conditions. It was made apparent by this analysis that the a priori estimates were often the best starting points for continued optimization. In general, optimization of this sort proved quite effective in enhancing the coverage of a priori constellation designs. A more detailed discussion of optimization and the SNOPT package used is found in Appendix 1.

5.2.1.3 Delta Pattern Approach

Star patterns are a variant of the delta pattern with specified polar inclinations for all satellites in the constellation. For this reason, the delta pattern designs appear very similar to those of the star pattern designs with the flexibility of common inclinations other than 90 degrees. The use of the abstracted streets of coverage method is again an integral part of delta pattern design. In keeping with classical delta pattern design, constellations in this work will be identified by Walker's three parameters: the total number of satellites (T), the number of orbital planes (P), and the inter-plane satellites phasing parameter (F). With Walker's three parameters, one can quickly establish the placement of each satellite in a delta pattern. Orbital planes in this constellation type now

106

have many crossing points. This makes delta patterns better suited for lower to mid-latitude coverage. This research develops the delta pattern by adapting the streets of coverage meshes approach shown in Chapter 3 and used by Rider[44].

The reader is reminded that a mesh is an area enclosed by the orbital traces. The notion of meshes is illustrated in Figure 3.5 and discussed in greater detail in Chapter 3. Meshes are numbered by m, where $m = 0$ indicates a polar region. Larger values of m indicate the number of different orbital traces that cross above the mesh. There may be many of these meshes in a constellation.

While this constellation design method is capable of defining the constellation configuration needed to cover any mesh, only the meshes in the region of the fence must be considered. In this way, fewer total satellites will be required for fence coverage versus whole-Earth coverage. Since the fence resides in a high latitude band, at a specific longitude, the coverage can be tailored for that region. Constellations developed in this manner will provide similar effective coverage at any longitude over an entire latitude zone. Equation (3.3) and (3.4), previously used in Rider's determination of constellation coverage, will be selectively used to provide coverage in only the meshes of interest. In this way, an a priori constellation can be developed around complete coverage of the fence using the new coverage footprints.

It was apparent to Rider and others, that satellites with inclinations near the latitude of the desired coverage area will have the greatest opportunity for sustained coverage periods[23],[44]. Equations (5.1) and (5.2) describe the lower and upper bound on the streets of coverage crossing points[44]. Equation (5.1) is the lower latitude bound (ϕ_p) of the $m = 0$ crossing point as illustrated in Figure 3.5. Equation (5.2) is the upper latitude bound (ϕ_h) for the $m = 2$ crossing point. An ideal inclination (i) to achieve complete mesh coverage can be found by combining Equations (5.1) and (5.2). The ideal inclination is given in Equation (5.3). The unknown parameter in this equation is the number of planes in the constellation (P). However, this parameter is specified for each constellation configuration. The C parameter serves as the common street of coverage half-width, as depicted in Figure 5.3. This parameter for coverage swath half-width can

then be directly solved for from either Equation (5.1) or (5.2). In this manner, complete coverage can be achieved as long as $m = 1$ is always completely filled by the surrounding streets of coverage. Equation (5.4) is used to ensure that the $m = 1$ is completely covered given an ideal i and C with some number of planes, P.

$$\sin(C) = \sin(\phi_p)\cos(i) - \cos(\phi_p)\sin(i)\cos(\pi / P) \tag{5.1}$$

$$\sin(C) = \cos(\phi_h)\sin(i)\cos(\pi / P) - \sin(\phi_h)\cos(i) \tag{5.2}$$

$$\tan(i) = \frac{\sin(\phi_h) + \sin(\phi_p)}{\left(\cos(\phi_h) + \cos(\phi_p)\right)\cos(\pi / P)} \tag{5.3}$$

$$\sin(C) = \frac{\sin^2(\pi / P)\sin(i)\cos(i)}{\sqrt{\cos^2(i) + \cos^4(\pi / P)\sin^2(i)}} \tag{5.4}$$

Constellation configurations capable of 100% coverage, by meeting these abstracted coverage requirements, can now be established. The P and T parameters define the initial constellation configuration. In an effort to explore various constellation configurations, the number of planes were varied from 2-200. At a minimum, eight planes are necessary to provide complete coverage over the latitude zone with an ideal inclination of 62.27 degrees. As the number of planes increases, the ideal inclination tends toward the central latitude, between the upper and lower bounds of the fence, at 60.36 degrees. During these calculations the required C, to ensure complete $m=1$ coverage, varied from 4.68 degrees to 4.98 degrees. Each of these values is well within Ψ, the maximum half-width of the interceptor reachability coverage footprint of 6.57 degrees. This implies that an a priori delta constellation can be developed using the mesh coverage abstraction. Such an a priori constellation configuration will be the stepping off point for further optimization.

Optimization is necessary to tweak the constellations to provide three-dimensional coverage from the two-dimensional coverage estimation. Similar to the star pattern, mesh coverage with streets of coverage approach does not account for inter-plane

108

satellite phasing between orbital planes. However, the parameter F will be included here in an effort to enhance coverage by meshing the footprint lobes. Using the inter-plane satellite phasing parameter (F), the inclination (i), and the altitude (h) as optimization parameters, any delta pattern configuration can be optimized to maximize interceptor coverage. The total number of satellites in a constellation configuration was limited to around 200 satellites for this exploration. Only constellations that provided at least 90% coverage are reported in this work. In the initial delta pattern analysis, between 6 and 27 orbital planes were considered, with each plane containing an equal number of satellites. Using these bounds a great many configurations were explored around the a priori configuration estimate.

Because F is allowed to be a non-integer, the constellation periodicity is not readily apparent. The first and last satellites in the constellation are not phased in the same way as the remaining satellites. In order to ensure continuous constellation coverage it is necessary to understand the repeat periodicity of the delta pattern. Both Figure 3.7 and Figure 5.4 below, show how delta patterns develop a polygon shaped mesh ($m = 0$) over the North Pole[§§]. This polygon has the same number of curved sides as planes in the constellation. The pattern will repeat itself once two vertices, or peaks, have passed over the same point on Earth. The coverage area will see the same coverage just mirrored once it passes the trough of a side. The troughs of these patterns occur at the mid-point to each side of the polygon. Figure 5.5 depicts the simulation time needed for a ground point to view the constellation from peak to peak and from peak to trough. This figure was created by comparing the J_2 perturbation rate of the ascending node with the rotation rate of the target site over Earth. While this does not encompass the full repeat cycle due to the broken symmetry, the fundamental nature is captured. Approximately twice this repeat pattern period is used in the analysis to optimize coverage simulations.

[§§] Interceptor reachability envelopes with twelve-minute capture times are shown in this figure extending from each satellite. This graphic has the effect of showing the street of coverage of each orbital plane.
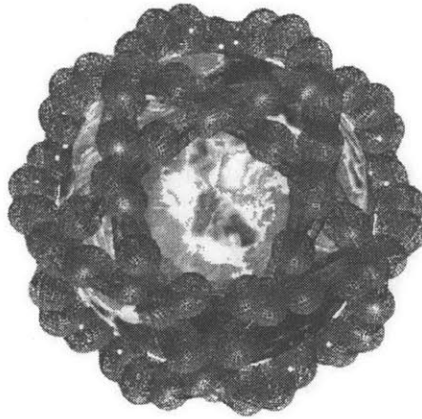
Figure 5.4: Five Plane Delta Pattern, *m* = 0 Polygon View
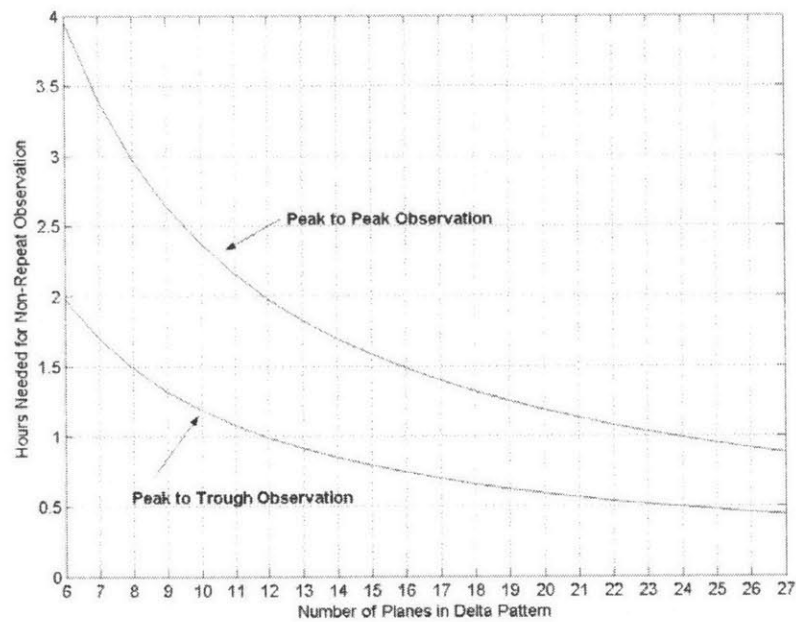
Figure 5.5: Walker Delta Pattern Repeat Observation Times

5.2.2 Single Satellite-per-Plane Approach

A noticeable trend emerged throughout this analysis and exploration around the a priori constellation configuration of the delta pattern. The actual results of the analysis of the delta pattern will be discussed in the following chapter; however the trend of the

110

solutions will be mentioned here. In delta pattern configurations with an equal number of total satellites, configurations with more planes often had noticeably better coverage. This is very similar to the results Walker and others noticed for area specific coverage in their constellation coverage analysis[52],[23]. Some of the best coverage results, with the fewest number of satellites, often come from constellations with a single satellite-per-plane. This configuration layout has the effect of braking down some of the inner symmetry apparent in delta patterns and the street of coverage method. The same three parameter scheme is used to construct these constellations with the number of planes equal to the total number of satellites, $P = T$.

While single satellite-per-plane constellations are simply a sub-set of the delta pattern, in this research they are studied apart from the delta pattern. This distinction is due in part to the fact that there is not a good understanding of how to create an a priori constellation. There is no longer a discernable street of coverage with one satellite per orbital plane. The constellation relies heavily on a good inter-plane satellite phasing to place satellite from several planes in the area of interest. Results generally show that constellations which place several interceptor reachability envelopes on the fence area at any one time provide better coverage results. For this exploration, the same design parameters: (i), (F), and (h) were allowed to vary. Equation (5.3) can be used, in the same fashion as in the delta pattern analysis, to obtain an approximation for the ideal inclination. As will be discussed in the results section, the value of F for each configuration was obtained through several gradient based optimization attempts using the SNOPT toolbox. Picking the appropriate starting F for optimization required several attempts to avoid sub-optimal local minima. Through this detailed search procedure, one satellite-per-plane constellations also appear to provide the best missile defense coverage results with the fewest total numbers of satellites.

5.2.3 Timeline Optimization Approach

One of the most beneficial aspects of single satellite-per-plane constellation is its ability to slightly break the symmetries apparent in the delta and star patterns. The ability to break from a symmetrical design allows a constellation designer more freedom in the

111

type of orbit used. One more recent constellation design method deals with the use of coverage timelines from repeat ground track orbits[23],[37]. This allows for a much greater freedom of design; however more variables are required to describe the complete arrangement of satellites in a constellation. Simple three-variable representations for constellations will not suffice. Additionally another, more accurate, abstraction of constellation design must be applied beyond the streets of coverage method.

Repeat ground tracks are very desirable for area specific coverage because the ground track is guaranteed to follow the same path over on the ground day-after-day***. This method has the distinct feature that constellations can be constructed without any apparent symmetry other than the desire repeat cycle. The first step in this type of classical constellation design required that the coverage capability of different orbits be pre-analyzed. In classical timeline optimized constellation design, a satellite was allowed to orbit for its repeat cycle, commonly some number of orbits per Earth revolution. The time and duration of any observations of a particular ground site were recorded for a specific orbit inclination. In this manner, each orbit inclination has a specific timeline for ground site observations. The classical method of timeline optimized design takes these timelines and builds a constellation to obtain the desired coverage results. The classical approach to this method is described in greater detail in Chapter 3. However no work, as known by this author, was done to develop a constellation for continuous coverage based on this method. The drawback to using repeat ground track orbits is that they must have a specified semi-major axis if the eccentricity is fixed. To simplify the variability of this design the eccentricity will be set to zero. This simplification will be removed later.

To abstract the timeline optimized constellation design method for fence coverage a circular repeat ground track was found that nearly matched the desired mid-fence altitude. The repeat ground track of 27 orbits for every two Earth revolutions was chosen because it has the shortest repeat time, two Earth revolutions, with an altitude within 74 km of the desired fence altitude. The ground track of a 27/2 repeat cycle orbit can be seen

---

*** The usefulness and method of construction for a repeat ground track orbit is described in more detail in Chapter 2.

in Figure 2.8. As this figure illustrates a repeat ground track of a particular inclination will traverse much of the Earth in 27 orbits. After the coverage analysis of each orbit, constellation design becomes a matter arranging the ground tracks to provide continuous fence coverage.

5.2.3.1 Timeline Analysis

Timelines for repeat ground tracks are easily produced; however, using the coverage method to optimize the timelines and create a constellation a harder task. Timeline analysis per orbit was performed by initializing a satellite at a longitude of the ascending node (Ω) from 0 to 45 degrees, at half degree increments, and at an inclination (i) from 50 to 130 degrees at half degree increments. Varying inclinations leads to slight changes in the semi-major axis to ensure the same repeat cycle. Inclinations outside of this range provide no coverage of the fence area. A satellite was propagated forward two full days to acquire a complete repeat ground track timeline from each orbit initialization. Creating timelines for coverage of each point on the exterior of the fence, the approximate coverage over the whole fence can be determined. The time of day and duration of fence coverage for each inclination, at zero degrees longitude of the ascending node, is shown Figure 5.6. Timelines, represented in this figure, are vertical strips starting near the inclination designation and continuing upward over the two-day interval. The horizontal bars, common across sets of timelines, are indicative of the orbital period of each orbit. Some of the coverage spikes, indicated by the slightly darker shaded dots, reach 100% coverage. This figure is very similar to that created for classical designs seen in Figure 3.10; however Figure 5.6 covers a larger range of inclinations for a longer time period. The coverage in most timelines does not reach 100% during every observation. This lack of coverage capability is further illustrated in the accompanying 3-dimensional graph of Figure 5.7. This figure represents the same data as in Figure 5.6, however the vertical axis represents the percent fence coverage during each observation. No information is given in either of these figures about where on the fence the partial coverage is located.
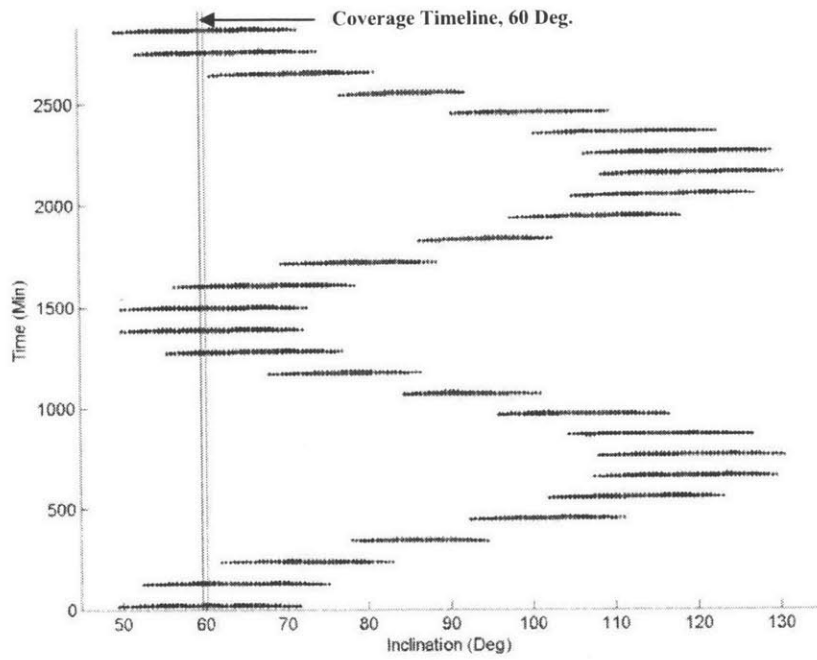
Figure 5.6: Two-day Coverage Timelines for all Applicable Inclinations
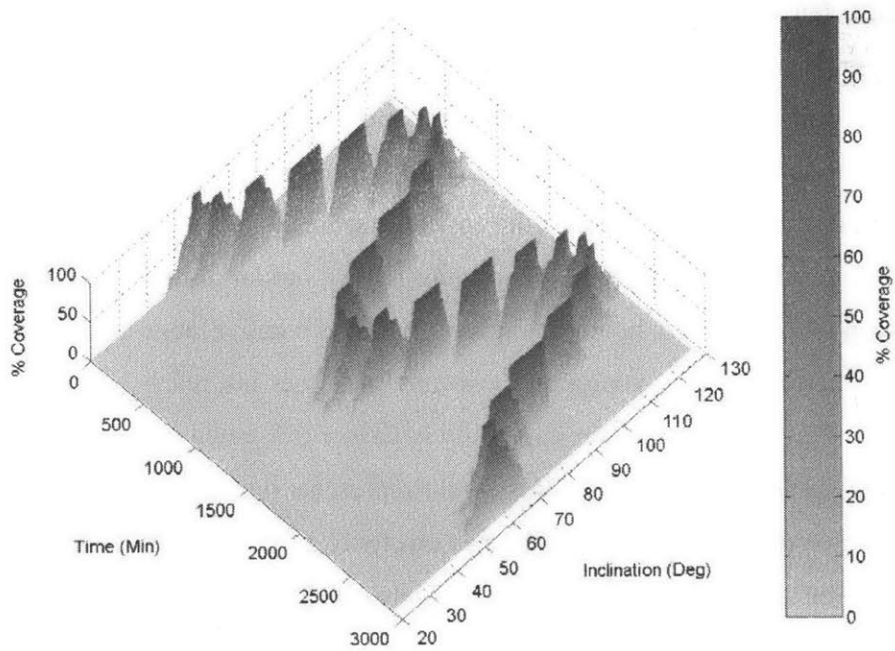
Figure 5.7: Two-day Coverage Timelines Showing Partial Coverage

114

Several facts of coverage can be gained from the timeline analysis for implementation in constellation design. The 100% coverage durations along each timeline ranged from a single minute, at lower inclinations, to seven minutes at inclinations around 90 degrees. If only the 100% coverage time segments were used in a greedy algorithm approach at adding together timelines, nearly 200+ satellites are needed to create a constellation for continuous 100% coverage over two days[†††]. If partial coverage durations are factored into the total coverage time per inclination, higher inclinations approached 17 total minutes of partial coverage at a maximum. This maximum was reached at an inclination of 89 degrees. If the total partial coverage time is factored in, 169+ satellites would now be required from greedy algorithm approximation. This shows that there is greater potential for fewer satellites in a constellation if partial coverage is used in the design.

Preliminary analysis indicates that there is a trade space between coverage duration and inclination. As shown in Figure 5.6, lower inclinations have many more coverage opportunities. These opportunities are shorter in duration than those near polar orbits having fewer total opportunities. This analysis done in this research extends farther than classical examples by allowing for retrograde orbits and additional longitudes of the ascending node. The longitude of the ascending node range is roughly equivalent to the angle between three consecutive ascending node crossings over the equator. With this range all possible coverage variations can be thoroughly explored. Classical methods of this type did not look at the effect of varying the initial longitude of the ascending node. The net affect of this extra analysis is negligible for single point observations. For the new definition of coverage over the fence area, many different longitude placements will allow orbits to see different parts of the fence at different times. Constellations can be pieced together from partial coverage results. As satellite timelines are chosen, a satellite can be placed at any point in its timeline. This ability allows constellation designs using either common or multiple inclinations. The next step in the design process involves intelligently selecting which orbit timeline to use, and where in that timeline to start a particular satellite.

[†††] The methods and purposes of a greedy algorithm approach to optimization can be found in Appendix I.

5.2.3.2 Constellation Development

Creating a working constellation from the coverage timeline analysis is the next step in the timeline optimized constellation design process. Fence coverage is more complex than the visual coverage used in classical timeline analysis. For this reason, simple classical sorting algorithms are insufficient to create a constellation based on partial fence coverage timelines. In this research, a genetic algorithm package is used to place timelines of a particular inclination, longitude of the ascending node, and at precisely the right starting time. The package used in this research was developed in the Automatic Control and Systems Engineering Department of Sheffield University, UK[‡‡‡]. Details of the functionality and uses of genetic algorithm optimization can be found in Appendix 1.

A drawback to the use of a genetic algorithm for this purpose is the run time needed for simulations of an entire a population of constellation arrangements. Constellations in this analysis need only be observed for their repeat cycle, i.e. two-days. The total percent coverage of the fence area by a constellation was used as the fitness level to evaluate particular individuals. To improve the speed of a simulation a discrete binary analysis of each fence point was used on a one-minute interval. A binary value of one indicates no interceptor coverage of that fence point at that time. Each of the 16 fence pointes were initialized with an array of ones for each of the 2880 minutes of a two-day simulation. Full fence coverage at some time is obtained when the sum of the values for all 16 binary values add to zero. 100% simulation coverage means that there are no ones within the 46080 binary values. An analogy of this binary process can be imagined with a bowling lane filled with 16 pins across and 2880 pins deep. The goal for complete coverage is to simply knock over all the pins. The bowling ball represents a satellite's intercept capability as it moves in and out of range over the course of two-days. Using the genetic algorithm, a collection timelines can be arranged and overlaid to ensure complete coverage over the whole two-day simulation. The genetic algorithm optimization for timeline placement is not constrained to the same symmetric satellite arrangement of

---

‡‡‡ The source code for this genetic algorithm package is freely distributed on the internet[18].

116

previous design methods. In this manner, an asymmetric constellation of repeat ground track orbits can be constructed for fence coverage missile defense.

5.2.4 Repeat Delta Pattern Approach

Results, given in the following chapter, illustrate that timeline optimized constellations generally have worse coverage capabilities than single satellite-per-plane constellations of the same number of satellites. One of the most beneficial aspects of the one satellite-per-plane constellations is their ability to break apparent symmetries of delta pattern constellations. An important lesson learned from the results of the previous constellation designs is that some symmetry can be beneficial to the coverage. Symmetry in timeline optimized constellations is difficult to create with a random arrangement of satellites. It is also more difficult to launch a large number of satellites into precisely timed and completely different orbits, than it is to send the same number of satellites into commonly inclined symmetric orbits. Both symmetric and timeline optimized methods have their own unique benefits within constellation design. Thus a new constellation design method can be created by combining these strengths.

Applying the symmetry of a delta pattern and the repeat ground track orbit of the timeline optimized method, the repeat delta pattern constellation can be created. This design uses only one common ground track and symmetrically places a given number of satellites along the ground track. While the constellation is not a true delta pattern, Walker also attempted to develop delta patterns with the repeat ground track feature[52]. However, Walker's work was based solely on the two-body motion and spherical trigonometry. When these designs were tested by the author, the constellations did not maintain a repeat ground track under J_2 perturbations. In this work, each satellite comprising the repeat delta pattern constellation will have its own orbital plane. All of the orbital planes will share the common characteristics of: inclination, semi-major axis, and eccentricity. The phasing angle of each satellite, and thus the true anomaly, is precisely described to ensure that it will follow a common ground track. Once again the 27/2 repeat ground track was chosen for the repeat cycle for the constellation. A circular orbit with this repeat pattern will have a semi-major axis very close to the mid-altitude of the fence.

Describing the constellation in this manner defines a strict symmetry along a common repeat ground track. Placing satellites back to back to provide a continuous street of coverage would require approximately 412 satellites. However, taking a lesson from the single satellite-per-plane results, evenly distributing satellites along the same ground track can achieve the same coverage results for the higher latitudes where many of the orbit traces cross. The goal is similar to filling in the first mesh with coverage from different orbital traces. Unfortunately the phasing parameter is no longer a free variable to manipulate due to the repeat nature of the ground track. The benefit to this pattern is that a portion of the constellation, with good coverage from crossing orbital traces, can be fixed over the fence location.

5.2.4.1 Constellation Development

The following section describes the mathematical method of developing a repeat delta pattern constellation. Equation (5.5) must be used to place longitudes of the ascending nodes from each consecutive satellite into the same ground track taking into account orbital perturbations. Much like a delta pattern, many orbital elements of each satellite are common throughout the constellation. Only the true anomaly (v) and the longitude of the ascending node (Ω_n) are different from satellite to satellite. The subscript n, in Equation (5.5), refers to the sequential satellite number, i.e. $n = 1...T$. The true anomaly separation angle between satellites is specified as 9720 degrees divided by the total number of satellites in the constellation. This separation angle places the satellites evenly over a 27/2 ground track. The node rate ($\dot{\Omega}$) is determined from the J_2 dynamics as described in Chapter 2. Note that $\omega_\oplus$ is the rotation rate of the Earth.

$$\Omega_n = (\dot{\Omega} - \omega_\oplus)\left(\frac{2\pi * 27 * (n-1)}{v * T}\right) \qquad (5.5)$$

Each satellite in the constellation follows the same ground track but resides in its own unique orbital plane. A benefit to this constellation type is the ease of its design and construction. Only two design variables remain for optimization once the total number of satellites and the repeat cycle are established: the common inclination (i), and the starting

118

longitude of the ascending node (Ω_i) (Note that the semi-major axis is dependent on the inclination to maintain the repeat ground track.) The nonlinear optimization package SNOPT was used to optimize these design parameters. Simulations of this constellation type must be run over the full two-day time period to see all parts of the constellation. The simulation configuration and design results follow in the next chapter. This design scheme was founded on the idea that it would use the best of several methods in designing constellations for area specific coverage. A fixed ground track together with a bit of symmetry is created in an effort to provide fence coverage with fewer numbers of total satellites needed.

5.3 Constellations for Coverage Gap Filling

Throughout the design, construction, and testing phases of the above mentioned constellation designs, a method was created for enhancing the coverage results of constellations not quite capable of 100% coverage. The constellation gap filling idea involves intelligently placing additional, non-symmetric, satellites into an existing constellation to fill any existing coverage gaps. The goal of this method is to use a few additional satellites to bring a constellation configuration up to 100% coverage.

To properly fill the coverage in a constellation, it is necessary to determine the repeat pattern of coverage outages. In the case of the repeat delta and timeline optimization constellations, these patterns repeat with a two-day cycle. Outages patterns within the star and delta patterns varied with the configuration of the constellation. Through inspection, it was observed that their coverage outages also appeared on a one- to two-day repeat cycle. Since this is not a constellation design method, test cases of less than 100% coverage are used to investigate the method of constellation gap filling.

5.3.1 Satellite Placement for Coverage Filling

The process of filling the coverage gaps in a constellation has three parts. The first part is simply determining the patterns of coverage outages over the course of a constellation's repeat cycle. To accomplish this, a matrix of binary points was created

119

representing each exterior fence point at each minute. This approach is identical to the coverage timeline determination process used for the timeline optimization method. The next step of this process involves identifying the coverage timelines for every available orbit. This process was also completed earlier for the 27/2 repeat ground track orbits, see section 5.2.3.1 . The third part of this design involves taking the coverage timelines from available orbits and matching them to the coverage outages of the original constellation. Again, this process is similar to the genetic algorithm timeline sorting process used for constructing timeline optimized constellations.

Going back to the analogy of the bowling lane filled with pins, where pins represent points of the fence without interceptor coverage. The original constellation is capable of knocking down several of these pins leaving only isolated pins placed sporadically throughout the lane. Each orbit has its own specific path through the lane, and may or may not be capable of knocking over some of the remaining pins. At this point, a genetic algorithm is used to pick which orbit timeline to use to best knock down as many pins as possible. One interesting note on this process is that genetic algorithm is capable of filling coverage gaps with the timelines from several obits at once, or gradually filling coverage with single orbit timelines. In this analysis both approaches were explored. The genetic algorithm optimization was first used in a greedy algorithm fashion. The optimization algorithm was allowed to randomly select the timeline to best remove as many coverage gaps as possible. As the algorithm reaches convergence, there may still be some coverage outages from the original constellation plus the new satellite. In this fashion, orbits are added one at a time until complete 100% fence coverage is achieved. The use of a genetic algorithm in a greedy manner allowed for a faster determination of an approximate number of satellites needed for constellation gap filling. Additional genetic algorithm runs, optimizing several orbit timelines at once, may help to decrease this total number of additional satellites needed. While not a complete constellation design method, this procedure completes coverage in otherwise deficient constellations. The resulting constellations achieve complete fence coverage but lack coherent design structure due to the random orbit placement.

120

5.4 Eccentric Orbit Modifications

Constellation design methods, abstracted from classical methods, are only a starting point for additional constellation design approaches using the new coverage definition. Star, delta, one satellite-per-plane, timeline optimized, and repeat delta pattern constellation types are identical to or abstracted from classical methods. However, these constellations are still limited to only using simple circular orbits. Circular orbits are good for ensuring constant coverage footprints in the classical coverage method. The next step in the constellation design process is determining what missile defense coverage improvements can be made by adding eccentricity to existing constellations.

Eccentricity has the potential to open up the constellation design space. Only a very few classical methods incorporate eccentricity into constellation design[14]. Orbits in a constellation type shared many common orbital elements. One orbital element that is common to all of the above mentioned constellations is zero eccentricity. Circular orbits are simple to work with because mean anomaly is the same as true anomaly, and iteration using Kepler's equation is not required for orbit propagation. However, there are also some enticing benefits in the use of eccentric orbits. Eccentric orbits allow satellites, evenly spaced in mean anomaly in a common orbit, to congregate around apogee were the relative velocities are slower. The size and shape of reachability envelopes vary, since the satellite speed is slower at apogee. Varying the eccentricity of an orbit allows for a selection of the drift rates in perigee and ascending node locations, even while maintaining the same inclination.

As a side focus, this research explores the use of eccentric orbit modifications to developed constellations. Adding eccentricity allows several design parameters to be variable within a constellation. In addition to semi-major axis, inclination, and starting longitude of the ascending node; the constellation design process can now allow for a variable argument of perigee and eccentricity. To maintain the symmetry of a constellation, both eccentricity and argument of perigee must be common to all satellites in the constellation. The reason for this constraint in individual satellite freedom comes from the desire to keep constellation cohesion. Constellation cohesion refers to the

121

symmetric placement of satellites in a particular phasing at particular longitudes of the ascending node. Previously developed symmetric constellations generally experience J_2 perturbations equally among all satellites in the constellation. Common geo-potential perturbations cause shifts in all of the orbits of a constellation equally[§§§]. Allowing all the design variables to be common will have the same cohesion effect on eccentric orbit constellations.

The procedure for designing constellation with eccentric orbit modifications involves adding the new design inputs to the optimization, used to develop the previous circular-orbit constellations. Several initial values of eccentricity were explored for each constellation type. With this new design freedom, constellations from previous circular orbit designs are adapted to take advantage of any possible eccentric orbit benefits. The design results of eccentric orbit modifications can be found in the following chapter.

5.4.1 Constellation Design Extensions

Eccentric orbit modifications are a jumping off point into satellite arrangements within a constellation. Constellations developed in this chapter are built for missile intercept and focused around fence coverage. Abstractions of several classical coverage methods were used to develop many classical constellation types and design modifications. Optimization schemes discussed in this chapter are used to further tweak and modify constellation parameters to obtain the greatest coverage results per configuration. Large numbers of configurations from each constellation type are developed to present a picture of that constellation type's coverage capability. The reader should note that there may be better ways of constellation design for fence coverage that were not conceived of in this research. Coverage results of the constellations developed here, as well as the gap filling and eccentric orbit modification results are given in the following chapter. Many additional approaches to classical constellation design are given in the reference section of this paper. The reader is encouraged to further explore these possibilities.

[§§§] This assumption is not accurate when dealing with higher order, and third-body perturbations. Such affects on constellation cohesion will be discussed in the concluding chapter of this work.

As a side note to the development of this chapter, additional constellation design schemes also showed promise for creating constellations capable of fence coverage. Some of the more intriguing ideas for constellation design, not explored in this research, involve mixed integer programming, ergotic analysis, and all variable designs with genetic algorithms. The very nature of building a constellation for fence coverage has discrete characteristics. A mixed integer program might be capable of capturing the mechanics of orbital motion and interceptor coverage to develop a working constellation. The objective function should maximize coverage over the scenario. The orbital motion of satellites and interceptor flight are dynamic constraints. The total number of satellites in a constellation could either serve as another constraint or possibly an additional objective function. In this case, 100% coverage would be a constraint. Near random placement of satellites by an integer program or even a genetic algorithm may provide a foundation for an ergotic analysis of constellation coverage. This analysis explores the time-invariant coverage capability from the semi-random passes of satellites[36].

Recent design work has employed genetic algorithms to obtain optimal constellations. A fully variable genetic algorithm design was examined for this research. In this algorithm all orbital elements from each satellite were allowed to vary. Each orbital element was varied within specified bounds. Constellations in this scheme had $6*T$ total variables. This many variables resulted in slow computations of coverage. If a repeat ground track orbital constraint was not specified, there is no way of determining the length of the repeat cycle and thus the length of the coverage simulations. Techniques used in classical approaches to genetic algorithm were applied as illustrated[16],[17],[19],[33]. For convenience a 27/2 repeat ground track was specified to remove one variable per satellite and fix the simulation time.

[This Page Intentionally Left Blank]

Chapter 6

Fence Coverage Design Results

The purpose of this chapter is to present the design and simulation results of constellation design for ballistic missile intercept using the fence barrier definition of coverage. The process of space-based constellation design begins with the understating of missile defense, astrodynamics, constellation design, and interceptor coverage. These concepts can be strung together into a defense system using the constellation design abstractions developed in the previous chapter. This chapter will determine the effectiveness of the design methods for maximizing missile defense coverage at the fence boundary. The methods and processes involved in this work are the framework for space-based missile intercept constellations.

The work of this thesis is intended to be a realistic approximation of the general design process and not an in-depth analysis into every aspect of ballistic missile intercept. More accurate analysis and design methods can be developed from this work. With that being said, the results presented here maybe subject to small errors due to discrete time step approximations and incomplete orbital perturbation models of orbital motion. The results presented here pertain only to those constellation designs developed in the previous chapters. It is possible that alternative constellation types or configurations, beyond the extensive study involved here, could provide better coverage results. The results presented here provide an extensive examination of satellite based missile defense using the fence definition of coverage.

6.1 General Simulation Design Process

This section describes the general design, optimization, and simulation processes used for generating coverage results. The code compiled for this research was developed

using Matlab$^{\circledR}$. The upper level algorithmic flow of the constellation design process has three parts: 1) a priori constellation development, 2) constellation type initialization, and 3) configuration optimizations. The functional algorithms used to establish coverage, and to optimize configurations will also be discussed in this section.

6.1.1 Constellation Design Process

Due to the complex nature of the constellation coverage function, constellation design is not complete with an a priori estimate. Additional levels of refinement are required to ensure the best possible coverage for a given constellation type and configuration. The a priori constellation estimate is based on the abstracted methods described in the previous chapter. Constellation type initialization is the next step in the constellation design process. In this step, the common semi-major axis design parameter is optimized, holding all other parameters to their a priori values. This optimized semi-major axis remains fixed for the remainder of the design process. Due to scaling, interceptor coverage is very sensitive to this value. Solving for the optimal semi-major axis together with other design parameters led to poor performance. Incorrect variations in the semi-major axis that are too big or too small often resulted in a locally flat region of zero percent coverage. In retrospect, it was observed that this optimum constellation semi-major axis varied only slightly from the a priori estimate. Post-optimization of this parameter also resulted in little to no change. However, not all constellations require an initial optimization of the semi-major axis. Constellations with repeat ground tracks employed a defined semi-major axis. Eccentric orbit modifications to constellations allowed this parameter to vary during the optimization of the other design parameters because the effects were not as dramatic.

Having derived an optimum semi-major axis, constellation configuration optimization continues by adjusting parameters such as: inclination, inter-plane satellite phasing, and/or initial longitude of the ascending node to maximize coverage. Either a non-linear programming package or a genetic algorithm was used to optimize these parameters. In the case of the non-linear programming package, partial derivatives of the simulation coverage were approximated by the software using finite numerical

126

differencing. The optimization processes of these two programs are developed in greater detail in Appendix 1. The starting points for parameter optimization were based on the a priori estimate. Initial values from other points, in the allowable design range, were also used to restart this design process. The reason for the additional design runs is to ensure that the maximum global constellation coverage is obtained and not a local coverage maxima. Once the design parameters are established a final simulation run was created to develop the coverage results for that optimized constellation.

6.1.2 Simulation Process

The percent coverage that a constellation is capable of achieving is a complex function. This function is based on a discrete number of satellites attempting continuous fence coverage over some period of time. The length of the simulations are based on the constellation type, and established to show coverage over a complete repeat cycle. The top level algorithmic process for the coverage computation is given in Figure 6.1. A generic constellation design will be used to demonstrate the algorithm behind the simulation process. The simulation inputs and outputs are noted by the blocks without backgrounds. Matlab® functions are given by blocks with lightly shaded backgrounds. The inputs consist of: the configuration parameters, the allowable design parameters (using the process described in the previous section), and the fixed simulation inputs. The simulation input values are fixed for the series of optimizations under a constellation type. These can be adapted for constellation design about a different objective or with different capabilities. The state building function for a particular type is based on the design methods of Chapter 5. The constellation is propagated in its orbit based on the orbital dynamics of Chapter 2. Finally, the coverage at some particular time is determined by the interceptor coverage determination function. The functional coverage determination algorithm can be found in Figure 4.10. Looping through the entire simulation time at a given step-size, fence coverage for the whole simulation is established. The results of this process were plotted as needed.
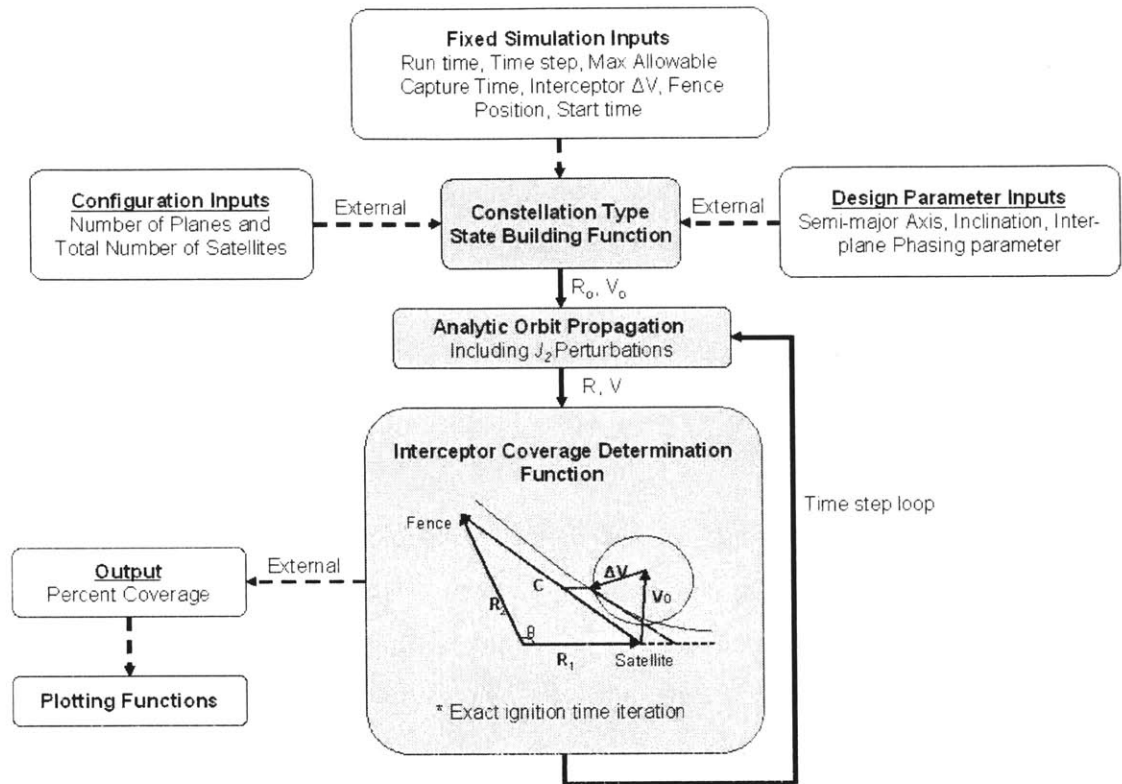
Figure 6.1: Algorithmic Flow Diagram of the Coverage Determination Simulation

The coverage determination simulation is the basic element of constellation design. As discussed earlier, the constellation design process requires the use of an optimization tool package to tweak the simulation design parameter inputs. A set of Matlab® functions were created to interface with either the SNOPT non-linear programming package or the Genetic algorithm package. Both of the optimization packages could be directly interfaced with the coverage simulation described above. The goal of either package was to maximize constellation coverage for each configuration. A generic functional block diagram of the SNOPT non-linear programming optimization process is given in Figure 6.2. Again the input and output from this algorithm are given by blocks with un-shaded backgrounds. In this process, a user defined SNOPT setup function was used as an interface with the package. This function takes in the constellation type and the individual configuration parameters to be explored, and passes the data to SNOPT. This function also defines the available design parameters and their allowable ranges. SNOPT properties, such as convergence and finite differencing

128

tolerances, are also assigned in this command function. The SNOPT package itself takes the configuration and the design parameters and passes them to the coverage determination simulation function. The resulting percent coverage output is fed back to SNOPT to tweak the design parameters for maximum coverage. A priori constellations with 100% coverage are not modified from the a priori design parameters. This process was sometimes prone to designing constellations with less than optimal coverage results. This was often due to the initial conditions and the parameter step-size selected by the software. Note that coverage is a zero-one condition, where small changes in design parameters may not have any effect on coverage estimates. While this process did not always provide the best optimal coverage parameters, it did provide a very good approximation with better constellation coverage results. Several runs starting from different initial conditions helped to enhance the results and design parameter selection. After the optimization process, SNOPT passes back the optimal design parameters and coverage results to the user defined setup function.
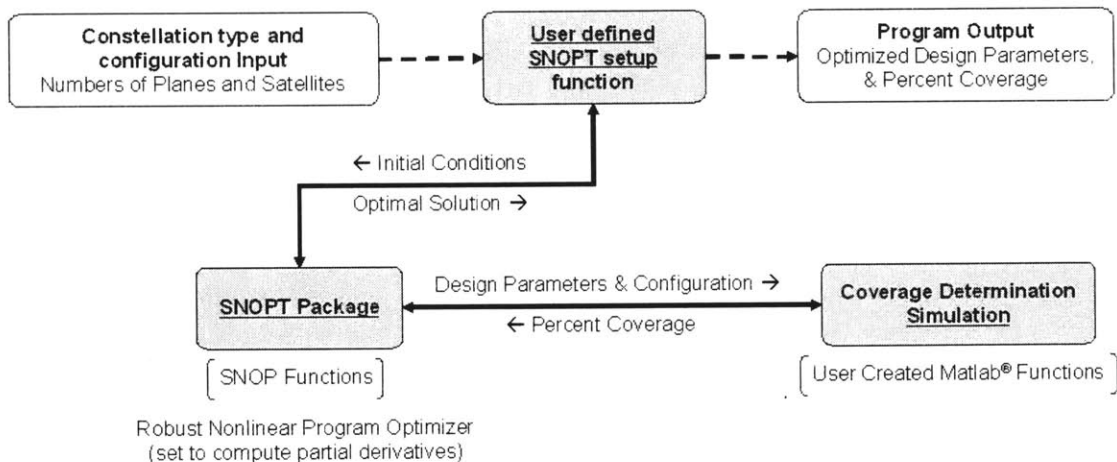
Figure 6.2: Typical SNOPT Constellation Design Optimization Functional Flow

The genetic algorithm optimization package was also used to obtain optimal constellation design results. Using a genetic algorithm varied significantly from the SNOPT design process. An example of the top-level genetic algorithm functional flow is given in Figure 6.3. The genetic algorithm requires a large set of initial inputs. However, the only specification on a constellation configuration comes in the form of the total

129

number of satellites to be used. Other constellation design parameters are randomly chosen, within a stipulated range, for each member in a population. The number of constellations in a population and the number of generations were also initialization parameters to the algorithm. In this figure, the lower blocks are those used by the genetic algorithm package. The genetic algorithm checks the fitness of each member of the population, each constellation, by calling a constellation fitness function. This function is similar to the coverage determination function except, that it uses precompiled coverage timelines, from multiple runs of the coverage determination function. This segment contains many data sets like those shown in Figure 5.6 and Figure 5.7. The genetic algorithm specifies which individual satellite timelines to use and how to place them together. The purpose of this function is to piece together the timelines calculate the percent coverage. The best constellation coverage results and design parameters are passed back to the genetic algorithm and to the output. The genetic algorithm then ranks all of the constellations in a population to determine the fittest members. Much like the natural evolutionary process, the fittest members are mated and reproduce constellation offspring for the next generation population. In this manner, the best constellation configuration is produced from randomization without a need for partial derivatives. The genetic algorithm process is further detailed in Appendix 1.
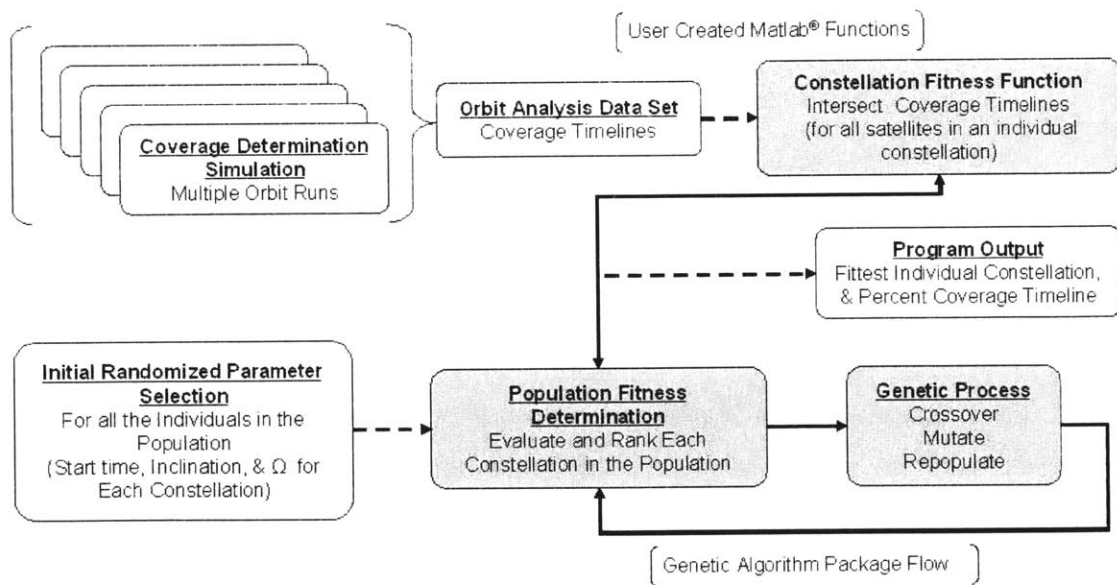
Figure 6.3: Typical Genetic Algorithm Constellation Design Functional Flow

130

6.2 Simplified Non-Rotating Earth Design

The first attempt at any sort of constellation design for fence coverage used a non-rotating Earth approximation. This approximation is not realistic but, it allowed for a general understanding of satellite placement for missile defense. The fixed-Earth scenario provides as a lower bound on the total number of satellites for 100% fence coverage. In this scenario, only one orbital plane was used. The initial design parameters were the common semi-major axis, inclination, and longitude of the ascending node. Mid-fence altitude (plus the radius of the Earth) was selected as the a priori semi-major axis value. Two a priori estimates were created for the inclination. The first was an inclination of 60 degrees placing the highest ground track latitude of the plane in the middle of the fence. The second estimate for an inclination was 90 degrees, a polar orbit. The initial longitude of the ascending node was placed to ensure the orbit trace went through the fence area. Using the design process described in the last section, SNOPT was used to tweak these parameters to achieve the best coverage for a non-rotating Earth constellation. SNOPT was also used in another fashion for this analysis. 100% coverage was set as an optimization constraint and the total number of satellites, symmetrically placed in an orbital plane, was the minimization objective. This is the only time this optimization scheme could be applied due to the complex configurations of constellations for actual rotating Earth coverage.

Results of this analysis found that eleven satellites in one plane was the minimum total number of satellites needed for 100% fence coverage. This small number of satellites is based on the use of twelve-minute capture times over a fixed-Earth. A visual depiction of the relative placement of each satellite in the plane and their reachability envelopes was created from a set of Matlab® plotting functions developed by the author. This depiction can be seen in Figure 6.4. The fence area cannot be seen in this figure because it is entirely contained within the reachability envelope of a satellite. The general fence location is in the upper right side of the figure, over the Bering Strait. The optimal semi-major axis was found to be 7470.3535 km at an inclination of 88.96 degrees. The longitude of the ascending node was initially set to zero degrees and was not modified.

Figure 6.4: Simple Non-Rotating Earth Constellation

The non-rotating Earth constellation, while not realistic, suggests an altitude for good circular orbit coverage. Throughout this investigation, the common semi-major axis for circular orbit constellations did not vary much from this initial approximation. This semi-major axis value allows the reachability envelopes to encapsulate the fence area for the longest view period. These results indicate the potential of using polar orbits for actual constellation design. These results were also a successful test of the optimization scheme. Earth rotation makes ballistic missile defense a much more challenging problem, and is included in the remainder of this thesis.

6.3 Star Pattern Constellations

The first constellation design scheme to be investigated focuses around the abstraction of Walker's star pattern. In this constellation type, all orbits are circular and share a common polar inclination. Satellites are placed evenly among all the planes of the constellation, and the planes are spaced symmetrically about the equator. Only the inter-plane phasing parameter, F, and the Δ parameter are adjusted given a specific configuration, i.e. total number of planes and total number of satellites. The a priori estimate for a constellation, developed from the abstraction in Chapter 5, called for thirteen planes with eleven satellites per plane, or 143 total satellites. The F parameter

132

was initially estimated to be 0.2274. The Δ parameter was initially estimated to be 2.2923 degrees. The semi-major axis was set to the optimal non-rotating Earth value. This a priori constellation will serve as the basis for further star pattern exploration.

6.3.1 Simulation Design

Using the coverage function described earlier, coverage results of the a priori constellation over the twelve-hour simulation resulted in 93.53% fence coverage. This value is very low as was expected from the initial abstraction. Recalling that parameter optimization is a two-step process, SNOPT is employed first to adjust the initial semi-major axis for the constellation. In this case, the value did not change from the fixed Earth results, 7470.3535 km. The next step in the constellation design process calls for the a priori estimate to be optimized around the design parameters, F and Δ, to maximize coverage. The result of optimization of the design parameters reveals that the optimal fence coverage from the a priori configuration is 98.3703%. This is an improvement of 4.837%. The final values of the F and Δ parameters were 0.5610 and 1.4027 degrees respectively. The SNOPT design optimization process proved to be effective at reorganizing the constellation to maximize the coverage.

6.3.2 Constellation Design Space Results

The previous a priori star pattern constellation configuration did not reach 100% coverage after optimizing its design parameters. Configurations around this design were tested to determine the configuration with the fewest number of total satellites capable of 100% coverage. The a priori optimization illustrated the need for more satellites per plane or more total planes. The non-rotating Earth scenario illustrated that at least eleven satellites per plane are need to ensure a complete street of coverage. The number of planes and satellite per plane were limited to a range from 11 to 19. These limits allowed the total number of satellites to vary from 121 to 361 satellites. This configuration design space was parametrically tested and optimized using the scheme devised earlier. The constellation coverage results are shown in Figure 6.5. Eleven planes did not establish 100% coverage even with 19 satellites per plane. Thirteen planes with fourteen satellites

133

per plane, or 182 total satellites, proved to be the smallest configuration capable of complete coverage. The optimal values of the F and Δ parameters for this configuration were 0.4614 and 0.0284 degrees respectively. The coverage result of this constellation is identified as the best configuration in Figure 6.5. In general, configurations on the border of the 100% coverage plateau will provide complete coverage with the fewest number of total satellites. The optimal constellation is relatively close in configuration to the a priori estimation. This is because they both used thirteen orbital planes; to ensure complete coverage far more than the estimated numbers of satellites per plane were needed.
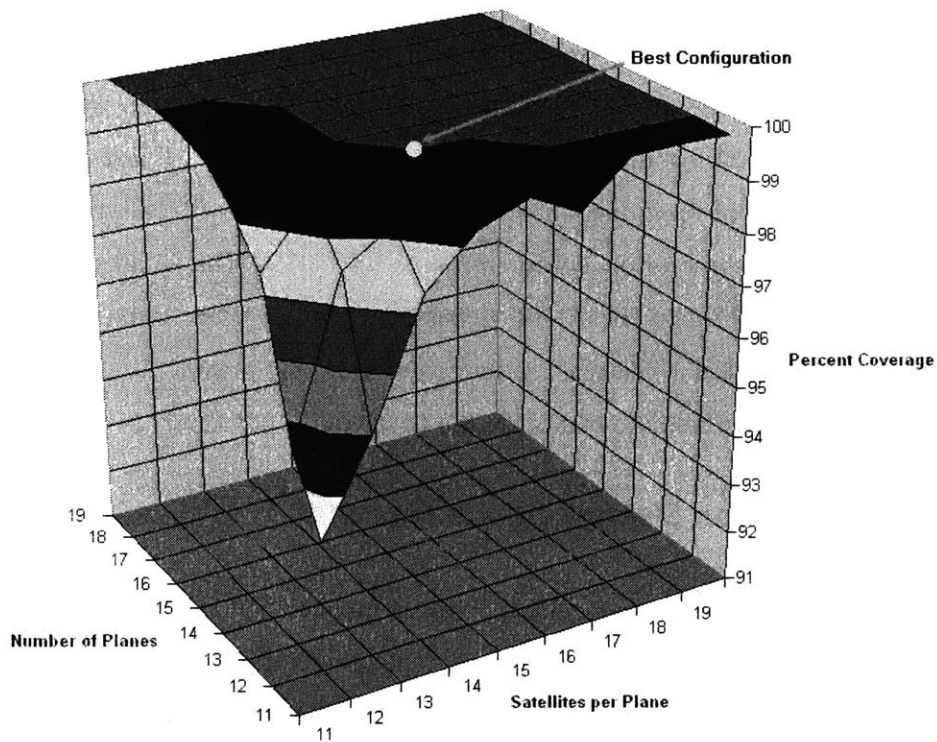
Figure 6.5: Design Results for the Star Pattern Constellation Type

The star pattern constellation type is not efficient for area specific coverage. However, it is capable of defense over the entire polar region down to the lowest fence latitude. Thus any missile launched over the polar region has a high probability of being intercepted. An accurately scaled representation of the optimal constellation can be seen in Figure 6.6. Reachability envelopes from each satellite in the constellation appear to

134

blanket Earth with coverage. This figure shows that the constellation is also capable of providing significant partial coverage to many other parts of the world. A drawback to the implementation of such a constellation is the sheer number of satellites required. It should be noted that if less than complete coverage is acceptable, 99% coverage requires 154 satellites. Other constellation types will be given to lower the total number of satellites required for missile defense.
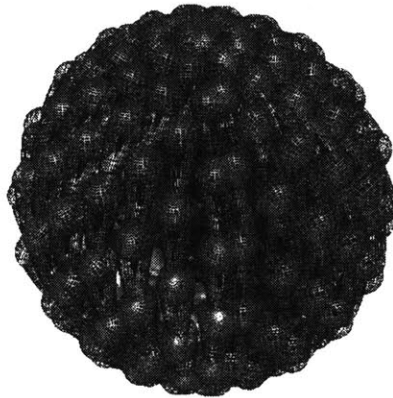
Figure 6.6: Optimal Star Pattern Constellation

6.4 Walker Delta Pattern Constellations

The Walker delta pattern constellation is commonly developed for Earth coverage. This constellation, simply an extension of the star pattern, was applied to missile defense coverage. Walker used the P, T, and F parameters to define a delta pattern configuration. Only P and T will be used here to define a configuration since F is one of the design parameters. F can not be initially determined from the mesh coverage abstraction. An a priori constellation was constructed from the coverage abstraction method described in Chapter 5. The a priori constellation configuration called for eight orbital planes with 16 satellites per plane, or 128 total satellites. The semi-major axis was initially set to the optimal fix-Earth result. The initial inclination was chosen to be 62.27 degrees from Equation (5.3) for the ideal inclination with an eight plane constellation.

The F parameter was set to one initially. Constellation design, optimization, and coverage determination of the delta pattern was very similar to the analysis used for star patterns.

6.4.1 Simulation Design

As expected, the two-dimensional coverage abstraction did not produce an a priori constellation capable of 100% coverage. The a priori configuration, $T=128$ and $P=8$, delta pattern provided 99.0677% fence coverage. This was improved by optimization to 99.9309%, a difference of only 0.8632 percent. These results were from a six hour simulation. After applying SNOPT for optimization the initial semi-major axis for the constellation type was determined to be 7470.3535 km. Again, this value did not change from the fixed Earth results for the decimal results given here. The optimized value of the F was 2.86. This value served to best mesh reachability envelopes for better fence coverage results. The optimized inclination was found to be 62.67 degrees. This value was only 0.4 degrees greater than that predicted for the idea eight-plane inclination. A parametric analysis of the surrounding configurations is again required to obtain an understanding of the delta pattern capability, and to find a configuration capable of 100% coverage.

6.4.2 Constellation Design Space Results

Optimizing the design parameters of inter-plane satellite phasing (F), and the inclination (i), many delta pattern configurations were developed. The goal of this exploration was to discover feasible (i.e. 100% interceptor coverage) constellations. Only constellations that provided at least 90% coverage are reported in this thesis. Between 6 and 27 orbital planes were considered. The number of satellites per plane was restricted within a range from 4 to 22 satellites. The optimized coverage results for the delta-pattern design space are given in Figure 6.7. A six hour simulation time span was used as a standard for all the constellations of this type. This was determined earlier to be roughly twice the required observation time for peak to peak repeatability of the smallest configuration. Both the $P=7$, $T=126$ and $P=21$, $T=126$ configurations were found to provide complete coverage with the fewest total number of satellites. These constellations

136

are designated on Figure 6.7. The optimal inclination and F of the $P=7$ configuration were 62.64 degrees and 2.484 respectively. The inclination and F of the $P=21$ configuration were 64.23 degrees and 3.208 respectively. These results show that there are multiple constellations achieving 100% coverage. These results also show that there is a large 100% coverage design region to allow exploration of other constellation design elements. The choice of which constellation to employ can be based on other considerations such as: launch costs or sparing. Additional constellation design elements will be discussed in the concluding chapter of this thesis. Regions with either 100% capability or less than 85% capability are also identified on the figure. As a note, 99% coverage can be obtained with a constellation of only 98 satellites.
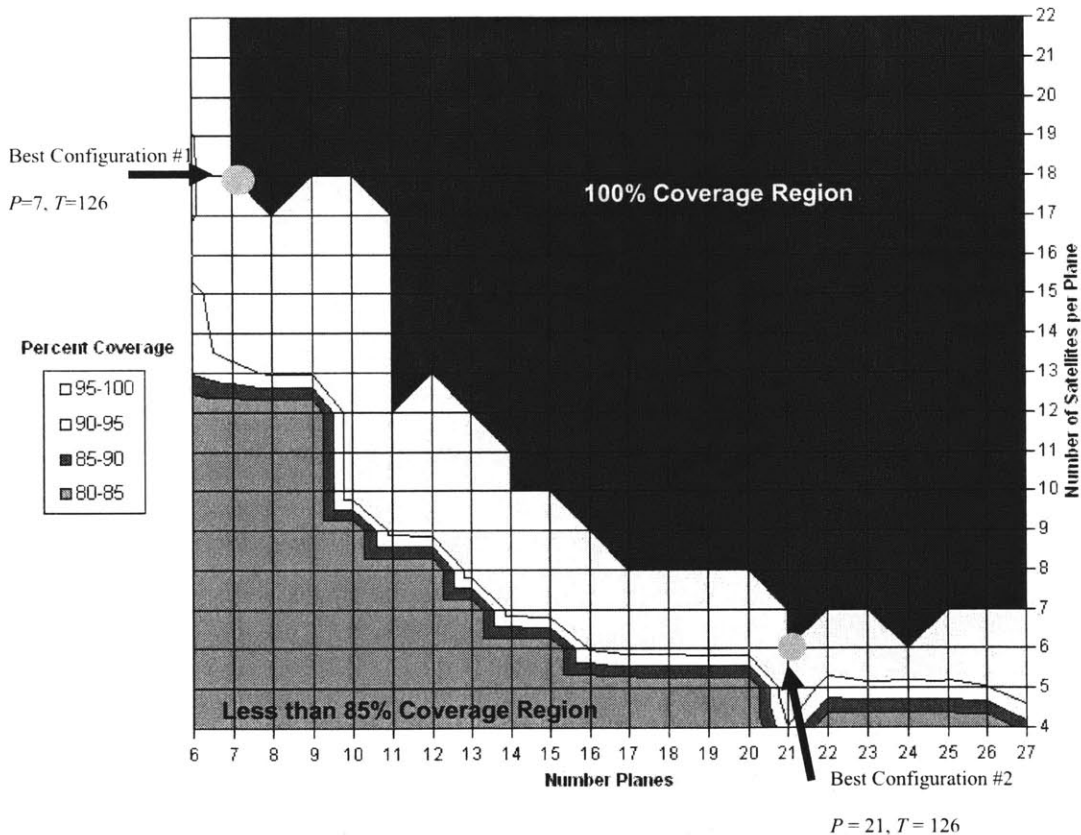
Figure 6.7: Design Results for the Delta Pattern Constellation Type

Inclinations for all cases tended to increase as the total number of planes increased. The values of F varied from 2.27 to 4.21 in the optimum results. This

constellation type relies on complete zonal coverage between the fence latitude bounds. This appears as a ring of 100% coverage at the fence latitudes over the Northern and Southern hemispheres. This band of latitude is highlighted on the $P=7$ configuration in Figure 6.8. The view point of this figure, as well as many of the other constellation representations in this thesis, is shown looking down at the approximate location of the fence over the Bering Strait. It is apparent from this figure that complete coverage can be obtained with fewer total satellites using proper meshing of reachability envelopes. In general, delta pattern constellation types appear to provide better coverage, for a given number of satellites, than other constellation types.
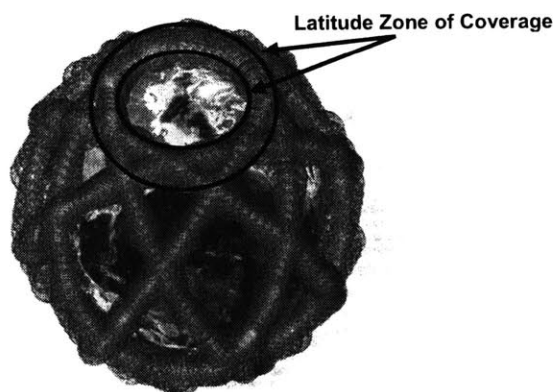
Figure 6.8: Optimal Delta Pattern Constellation with Zonal Coverage

In testing the 100% coverage results well beyond the time span used for optimization, it was observed that there could be coverage drops. This occurs only for "extreme" configurations, i.e., the boundary of 100% coverage plateau shown in Figure 6.7. The interior region of the 100% covered constellations does not appear to exhibit this "flaw". Certain measures and constellation modifications will be developed in the following sections to help fix such coverage drops.

6.5   Single Satellite-per-Plane Constellations

During the analysis and exploration with the delta pattern constellation configurations, a notable trend emerged. For the same number of satellites, constellations

with more planes often had noticeably better coverage. This is similar to the results Walker and others noticed for area specific coverage in classical applications[23],[52]. This trend is visible in Figure 6.7. Using a single satellite-per-plane configuration has the effect of breaking down some inner symmetry apparent in delta patterns. As mentioned in Chapter 5, the single satellite-per-plane constellation type is a specific case of the delta pattern constellation type. The restriction to one satellite per plane has the effect of limiting the configuration design space. No a priori design parameters were established other than to use the ideal inclination for the total number of planes in a configuration. The fixed-Earth scenario was used an approximate starting semi-major axis. Analysis of this single satellite-per-plane constellation type proceeded over a large range of configurations to identify any trends in coverage results.

6.5.1 Constellation Design Space Results

To explore the single satellite-per-plane design space, only an exploration of the total number of planes is required. The semi-major axis for the constellation type was optimized with SNOPT from the non-rotating Earth value. No change in semi-major axis was found to produce more favorable coverage results. For this exploration the same design parameters of i and F were allowed to vary. An F of about 4 was found to be the best starting value for optimization. However, the final value varied wildly with each configuration after optimization. Several initializing values of F were attempts for each configuration to avoid small local coverage maximums to reach the global maximum. The design space was limited to constellations with greater than 90% coverage.

The optimization results for this constellation type, with one satellite per plane, can be found in Figure 6.9. As seen in this figure, the percent coverage per constellation varied dramatically with the number of satellites. However, the general trend showed improved coverage with an increased number of planes and thus total number of satellites. A trend line has been overlaid on the data in the figure. It is apparent from the results that the last several percentage point improvements come at a significant cost in the required number of satellites. The smallest configuration capable of 100% fence coverage employed 116 satellites. The optimal inclination and F of this configuration

139

were 63.41 degrees and 6.485 respectively. A graphical representation of the constellation can be seen in Figure 6.10. Note that 91% coverage could be achieved with only 69 satellites. The graphical representation of this smaller constellation can be seen in Figure 6.11.
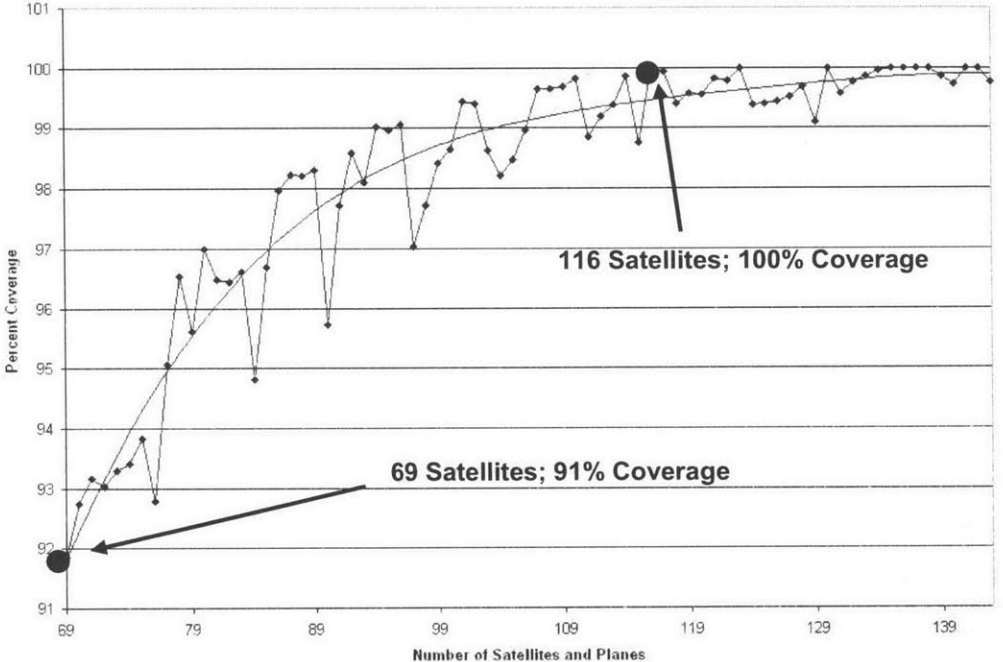
Figure 6.9: Design Results for the Single Satellite-per-Plane Constellation Type
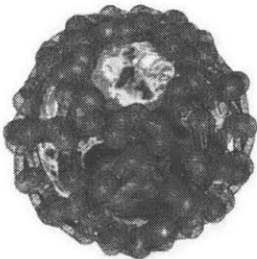
Figure 6.10: Best 116-Satellite Constellation
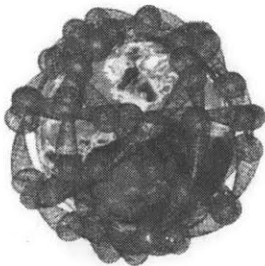
Figure 6.11: 91%, 69-Satellite Constellation

The one satellite-per-plane constellation proved to be the most efficient constellation type for fence coverage. This constellation type obtains 100% coverage with fewer satellites than any other constellation type analyzed. With 116 satellites, a 66 satellite improvement is exhibited over the best star pattern configuration. Because this constellation type is really a sub-set of the delta pattern, these constellations also provide latitude bounded coverage capabilities. This zonal coverage characteristic is apparent in both figures. The one satellite-per-plane constellation design abandons the streets of coverage design abstraction; however it allows for much improved coverage capabilities.

6.6 Timeline Optimized Constellations

Another more recent constellation design method that can be applied to the new coverage definition deals with the use of coverage timelines[23],[37]. As discussed in Chapter 5, these designs monitor the coverage at a particular location as a satellite is allowed to orbit over a repeat ground track. In Chapter 5, a data set was built with the coverage time and duration of the fence. This analysis included orbits from several inclinations with several different starting ascending node longitudes. A repeat pattern with a ratio of 27 orbit to every 2 Earth revolutions, 27/2, was used because it placed the semi-major axis approximately 74 km away from the optimal size found in other constellation design results. The results for fence coverage over all inclinations at one longitude of the ascending node can be seen in Figure 5.6 and Figure 5.7. In the classical approach, a sorting algorithm was used to piece satellites into a constellation based on the maximum revisit time over a particular location. This method is similar to a greedy algorithm approach. However no classical work was found that developed constellations for continuous coverage.

6.6.1 Simulation Design

Constellation design using coverage timelines requires a different method of optimization. Because all of the coverage data has been pre-calculated, a sorting algorithm is needed to appropriately layer the timelines from each satellite in a constellation and determine total coverage. A genetic algorithm package was used for this

141

purpose. This algorithmic design process was discussed in the first section of this chapter and can be seen in Figure 6.3. In this analysis, a population of constellations is generated. Each constellation is comprised of a fixed number of satellites. Each satellite in the constellation has three parameters to describe which precompiled timeline to use. The inclination (i), the initial longitude of the ascending node (Ω), and the starting point on the timeline comprise the individual design parameters per satellite. Inclination varied from 50-130 degrees at half-degree increments. Ω varied from 0-45 degrees at half-degree increments. The starting point time varied from 0-2 days at one-minute increments. These parameters are generated randomly, within their constraints, by the genetic algorithm. The constellation individual is comprised of the design parameters of each satellite stacked and converted into a binary string.

The number of individuals per population was tested between 100 and 200 constellations. The maximum generation of the algorithm was limited from 5,000 to 100,000 depending on the test. Fitness of each individual constellation was tested with a defined timeline function. This function generated a timeline of available fence observation times. Individual timelines were compiled on a master coverage timeline. Once coverage from all the satellites had been computed, the function would determine the percentage of the fence not covered for the entire scenario. This value determined the fitness of the individual. Once fitness of all constellations has been determined, the best coverage constellation results were saved and the genetic algorithm produced the next generation of constellations.

In another approach, a greedy algorithm was used in conjunction with the genetic algorithm. In these cases, the same general process as defined above was used to generate a small constellation. After the best constellation was produced from coverage convergence, single satellite coverage timelines were added, one-by-one, until 100% total coverage was achieve. This method served as a good estimation for the total number of satellites to use in a complete genetic algorithm approach.

142

6.6.2 Constellation Design Results

This complex timeline sorting approach was computationally intensive and slow to obtain results. Because of the random nature of a genetic algorithm, no initial a priori is required. The first approach to this problem simply started with a set number of satellites and let the algorithm optimize the whole constellation for the best coverage. This method was computationally demanding. The greedy algorithm approach to constellation design proved to be more efficient. Because satellite timelines only needed to be optimized over the remaining coverage gaps from the previous constellations, satellites were individually added until a complete constellation was developed. This method was significantly faster than optimizing all the satellites in a constellation at the same time. With either approach, the resulting constellations are highly asymmetric. Often each satellite has its own orbital plane apart from any other satellite in the constellation.

Using the basic genetic algorithm approach, several sets of design runs were accomplished with different numbers of satellites. The convergence of a 100 satellite constellation can be seen in Figure 6.12, as a function of the best fitness level per generation. These results show that all the fence area is left without coverage for roughly 1000 minutes. This number is the sum of the amount of time each fence point goes without coverage. This gives the constellation a total of 99.66% fence coverage over the two-day scenario. However, it should also be noted that after 100,000 generations this approach was only able to improve the fence coverage to 900 minutes of coverage outages. A graphical depiction of the 100 satellite constellation can be seen in Figure 6.13. This figure illustrates the magnitude of random satellite placement from timeline optimization. No apparent order or understanding can be gained from the arrangement of satellites in this constellation to improve future designs.

143
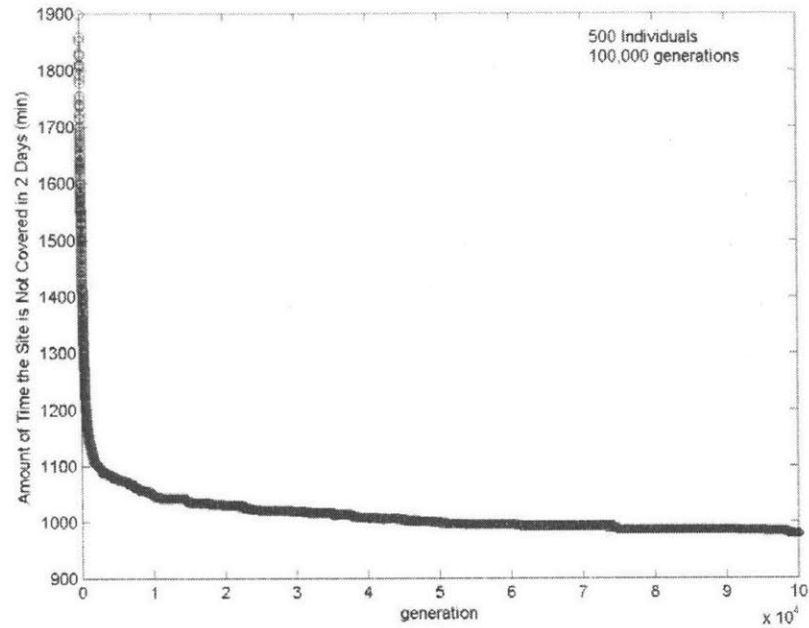
Figure 6.12: Fitness Results for Timeline Optimization of 100-Satellites
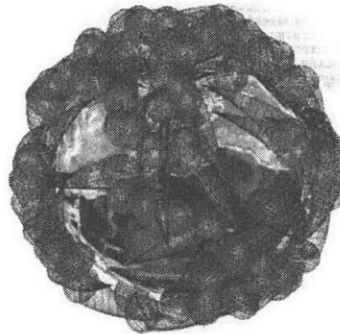
Figure 6.13: Timeline Optimized Constellation with 100-Satellites

Results of the combined greedy genetic algorithm approach, starting with 90 satellites, are show in Figure 6.14. This figure shows how the percent coverage changes with the addition of each satellite past 90. It can be seen in this figure that 173 satellites are needed to achieve full coverage. These results mimic the coverage trend of the one

144

satellite-per-plane constellation type, because far more satellites are required to obtain the last percent of coverage. These coverage results initially are not as good as those for a 100 satellite constellation. The 100 satellites in this approach are only capable of roughly 93% coverage. When this greedy algorithm approach was applied to the 100 satellite constellation, it was found that 65 additional satellites were needed for 100% coverage. This constellation proved to provide the best 100% coverage with the fewest numbers of total satellites using the greedy timeline optimization approach. Several normal genetic algorithm runs were completed using values near 165 satellites. None of these design optimization runs produced 100% coverage results within 100,000 runs. The combination of design approaches provided better coverage constellations.
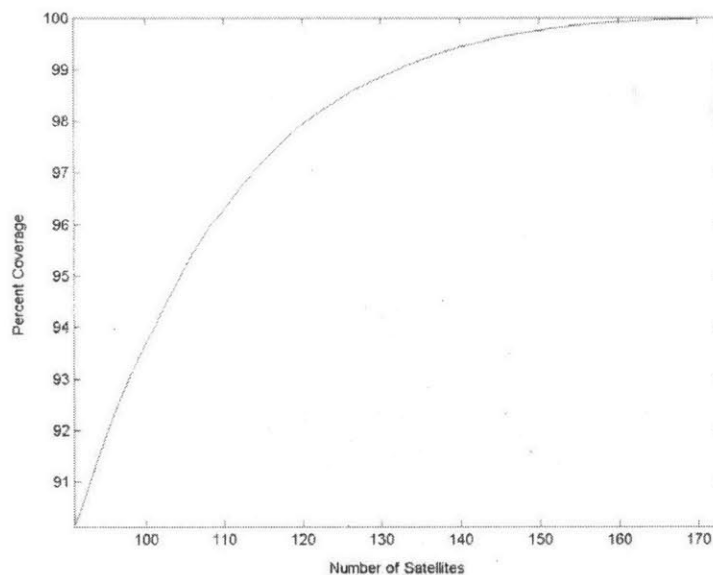
Figure 6.14: Percent Coverage Development Using a Greedy Genetic Algorithm

The results of this section were developed with several runs of the genetic algorithm processes described above. Each time the genetic algorithm's results could vary dramatically depending on how fit the initial constellations were. Given enough time and generation runs, perhaps the algorithm would produce constellations with coverage results closer to those obtained by symmetric constellations. While these constellations are deliberately off-set from the optimal semi-major axis to ensure repeat ground tracks,

145

optimal constellation results were not significantly different from the symmetrical constellation design results. While the constellation results from the timeline optimization were not as fruitful as symmetric constellations, several important lessons were learned. One of the most important is that coverage from multiple satellites at the same time is crucial to finding constellations with fewer satellites. Overlapping coverage helps groups of satellites obtain more coverage than the combination of all of them individually. The next important lesson is that some symmetry can be beneficial to the constellation design. This is because the constellation results are more tangible and designs can improve upon a standard starting position rather than a random one. An additional note when considering constellations of this type for real world purposes: It is much harder to launch 165 satellites into precisely timed and completely unique orbits than it is to send the same number of satellites into a commonly inclined symmetric constellation.

6.7 Repeat Delta Pattern Constellations

Utilizing the results established from both the symmetric and timeline optimized constellation design methods, a new constellation type was developed. The repeat delta pattern uses the same repeat ground track pattern with a little bit of symmetry added. The design is very similar to the one satellite-per-plane constellation type with the exception that the phasing parameter is defined to ensure satellites are evenly place over the same ground track. The reader is directed to section 5.2.4 where the design concept is developed in greater detail. Much like the one satellite-per-plane and timeline optimization constellations, no a priori estimate could be established.

This design scheme was founded on the idea that it would use the best of several methods in designing constellations for area specific coverage. Each satellite in the constellation follows the same ground track but resides in its own unique orbital plane. Only two variables remained for optimization once the orbital altitude was established for the 27/2 repeat ground track: the inclination and the initial longitude of the ascending node. Inclination was allowed to be optimized given a set number of satellites. Inclination was initially set to 60.5 degrees. This value is slightly less than the mid-fence inclination. Both one satellite-per-plane and delta pattern constellations resulted in inclinations close

146

to this value. The initial longitude of the ascending node was set to 4 degrees in an attempt to place a ground track crossing over the fence location. Simulations using SNOPT were optimized over the full two-day period. Between 54 and 154 satellites were explored in the configuration design space. The large design expanse was due to the unpredictable nature of the design results.

6.7.1 Constellation Design Space Results

Results for this constellation type were less effective. This constellation type contains too much symmetry. The inner symmetries created havoc within the coverage of individual configurations. Figure 6.15 depicts the coverage results for constellations ranging from 54 to 154 satellites. The first 100% coverage constellation contained 136 satellites. This configuration is identified on the figure and also shown graphical in Figure 6.16. The optimized inclination and initial longitude of the ascending node for this configuration are: 64.84 degrees and 30.47 degrees respectively. As the figure demonstrates, coverage with this type of constellation comes and goes in waves. In general, there is a noticeable increase in coverage with large jumps in the number of satellites as shown by a basic trend line.
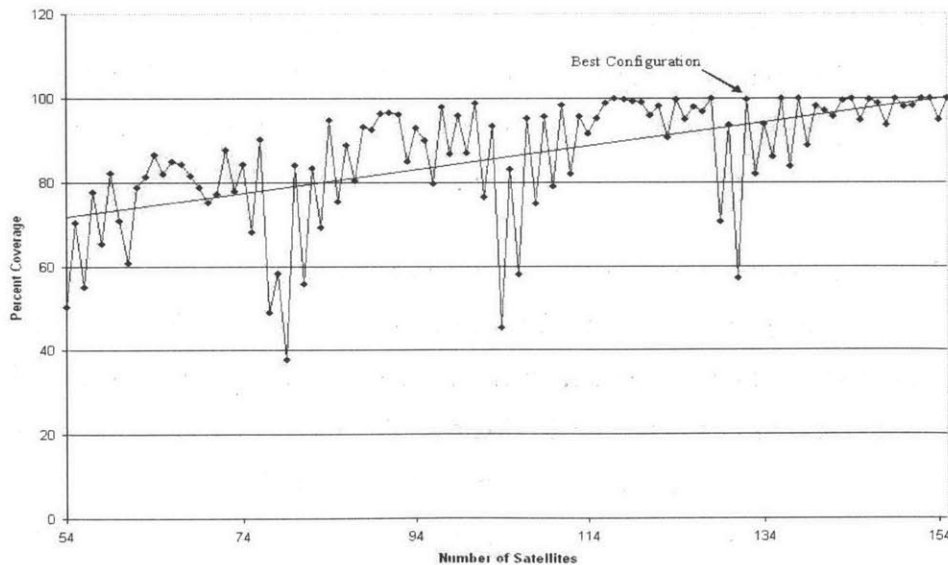
Figure 6.15: Design Results for the Repeat Delta Constellation Type

This method is not as good as some methods for obtaining coverage with the fewest number of satellites, and it also has some troubling side effects. Introducing more satellites does not always improve the coverage of the constellation. For the most part, the only conclusion that can be drawn is that the inner symmetries in the constellation cause massive fluctuations in coverage. Some of the most dramatic effects are shown in Figure 6.16, Figure 6.17, Figure 6.18, and Figure 6.19 which depict four constellations. In these figures, the inner symmetries of the constellation are readily apparent. The reachability envelopes emanating from each satellite help to accent how each constellation will evolve. Inner symmetries cause the odd distorted shape of the constellation reachability manifold patchwork. Each of these figures is a graphical representation of the constellation at one instant. The patterns shown here will evolve in their own way about the Earth. Every 30 or so satellites added allows a pattern to that seen in Figure 6.16 to be developed. These patterns are very symmetrical about the whole-Earth and tend to produce the flat coverage regions in Figure 6.15. The coverage from each satellite constellation is seen to vary wildly, from 38% to 100%, without an apparent relationship to the number of satellites in the constellation.
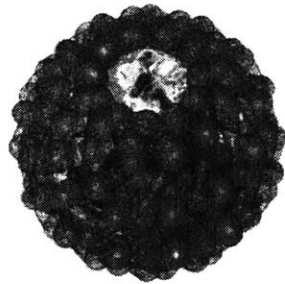
Figure 6.16: 136-Satellites; 100% Coverage
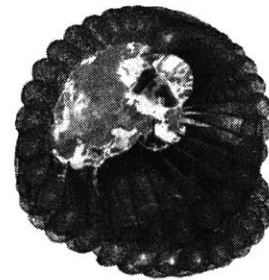
Figure 6.17: 79-Satellites; 37.77% Coverage
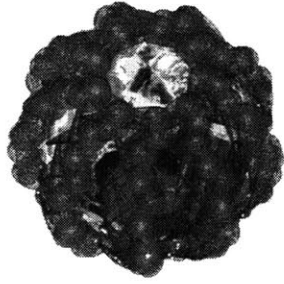
Figure 6.18: 117-Satellites; 99.96% Coverage **Figure 6.19: 131-Satellites; 57.04% Coverage**
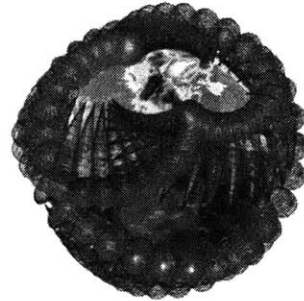
6.8   Constellations for Coverage Gap Filling

The results of this chapter have shown that there are a great many configurations of each constellation type that cannot reach 100% coverage, even after optimization. The following sections will outline two methods for modifying sub-optimal configurations to improve their coverage results.

The first method is a result of the timeline optimization design scheme. Coverage gap filling seeks to plug coverage gaps of optimized configurations with additional satellites. This approach uses the greedy genetic algorithm as described in Chapter 5. The goal is to improve coverage of symmetric constellations by infusing asymmetry to the design. Asymmetry is generated through the use of pseudo-random satellite placement. There are a vast number of constellations that could potentially benefit from this design method. However, constellation gap filling is not an independent design method and thus will only be explored to the extent of determining the method's usefulness.

6.8.1 Test Cases of Sub-Optimal Constellations

Four test cases were developed from the previous constellation designs. Two repeat delta pattern constellations are used as test cases in conjunction with a delta pattern and one satellite-per-plane constellation. Each of these constellations will have satellites added until the configuration provides complete coverage. Each constellation type and

configuration has its own repeat periodicity. Due to time restrictions, a timeline database of available satellite orbits for each repeat pattern of each test constellation was not created. For this reason only the 27/2 repeat ground track orbit analysis results were used to plug coverage gaps in each test case. This is not an accurate assumption for the repeatability of some constellations. Only constellations with a two-day repeat pattern, i.e. repeat delta patterns, will have coverage effectively filled for time beyond the two-day simulation analysis. The author recognizes this limitation, but presents the results to demonstrate the usefulness of the method.

The four test cases produced for this analysis come from configurations with greater than 90% coverage. The first test case is a $P=7$, $T=105$ delta pattern with 99.503% coverage over two-days. This configuration's coverage drops can be observed in the graph of percent coverage over two-days shown Figure 6.20. The second test case is a repeat delta pattern constellation with significant coverage loss at many points in the scenario. This is a $T=91$ configuration with 96.244% coverage over two-days. The coverage results of this configuration are shown in Figure 6.21. The third test case is another repeat delta pattern constellation with only minor coverage loss during the scenario. This is a $T=117$ configuration with 99.924% coverage over two-days. The coverage results of this configuration are shown in Figure 6.22. The fourth and final test case is a $P=110$ one satellite-per-plane constellation configuration with 96.869% coverage over two-days. This configuration's coverage results over the two-days can be seen in Figure 6.23. This configuration has two significant coverage drop regions. As seen in the figure, the drops occur at roughly one day intervals.
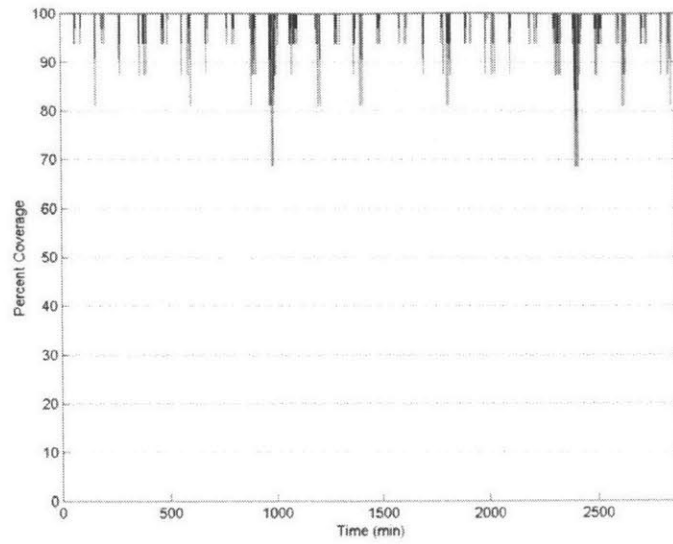
Figure 6.20: Test Case 1 – Delta Pattern Coverage over Two-Days
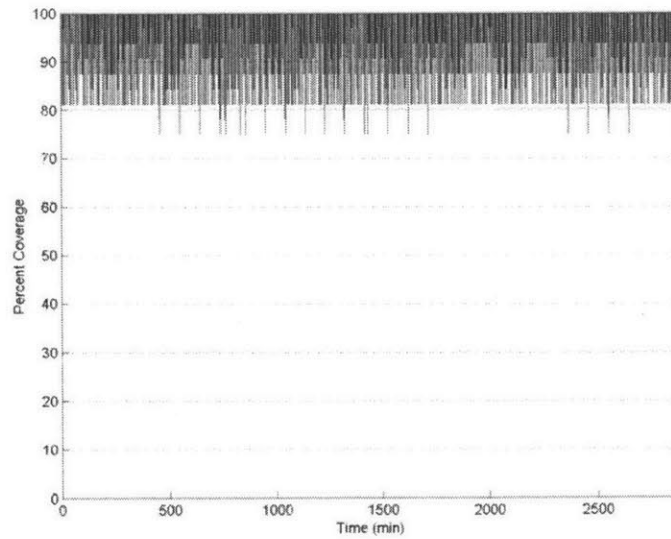
Figure 6.21: Test Case 2 – *T*=91 Repeat Delta Pattern Coverage over Two-Days

151
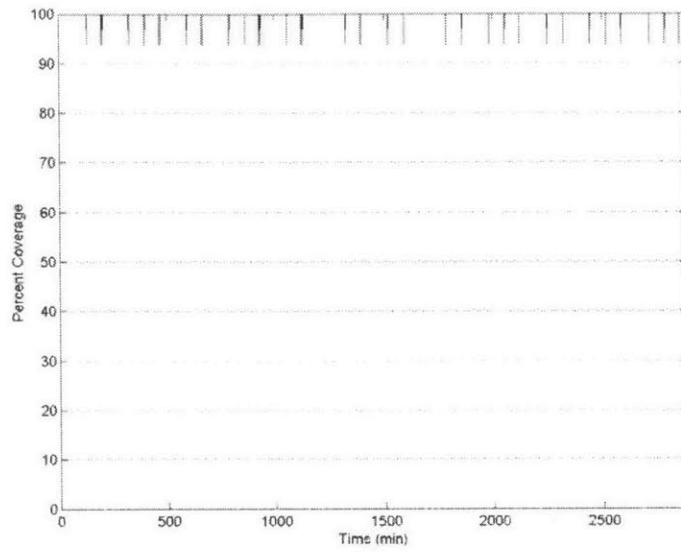
Figure 6.22: Test Case 3 – *T*=117 Repeat Delta Pattern Coverage over Two-Days
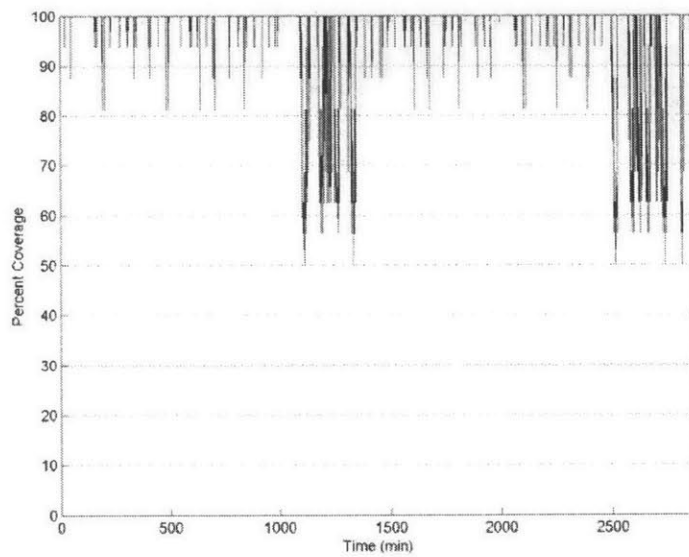
Figure 6.23: Test Case 4 – Single Satellite-per-Plane Coverage over Two-Days

6.8.2 Gap Filling Constellation Results

A greedy genetic algorithm approach was used to fill in the coverage timelines for each test case. Ten satellites were initially added to the constellation in a standard genetic algorithm approach. Ten satellites were insufficient to provide complete gap coverage in any of the test cases. From these results one satellite at a time was added in a greedy fashion. For each genetic algorithm run a population of 200 individual satellites was optimized over 1000 generations. This did not produce the single best satellite to fill coverage gaps; however the resulting "best" satellite was implemented from the generation after the large fitness level drop off. The general trend of fitness level per generation can be seen in Figure 6.12. After the large drop-off in fitness level usually little additional coverage capability is gained. The large initial population also allowed a broader sampling of the solution space. Genetic algorithm usage in this manner generates good gap filling satellites quickly within a reasonable number of generations.

Interesting results were obtained by applying this approach to the test cases described above. The delta pattern, of test case number one, required 29 additional satellites to provide complete coverage gap filling for the two-day scenario. The constellation's percent coverage improvement as satellites are added can be seen in Figure 6.24. The graphical results of this test case are given to show how coverage of a test constellation increases as satellites are added. Adding 29 satellites to this constellation raises the total satellites needed for complete coverage to 134. Unfortunately, this is not an improvement over the best symmetric delta pattern results. The second test case required 84 additional satellites. This brings the total number of satellites from 91 to 175. It was seen above that a repeat delta pattern with 136 satellites could provide 100% coverage. For large coverage gaps, as experienced by this repeat delta pattern, constellation gap filling does not appear to be beneficial. In the third test case, a repeat delta pattern with very few coverage gaps, 17 additional satellites were needed to provide complete coverage. The total number of satellites in this constellation is now 134. In this case, the gap filling was successful at reducing the total number of required satellites. The final test case was a one satellite-per-plane constellation. This constellation required 41 additional satellites to fill coverage gaps. The total number of

satellites in this constellation is now 151. This is far from an improvement on the best single satellite-per-plane constellation which required 116 satellites. This procedure is always capable of creating a constellation with complete coverage from an existing constellation with partial coverage. However, as demonstrated the constellation gap filling procedure does not always provide the fewest total number of satellites. This procedure is one possible method for seeking improved coverage capability from existing constellations.
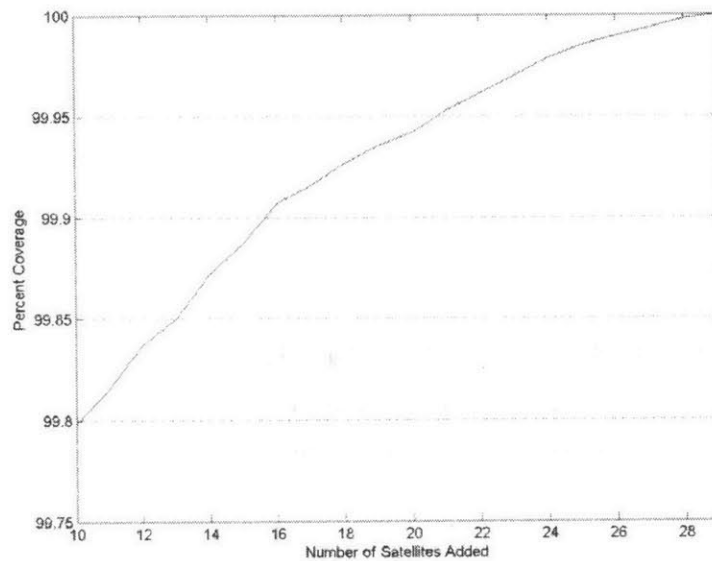
Figure 6.24: Constellation Coverage with the Addition of Gap Filling Satellites

6.9   Eccentric Orbit Modifications

Eccentricity has the potential to open up the constellation design space further or even improve on existing constellation designs. Only few classical methods have incorporated eccentricity into the constellation design process[14]. Eccentric orbit constellations often require fewer satellites. Eccentricity adds at least three more variables per satellite into each design: a, e, and ω. This thesis has left eccentricity set to zero, up to this point. To incorporate eccentricity into the design methods created thus

154

far, careful consideration is needed in order to maintain symmetry. The effects and the processes of adding eccentricity to an existing constellation were discussed in Chapter 5.

The same SNOPT design scheme that was discussed in the first section of this chapter will be used for design parameter optimization of eccentric orbit constellations. The input design parameters will now include the common argument of perigee, eccentricity, and semi-major axis. The semi-major axis will now be optimized per configuration rather than per constellation type. This is due to the fact that small changes in eccentricity can drastically change the semi-major axis. A check was added to ensure that the orbits did not have perigees less than 700 km above the Earth. This restriction will ensure that orbits will not experience extensive drag perturbations or impact the Earth.

The previously optimized parameters for each configuration in each constellation type were used as the initializing values for optimization. A starting argument of perigee value of 280 degrees was found to produce the best constellation design results. This value places the apogee of the orbits in the northern hemisphere. The initial eccentricity value was set to several different levels over a number of runs to ensure the best coverage results. Initializing eccentricities values of 0.005, 0.01, 0.015, 0.02, and 0.04 were used for this analysis. Certain constellation types seemed to favor specific starting values of eccentricity over others. The star pattern and the timeline optimization constellation types were not considered because of their generally poor performance when compared with the same number of satellites in other constellation types. The goal of this modification is to add a little eccentricity and arrange the satellites to improve fence coverage results.

6.9.1 Application to Delta Patterns

Introducing a non-integer inter-plane phasing parameter, F, as well as eccentricity, the delta pattern can lose a large part of its original symmetry. Using the method described above, SNOPT was allowed to re-optimize a configuration from its prior optimized design results. Several optimization runs, using different starting eccentricities, allowed the best coverage results to be pulled from all the different

initializations and compared with the original coverage results. In some configurations no improvement in coverage was observed, while other configurations showed significant improvements. Figure 6.25 depicts the amount of eccentricity that was used if an improvement was obtained. These results represent the same design space given in the results of Figure 6.7. A large portion of this space shows no improvement as noted on the figure. Constellations that were originally capable of 100% coverage were not explored in this analysis. Constellations with fewer numbers of satellites per plane were improved more by varying eccentricity.
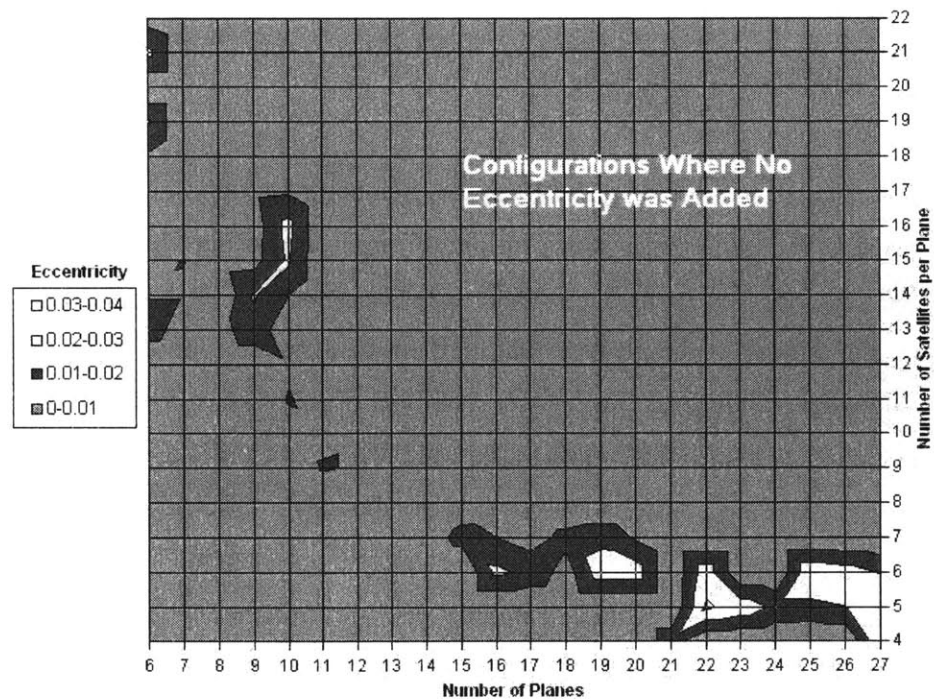
Figure 6.25: Eccentricity Added During the Modification of Delta Configurations

Figure 6.26 depicts the percent coverage improvement gained by each configuration. The greatest gains in percent coverage, and the largest eccentricity used, were in constellations with fewer satellites per plane. This figure covers the same design space as the earlier figures but is tilted to better show the gains in percent coverage. These results show that the majority of the constellations could not be improved with the addition of eccentricity. Only 0.01 to 0.02 percent coverage improvements were typically

achieved. The ability to add a small amount of eccentricity did allow several constellations on the verge of 100% coverage to obtain this goal. The new "best" delta pattern configuration, with the lowest total number of satellites and 100% coverage, is P=11, T=121. This is a five satellite improvement from the standard delta pattern approach. The eccentricity added to this constellation was 0.005. The new argument of perigee, ω, value was found to be unchanged from the initial optimization guess of 280 degrees. The semi-major axis remained unchanged while the new inclination and F were 63.57 degrees and 2.416 respectively. The small amount of eccentricity added to delta patterns gave no noticeable change in the reachability envelopes. However, adding the small amount of eccentricity had the effect of allowing for marginal gains in coverage at relatively little design cost. The optimal inclinations in this analysis varied from 62 to 69 degrees. Arguments of perigee ranged between 270 and 281 degrees. Figure 6.27 shows the new delta pattern design space after the eccentric orbit modification and optimization. The new "best" configuration is depicted on the figure. This figure can be compared with the results in Figure 6.7. Comparing the new modification results with the old results illustrates that there is now a steeper rise in coverage to the 100% plateau.
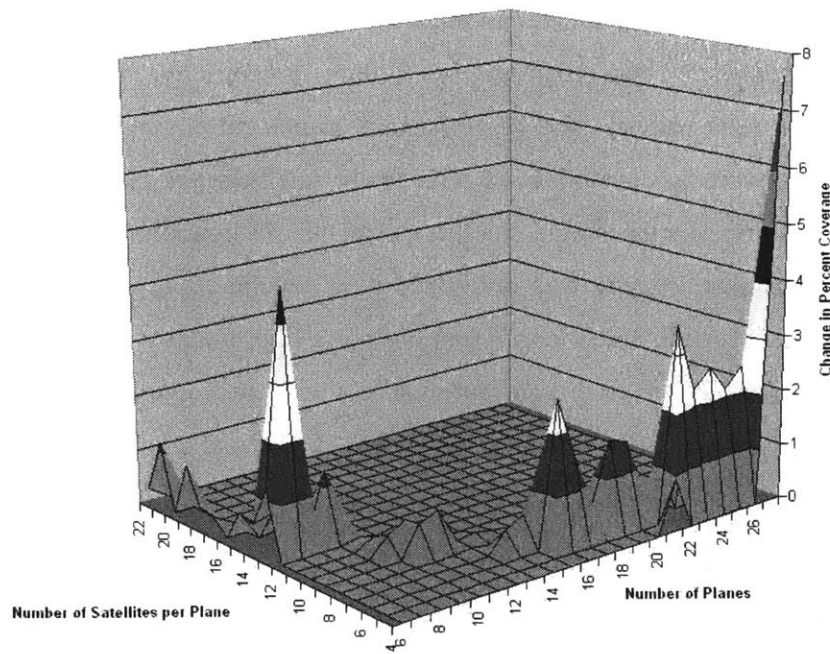
Figure 6.26: Percent Coverage Change for Delta Pattern Configurations
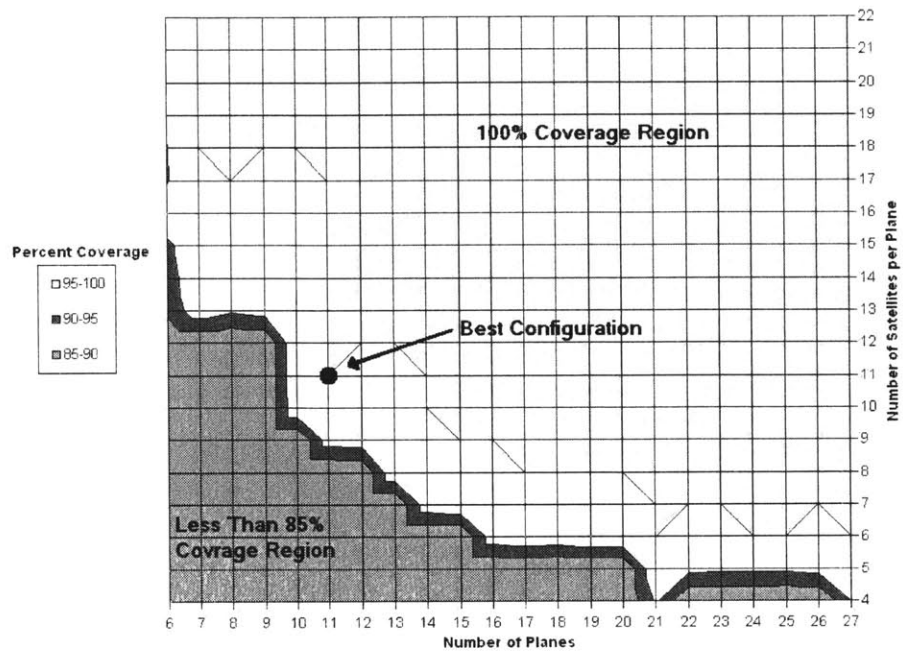
Figure 6.27: Design Space for the Eccentric Delta Pattern Constellation Type

6.9.2 Application to Single Satellite-per-Plane Patterns

Much like delta pattern constellations, only slight improvements were observed in single satellite-per-plane constellations by adding eccentricity. In eccentric orbit modifications for delta patterns, the greatest gains in percent coverage, and the largest eccentricity used, were in constellations with fewer satellites per plane. However, this trend did not continue to the single satellite-per-plane configurations. Similar to delta patterns, this constellation type was optimized over several runs with different initial eccentricities. However, far fewer configurations were improved by adding eccentricity. The optimal eccentricity for each configuration is shown in Figure 6.28. These results show that the value of eccentricity is very dependent on the total number of satellites. The only apparent trend was similar to that observed in delta patterns. Constellations near the cusp of 100% coverage were pushed to the plateau.

158
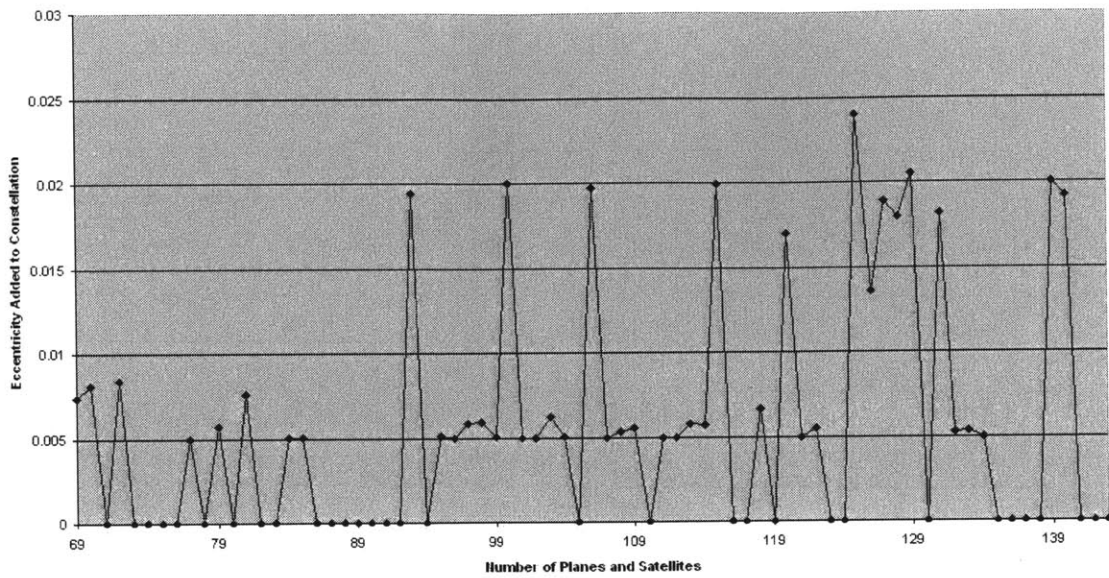
Figure 6.28: Eccentricity Added to Single Satellite-per-Plane Configurations

Large eccentricity use does not imply large improvement in percent coverage. The gains in percent coverage for each configuration are shown in Figure 6.29. The average gain in percent coverage was between 0.2 and 0.3 percent. Resulting inclinations varied by only a degree from the 63 degree mark. Arguments of perigee ranged between 270 and 281 degrees. A comparison of coverage results for the design space before and after the eccentric orbit modifications are shown in Figure 6.30. Eccentricity has the effect of smoothing out the coverage results curve. The most noticeable gains in coverage were in configurations that were initially close to 100%. For this constellation type, several additional constellations are now capable of 100% coverage. However, the smallest configuration capable of complete coverage remains the 116 satellite configuration. No eccentricity was added to this constellation. For this reason the semi-major axis, inclination, and F remained unchanged.
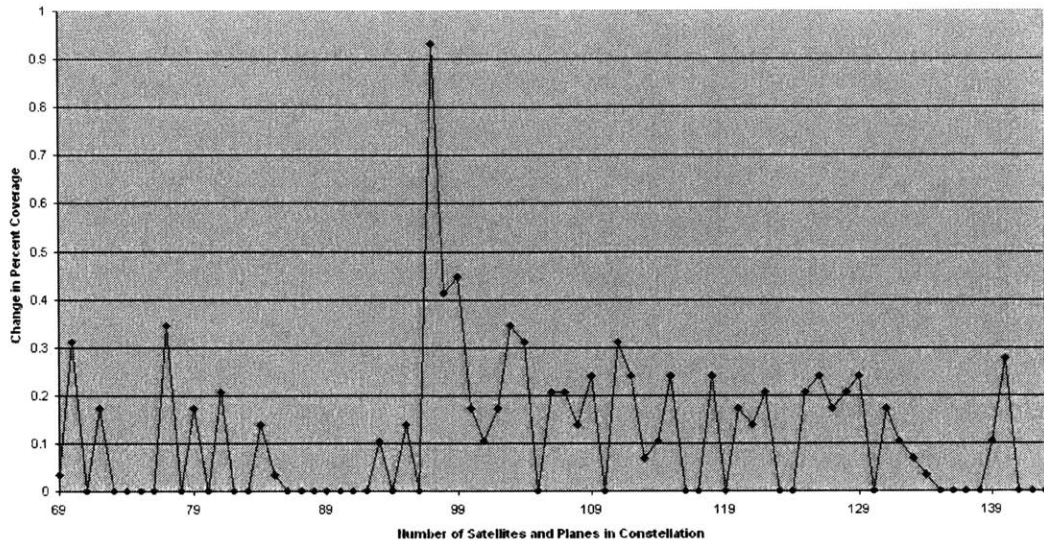
Figure 6.29: Percent Coverage Change for Single Satellite-per-Plane Constellations
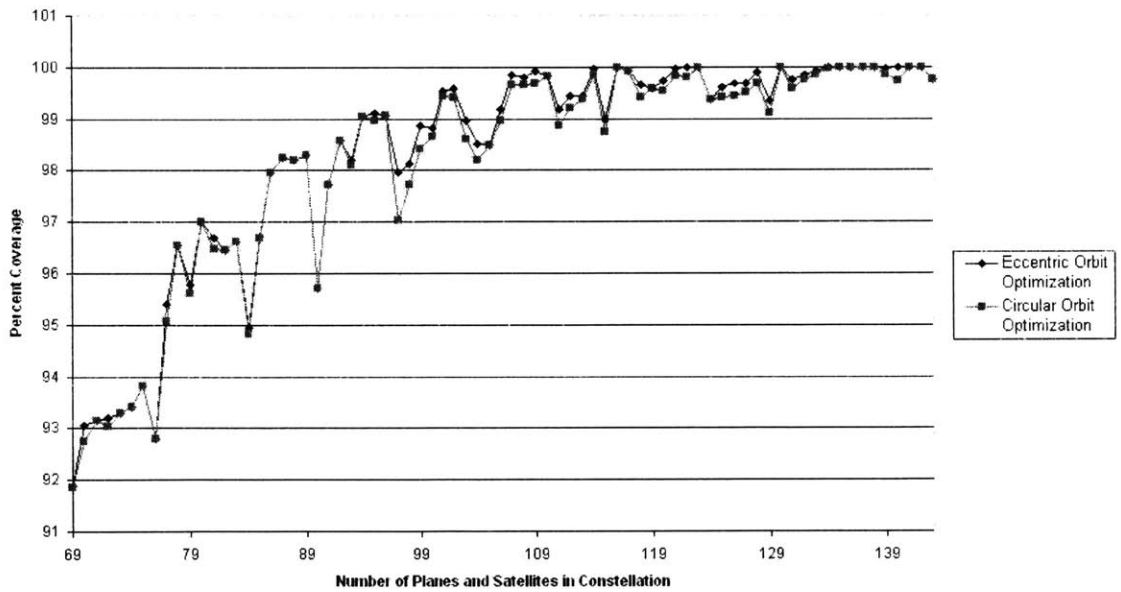
Figure 6.30: Design Space for the Eccentric One Satellite-per-Plane Constellations

6.9.3 Application to Repeat Delta Patterns

The final application of the eccentric orbit modifications was the repeat delta pattern. Previous constellation types did not benefit greatly from eccentricity. The repeat

160

delta pattern results were the most erratic, and thus have the greatest potential for improvement in coverage. The procedure used to add eccentricity to this constellation type was slightly different from the other constellation types. The semi-major axis was once again fixed to ensure a repeat ground track. The initial longitude of the ascending node, Ω_o, was allowed to vary. Additionally the eccentricity, inclination, and argument of perigee were also design parameters for optimization. The eccentricity obtained per configuration can be found in Figure 6.31. As seen in the figure, there was no apparent structure to how much eccentricity was added per configuration.
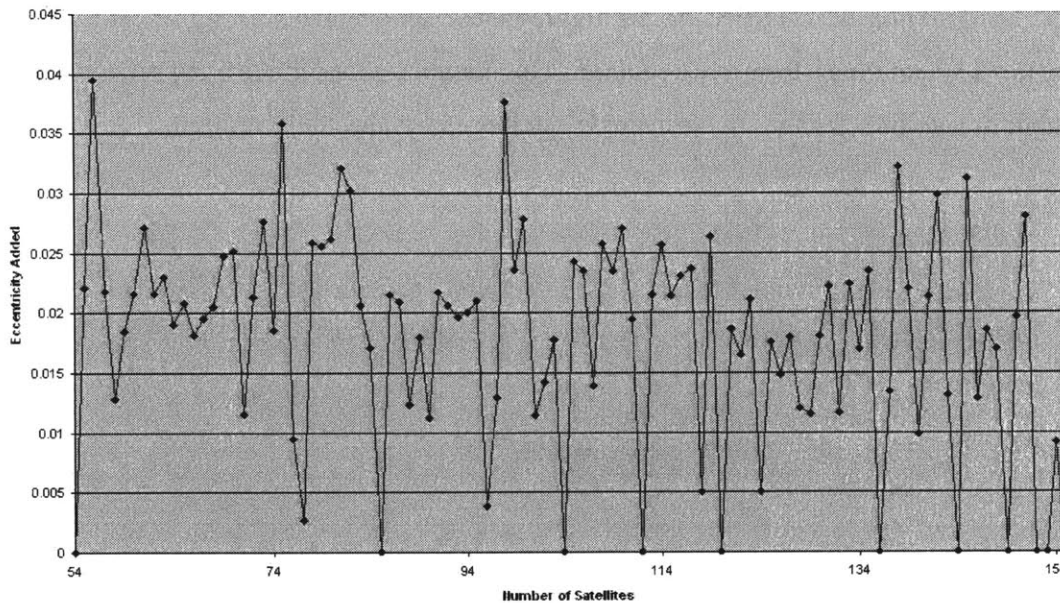
Figure 6.31: Eccentricity Added to Repeat Delta Configurations

The changes in percent coverage are given in Figure 6.32. The 93 satellite configuration experienced nearly a 14 percent improvement using an eccentricity of 0.0196. This was the largest improvement of all the eccentric orbit modifications. Of all the constellation types, this pattern gained the most from allowing eccentricity. This figure shows that nearly every configuration experienced some improvement in percent coverage. These results only partially smoothed the coverage curve of this constellation type. A coverage comparison of the modified constellations to the former constellations is shown in Figure 6.33. This figure shows the same basic structure; however the

161

coverage improvements by allowing eccentricity are nearly uniform for all configurations. For some configurations, improvements are substantial. The optimal inclinations in this analysis also varied wildly from configuration-to-configuration ranging from 61.5 to 70.0 degrees. The optimum argument of perigee stayed within a few degrees of the initial value of 280 degrees. The initial longitude of the ascending node also varied wildly ranging anywhere from 0 to 89 degrees. A new "best" configuration was established with 117 satellites. This configuration used an optimized inclination of 64.20 degrees with an eccentricity of 0.0236. The initial longitude of the ascending node, Ω_o, was found to be 38.76 degrees with an argument of perigee, ω, of 279.87 degrees. This configuration is identified on the figure below. This number is significantly lower than the 136 satellites formerly required. This number of satellites is approaching the number of satellites for the smallest single satellite-per-plane configuration.
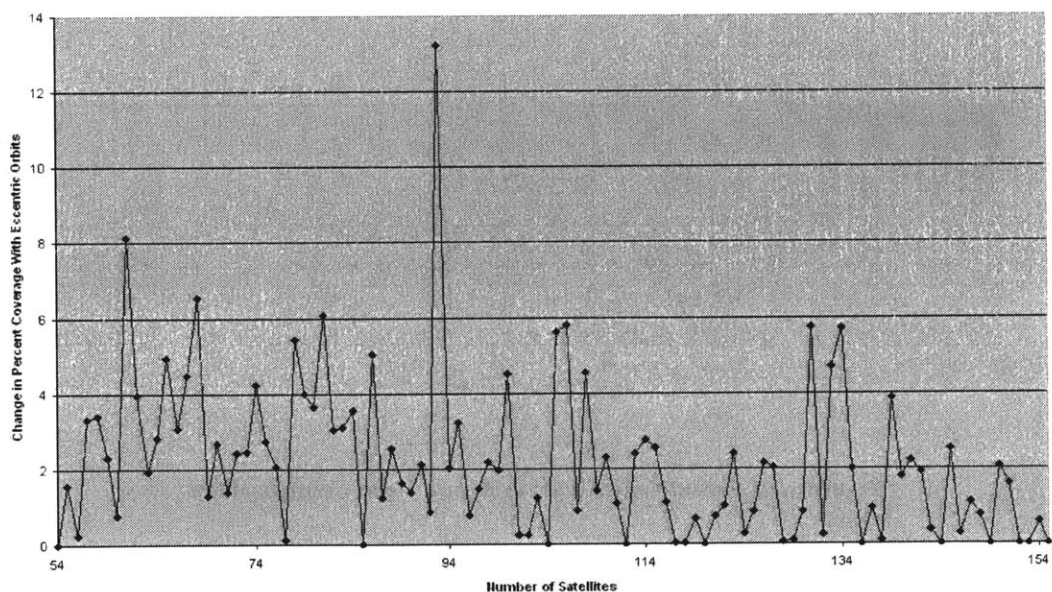
Figure 6.32: Percent Coverage Change for Repeat Delta Patterns

162
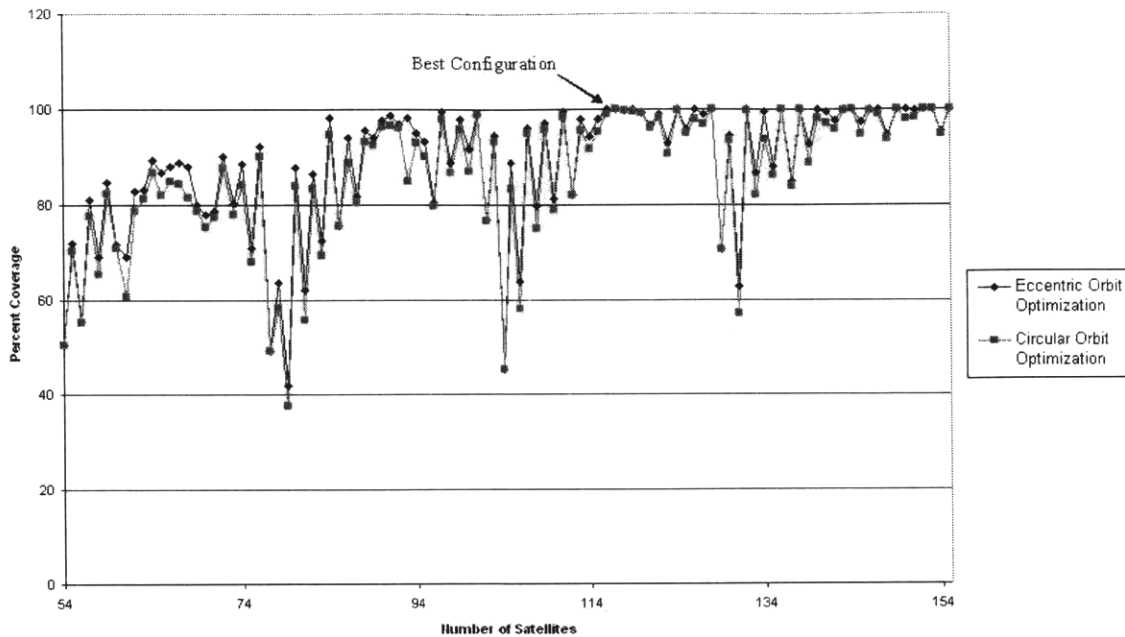
Figure 6.33: Design Space for the Eccentric Repeat Delta Constellation Type

6.10 Summary of Fence Coverage Results

This concludes the exploration of constellation design methods using the new definition of fence coverage. The constellation design methods described throughout this section comprise only a small minority of the possible ways that classical methods can be adapted for missile defense. These results also represent an upper bound on the numbers of satellites needed for 100% fence coverage. The classical coverage definition is line-of-sight visibility, based on observing a ground site with a nadir pointing sensor. The new coverage paradigm takes into account the capture time needed to intercept a target. For this reason classical constellations were "tweaked" to obtain the best coverage under the new definition. New methods of constellation design were created by modifying and abstracting earlier design approaches. Constellation design results presented in this chapter survey the capability of constellations for fence barrier missile defense. Table 6-1 below is a summary of the smallest configurations achieved per constellation type. This table also lists the configuration parameters and key design advantages.

Table 6-1: Minimum Satellite Configuration Summary

Constellation Type	Total Number of Satellites	Configuration Parameters	Key Design Advantages
Non-Rotating Earth	11	i=88.96° a=7470.3535 km	The semi-major axis of this result proved to be near optimal for many additional circular orbit constellations.
Star Pattern	182	P=13 F=0.4614 Δ=0.0284° a=7470.3535 km	Provides complete coverage of the polar region down to the fence latitude.
Delta Pattern	126	P=7 F=2.484 i=62.64° a=7470.3535 km or P=21 F=3.208 i=64.23° a=7470.3535 km	Common inclination makes for convenient launch and placement of satellites. Capable of coverage over an entire latitude zone.
One Satellite-per-Plane	116	F=6.485 i=63.41° a=7470.3535 km	Fewest total number of satellites required for 100% coverage.
Timeline Optimized	165	Repeat Ratio=27/2	Allows for asymmetric satellite placement.
Repeat Delta Pattern	136	Ω_o=30.47° i=64.84° Repeat Ratio=27/2	Combines aspects of the symmetric delta pattern design with the asymmetric timeline optimized design.
Eccentric Delta Pattern	121	P=11 e=0.0050 ω=280° F=2.416 i=63.57° a=7470.3535 km	Coverage improvements from eccentric orbits. Pushed several near 100% coverage constellations to that result.
Eccentric One Satellite-per-Plane	116	*Same as Unmodified Results*	No coverage improvement from modifications.
Eccentric Repeat Delta Pattern	117	e=0.0236 ω=279.87° i=64.20° Ω_o=38.76° Repeat Ratio=27/2	Large coverage improvements. The number of satellites required approached those of the best configuration.
Constellation Gap Filling	Configuration Dependent	Best Results Test Case # 3	Design modification which adds asymmetry to symmetric patterns using a genetic algorithm. The goal is to patch coverage gaps in existing constellations

164

Results presented here show that the smallest constellation capable of 100% fence coverage was a 116 satellite single satellite-per-plane configuration. This is a large number of satellites for realistic near term launch capability. However, this constellation also provides complete coverage over a latitude zone around the Earth. Several methods were devised to modify constellations to obtain better coverage results with only minor success. In order to make satellite based missile defense a more viable alternative, it is necessary to loosen the fence constraint, and open the possibility for interceptions at other points in a missile's trajectory.

[This Page Intentionally Left Blank]

Chapter 7

Volumetric Coverage Expansion

The objective of satellite based mid-course defense is to intercept any possible missile launched through a threat corridor. The spatial volume of the threat corridor represents an entire region of potential missile intercept locations. Previously, this goal was accomplished by creating an imaginary barrier, or "fence". This vertical slice through the missile corridor needed to have 100% coverage continuously to ensure that no missile could get through. The fence concept was a convenient simplification of the intercept problem to guarantee missile capture. It fixed the point of intercept and removed a degree of freedom from the timing problem. This allowed for a geometric picture of the capture area, but it did not allow for the possibility of intercepts at other locations in the corridor. Adding back this degree of freedom to the problem allows for a new definition of coverage. This coverage definition is an expansion of the fence concept and as such it includes the fence approach as a special, and restrictive, case.

This chapter will expand the coverage definition to include capture anywhere in the ICBM corridor. The missile trajectories defining the corridor will be used to define a discrete set of intercept locations. These trajectories are individually broken up into locations segmented by a common time step. This breakdown can be done at finer levels producing more intercept points, but at the expense of more computation requirements per simulation. The breakdown used here is conservative and sufficient to understand constellation intercept capability. Volumetric coverage (The ability to capture a missile anywhere in the corridor) enhances the capabilities of an interceptor. This benefit comes with a drawback; the simple abstractions from classical constellation design no longer apply.

7.1 Missile Corridor Volume

The potential ICBM mid-course flight paths capable of hitting the CONUS from North Korea constitute a volume of threat trajectories. The full missile corridor of trajectories can be seen in Figure 4.1. The corridor represents ICBM positions over a range of flight times in ECF coordinates. These points represent missile locations two minutes after the exo-atmospheric burnout point to the point of atmospheric re-entry for every trajectory capable of hitting the threatened region. In the previous fence coverage definition, capture time was limited to intercepting an ICBM at a specific location. An interceptor should be allowed to intercept an ICBM at any point in its trajectory, if it can. The starting and terminating ends to the volume are specific to this research. These bounds can be shortened or lengthened as needed. In particular, it is possible to reduce the terminating ends away from the CONUS. To develop an adequate defense for the entire volume, it is important to develop computational bookkeeping to track missile threats and intercepts throughout the corridor. The following sections of this chapter will describe the process developed for volumetric coverage determination.

7.1.1 Tubule Creation

In order to understand the full volumetric coverage capability of an interceptor, it is convenient to think of the coverage for only one ICBM trajectory at a time. A single trajectory is the flight path of a particular missile from the entry to the exit of the missile corridor, the mid-course portion of flight. The missile must be intercepted at some future location in this trajectory. An analogy of this concept is duck hunting. In this case, the duck is a particular incoming ICBM; the flight path of the duck is the missile trajectory. A particular satellite is the hunter waiting to shoot down the duck. The hunter is moving along his own trajectory and is only capable of hitting his target intermittently. In order to shoot down a duck, the hunter must lead his target. This is exactly the intercept timing problem developed in Chapter 4.

A continuous flow of missiles is postulated through each trajectory. If a constellation is capable of defending against a stream of incoming ICBMs along a

trajectory, then it can defend against any particular missile launched at any time. The ability to intercept any and all missiles in the flow, before any completely travel though the threat corridor, ensures complete missile defense of that trajectory. This single trajectory example must be expanded to a dense set of trajectories constituting the missile corridor. Realistically, a continuous wave of missiles in one trajectory cannot be simulated for constellation design purposes. Breaking the missile trajectory into a discrete series of points solves this problem in a conservative fashion. A discritized trajectory is known as a tubule. For this research, each tubule is broken up into a discrete one-minute grid along the trajectory. Continuing with an analogy, the single tubule situation is similar to an old carnival duck hunting game. In this game, it is only possible to hit a duck while it is visible in a window as it moves across the stage. A simplistic representation of this analogy is shown in Figure 7.1.
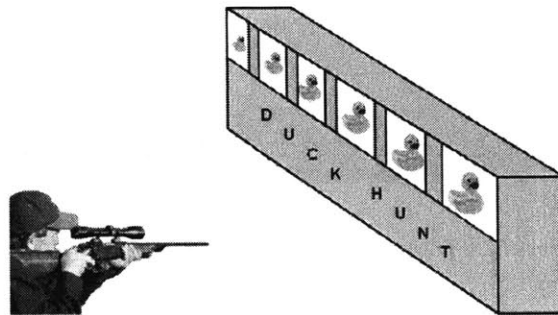
Figure 7.1: Duck Hunting Analogy for Missile Defense along a Trajectory

7.1.2 Coverage Development

The method of determining coverage at a particular point and time is exactly the same as the analytic algorithm described earlier. The reader is directed to Figure 4.3 and Figure 4.10 for a simple understanding of the ICBM intercept timing problem and coverage determination algorithm. The new degree of freedom to this problem means that the capture time of a given interceptor directly depends on which point in the tubule the interceptor is aiming for. A particular ICBM is vulnerable from its identification time, T_{ID}, until the terminal portion of flight, ranging 20 to 31 minutes after T_{ID}. Thus the maximum time of flight for the interceptor ranges from zero to the terminal ICBM time,

169

depending on the desired intercept location in the ICBM tubule. A ten by ten grid of missile tubules (100 total tubules) is used to define the threat volume. The set of these tubules is shown in Figure 7.2. Each tubule is shown as one line emanating from North Korea and terminating in the threat area. This figure can be compared to the similar missile threat corridor in Figure 1.2.

Figure 7.2: Tubule Representation of Missile Corridor

100% volumetric coverage means that no missile, from any tubule, can make to a terminal point. Volumetric coverage simulations are very similar to those used for fence coverage. A continuous wave of missiles starts at the beginning of each tubule at the start of a scenario. After each minute of simulation time, both the satellites in a constellation configuration and the missiles are advanced one minute in their respective trajectories. New missiles are started in the first location of each tubule creating a continuous flow. Also during each minute of simulation, coverage from each satellite is calculated against all the occupied missile locations. If a missile can be intercepted, it is removed from or flagged in its current location. In this fashion, if no un-flagged missile advances to the terminal state, 100% missile defense is attained. Missiles advancing to this state are tallied versus the total number of potential missiles to determine the percent coverage. In general, volumetric coverage results are computed for the first opportunity of intercept. Other interesting statistics can be accumulated during the simulations such as the location

170

of capture and, if possible, the number of times an ICBM can be captured. These statistics will be used to help determine the usefulness of a constellation type and configuration.

7.1.3 Constellation Development Method

At several points in this chapter it has been stated there is not a definitive method for constellation design using volumetric coverage. This is not an entirely true statement. It is true that the complex nature of the constellation's coverage "function" does not lend itself to a simple analytic method of constellation design. However, the fence coverage area is a sub-set of the full volumetric region. This means that volumetric coverage results will be at least as good as fence coverage results for missile defense. Some of the optimization schemes, used in previous designs to tweak parameters to maximize fence coverage, can also be used to tweak fence constellations to maximize volumetric coverage. Inclination, semi-major axis, inter-plane phasing parameter, and other design parameters per constellation configuration can be easily re-optimized from fence results. General constellation design trends can also be extended into the new definition of coverage. The method of creating a latitude zone of coverage can be directly applied to the full missile corridor. This new coverage definition will be applied to production of 100% coverage constellations with the fewest numbers of satellites. As of yet, this research has not developed a specific design method for volumetric coverage from the definition alone.

7.2 Additional Threat Deniability

Constellations to this point have been designed for protection against the missile corridor created from a hypothetical North Korean launch. ICMB trajectories were limited to those that could intercept the CONUS within the postulated North Korean range capability. However, a missile defense constellation would be more valuable if it were capable of defending the whole CONUS against future North Korean capability and other missile capable states. To examine the defense capability of constellations designed previously against these possibilities, additional missile tubules were created. A list of both possible threat launch locations and target locations was used to create a multitude

of tubules. The target locations were established with cities along the boundary of the CONUS and several cities in the interior. Table 7-1 lists the cities used for CONUS boundaries targets and those used for internal targets with their latitude and longitude. This set is an approximation of whole CONUS coverage. The layout of these cities on the globe used in the simulations can be seen in Figure 7.3. If a constellation can protect each of these cities then, by a convexity argument, it is capable of complete coverage over the whole continental United States.

Table 7-1: Target Cities on the CONUS Boundary and Interior

Boundary Cities:	North Latitude (Deg)	East Longitude (Deg)
Bellingham, WA	48.75972	-122.48694
Coer d'Alene, ID	47.67778	-116.77944
Harve, MT	48.55000	-109.68333
Minot, ND	48.23250	-101.29583
Duluth, MN	46.78333	-92.10639
Alpena, MI	45.06167	-83.43278
Detroit, MI	42.33139	-83.04583
Buffalo, NY	42.88639	-78.87861
Newport, VT	44.93639	-72.20556
Fort Kent, ME	47.25861	-68.59000
Calis, ME	45.18889	-67.27917
Boston, MA	42.35833	-71.06028
New York City, NY	40.71417	-74.00639
Atlantic City, NJ	39.36417	-74.42333
Norfolk, VA	36.84667	-76.28556
Wilmington, SC	34.22556	-77.94500
Savannah, GA	32.08333	-81.10000
Jacksonville, FL	30.33194	-81.65583
Miami, FL	25.77389	-80.19389
Pensacola, FL	30.42111	-87.21694
New Orleans, LA	29.95444	-90.07500
Houston, TX	29.76306	-95.36306
Brownsville, TX	25.90139	-97.49722
El Paso, TX	31.75861	-106.48639
Yuma, AZ	32.72528	-114.62361
Los Angeles, CA	34.05222	-118.24278
San Francisco, CA	37.77500	-122.41833
Eureka, CA	40.80222	-124.16250
Astoria, OR	46.18806	-123.83000

Interior Cities:

Las Vegas, NV	36.17500	-115.13639
Salt Lake City, UT	40.76083	-111.89028
Denver, CO	39.73917	-104.98417
Kansas City, MO	39.09972	-94.57833
St Louis, MO	38.62722	-90.19778
Chicago, IL	41.85000	-87.65000
Cincinnati, OH	39.16194	-84.45694
Atlanta, GA	33.74889	-84.38806
Washington, DC	38.89500	-77.03667
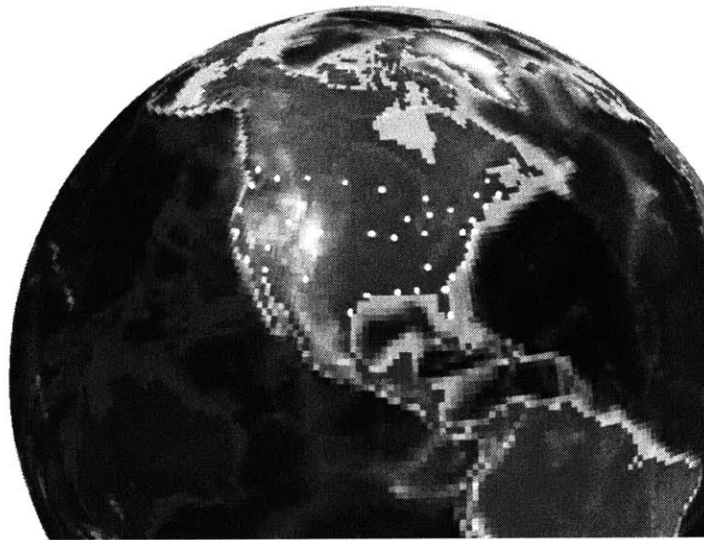
Figure 7.3: Geographic Location of Target Cities

The first extension in to the analysis of increased capability will come from an analysis of the potential capability of North Korea to strike any of the target cities listed in Table 7-1. This analysis will allow for assertions to be made on the coverage capacity of the optimized volumetric constellations. The tubules, emanating solely from North Korea, capable of hitting any of the target cities are shown in Figure 7.4. These tubules represent a future threat capability from North Korea.
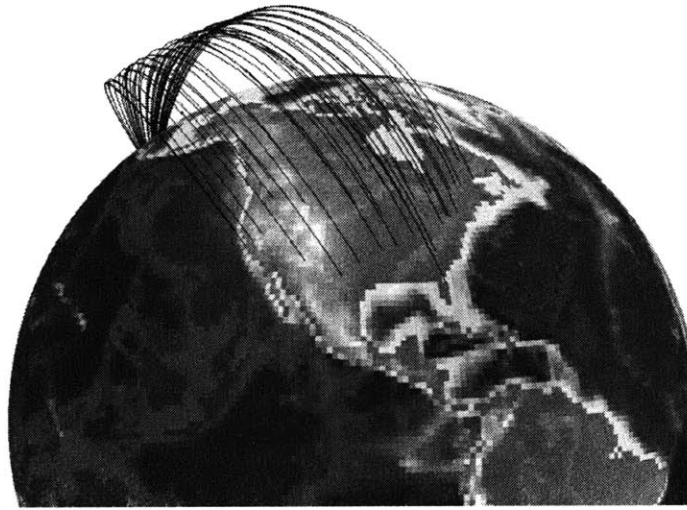
Figure 7.4: North Korean ICBM Tubules for CONUS Coverage Analysis

A list of possible threatening states with future ICBM ranges capable of hitting the CONUS was also created. The list is comprised of known launch locations from some ICBM capable states combined with a wide range of cities spread across each country. In this way, protection from all available launch sites in a country constitutes protection from that country. The missile trajectories created here represent a future capability for most states and are not representative of each country's actual launch capability. The list of countries and the cities used for launch sites can be found in Table 7-2 along with their latitudes and longitudes. The geographic layout of these launch locations is depicted in Figure 7.5. Missile tubules from each launch site to each target site can be created using the mathematics described in Chapter 4. A total of 38 target locations combined with 24 launch sites creates for a total of 912 individual missile corridors. A graphical representation of the new set of threat tubules can be seen in Figure 7.6. The first of these pictures depicts the tubules from a perspective over the launch sites on the Eurasian continent. The second graphic is a representation of the tubules near impact over the CONUS. The tubules shown in these figures only depict the mid-course portion of flight that will be used for analysis. Constellations will not be specifically created for global defense against these threats. Instead, a selection of constellations, designed to protect only against the North Korean threat, will be analyzed to determine their effectiveness

174

against the list of global threats. This analysis will express the capability of volumetric constellations for global defense.

Table 7-2: Launch Countries and Cites

Country	North Latitude (Deg)	East Longitude (Deg)
China		
Kashi	39.45472	75.97972
Altay	47.86667	88.11667
Yumen	39.80000	97.90000
Hailar	49.20000	119.70000
Qiqian	52.21667	120.80000
Tongjiang	47.64639	132.50167
Beijing	39.92889	116.38833
Fuzhou	28.01667	116.33333
India		
Dehra Dun	30.31667	78.03333
Patna	26.50000	85.11667
Iran		
Tabriz	38.08000	46.29194
Mashhad	36.29583	59.61194
Libya		
Tubruq	32.08361	23.97639
Zuwarah	32.93444	12.07917
Pakistan		
Quetta	30.20000	67.00000
Russia		
Bologoye	57.87833	34.07806
Tatishchevo	51.66833	45.59250
Dombarovskiy	50.75416	59.54000
Kopeysk	55.11167	61.64694
Aleysk	52.49444	82.77750
Bratsk	56.13250	101.61417
Yakutsk	62.03389	129.73306
Magadan	59.56667	150.80000
North Korea		
P'yongyang	39.01944	125.75472

175
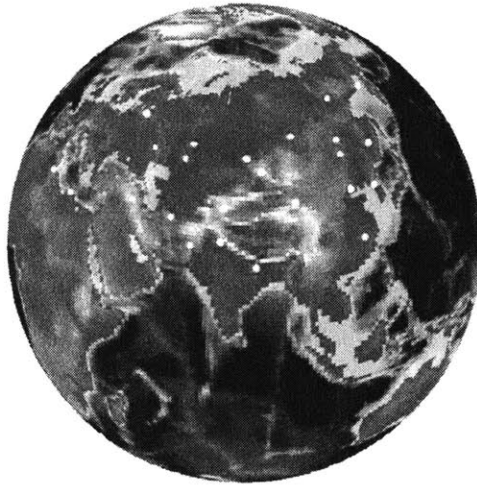
Figure 7.5: Geographic Location Launch Cities
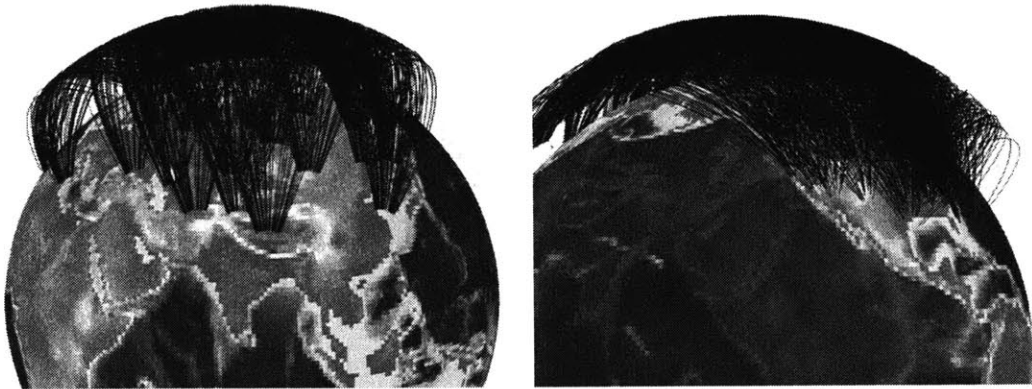
Figure 7.6: Global Defense Tubules

Chapter 8

Volumetric Coverage Results

This chapter presents coverage results stemming from the application of the new volumetric coverage definition. It will illustrate how the previous definition of fence coverage was too restrictive in its design requirements. A transition from design results of fence coverage to volumetric coverage is given by applying previously designed constellations to the new coverage metric. The results of these simulations illustrate that all fence coverage constellations can achieve 100% volumetric coverage. This will lead to the development of smaller constellations of satellites designed only about volumetric coverage. The constellation design and development process is more complex under the new coverage definition. For this reason, the great diversity of constellation design methods and their coverage results will not be explored here. Instead, this chapter will focus on the application of the delta pattern using volumetric coverage. Delta patterns, including single satellite-per-plane constellations, produced the smallest configurations capable of complete coverage. These results will also be expanded to look at additional constellation coverage issues such as the ability for multiple intercepts of a single ICBM. Additional design-space results are expanded to include: increased interceptor ΔV, total CONUS coverage, and the extent of a constellation's deniability. It will be demonstrated that realistic constellation sizes can now be obtained using volumetric coverage for ballistic missile defense. It will also be shown that these constellations are capable of exceeding their design goals.

8.1 General Design Algorithm for Simulations

The design process for volumetric coverage was very similar to that of the fence coverage process. As mentioned in Chapter 7, additional bookkeeping is required to keep track of the number and location of every intercept for a continuous wave of ICBM

threats. The simulation algorithm for the volumetric coverage determination, pictured in Figure 8.1, is similar to the simulation algorithm for fence coverage determination shown in Figure 6.1. The initial simulation inputs into this coverage algorithm are slightly modified from those required for fence coverage. In addition to the standard time regulation inputs, the maximum interceptor ΔV and the tubule descriptions are necessary. The tubule description contains the Earth fixed positions of an ICBM discretized over time. The interceptor coverage determination function must explore every potential ICBM tubule at every location in that tubule populated by an active ICBM. Missiles intercepted at some location are flagged and removed from the list of active incoming threats. In this way, the first opportunity of capture is considered for the active threats. This process can be altered to record additional intercepts of previously intercepted ICBMs if desired. Two additional functions are required before the simulation can step forward. First, the coverage statistics, containing the number and location of every intercept, must be gathered. A second function updates the list of active missiles and propagates their locations by a time step. Satellites and missiles are propagated forward in their own trajectories minute by minute as the simulation progresses.
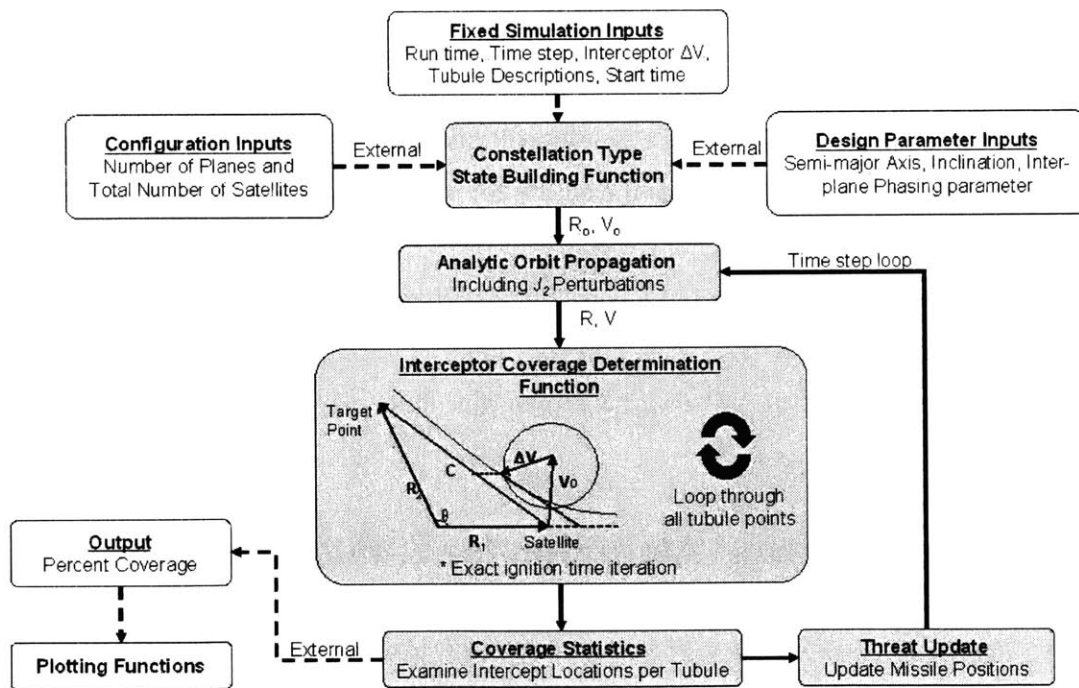
Figure 8.1: Flow Diagram of the Volumetric Coverage Determination Simulation

178

Volumetric coverage results are calculated for both existing constellations and for constellation design optimization (using SNOT.) The functional flow of the SNOPT design process is exactly the same as that given in Figure 6.2. Using this process, smaller configurations of existing constellation types can be developed using volumetric coverage. The algorithmic processes described here were implemented through functions in Matlab®.

8.2 Coverage Transition

Constellations optimized in Chapter 6, can be measured against the volumetric coverage metric. The optimized constellations from every constellation type and configuration, excluding eccentricity modifications and gap filling results, were tested using the volumetric coverage simulation. It was discovered that every constellation configuration achieved 100% volumetric missile defense coverage! One constellation of particular interest was the 69 one satellite-per-plane constellation that achieved only 91.85% fence coverage. This constellation now achieves 100% volumetric coverage. These results indicate that constraining interception to occur only on the fence is a severe limitation.

8.2.1 Histogram Understanding of Intercept Region

For Each tubule, an intercept can occur at any location. To gain intuition on volumetric coverage results, heuristics were created that measure the number of missiles intercepted at each point in the corridor. These results are best illustrated in a histogram of the number of intercepts per tubule location. Histograms show the first opportunity of intercept. Intercepts in the region of 21 to 31 minutes represent missiles approaching the terminating point of the tubules. Histograms with large numbers of intercepts in this region often indicate constellations with incomplete coverage. Using histograms helps to illustrate the lethality and robustness of a configuration. Constellations with intercepts closer to the beginning points of the tubules are more capable, since they may have more opportunities for additional intercepts. Several coverage histograms are given throughout this chapter.

8.2.2 Results from Fence Coverage Constellations

Due to all previously designed constellations resulting in 100% volumetric coverage, the coverage capability of the smallest configuration, explored under the fence coverage, is given as a test case. An interception histogram for the 69-satellite configuration of the single satellite-per-plane type is given in Figure 8.2. This simulation was completed over six hours for a total of 36,450 possible intercepts. The total simulation percent coverage, 100%, is denoted on the figure. A representation of the approximate fence location is depicted on the figure. As this curve shows, a great number of the missiles are intercepted well before the fence coverage barrier time, and all of them well before the terminal point. Additionally, it is known that this constellation can also provide 91.85% coverage at the fence barrier. This result shows that there are opportunities for multiple intercepts throughout the corridor.
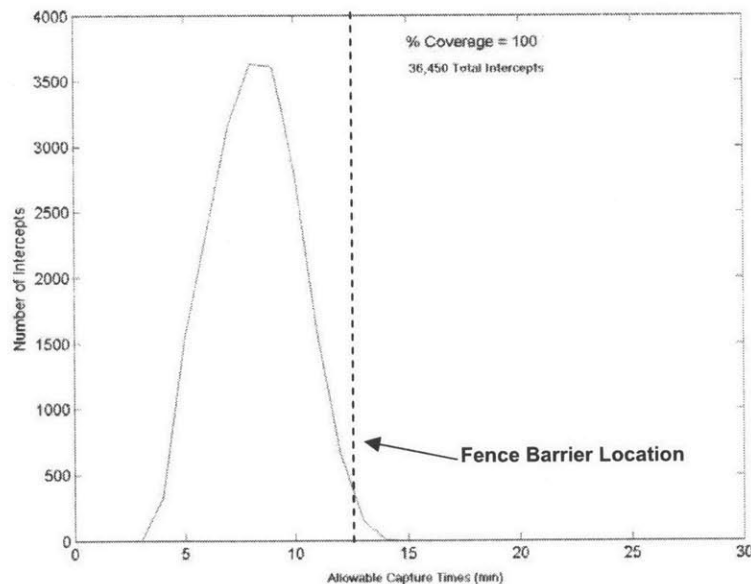
Figure 8.2 Histogram of Intercepts for a 69-Satellite Constellation

8.2.3 Coverage Simulation Animations

The design simulation in this scenario lends itself to the creation of coverage animations. Animations cannot be shown in this medium but will be described for the reader. They serve to visually depict coverage throughout the whole volume. As a simulation starts, missiles are initialized in each tubule. As time evolves, the location of the missiles and satellites will advance in their respective trajectories. Graphics of an example animation are given at 5, 10, and 14 minutes in Figure 8.3. Only the region of the Earth that contains the missile corridor is displayed in this animation. Each satellite is represented as a dot on the figure. The tubules in the missile corridor are represented by black lines emanating from North Korea. The light colored area in the missile tubules represents the continuous wave of active ICBMs. Both the satellites and missiles are shown advancing in their trajectories over the simulation time. Each of these figures was shot in an ECF frame moving with the Earth and centered over the missile corridor. Satellites begin to intercept missiles at the first available opportunity. Figure 8.4 represents the simulation at 15, 16, and 17 minutes. These snapshots from the animation show the missiles in the corridor being intercepted and thus removed from the tubules as the simulation progresses. Each satellite was capable of intercepting a significant number of ICBMs during its pass. Figure 8.5 is a final snapshot of the same constellation at the 18th minute. This figure shows the wave of active ICBMs knocked back to roughly the same point as the 5-minute snapshot. The simulation continues as waves of active missiles progress forward in their tubules and are knocked back again. In the animation of this example, the forward progression of the active missiles appears to throb within the corridor.
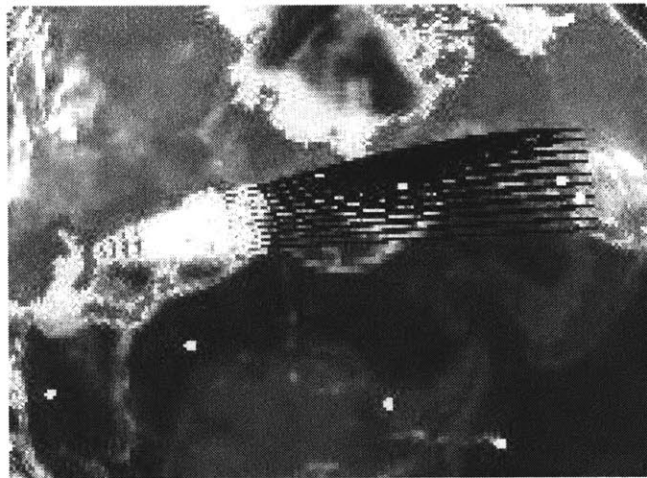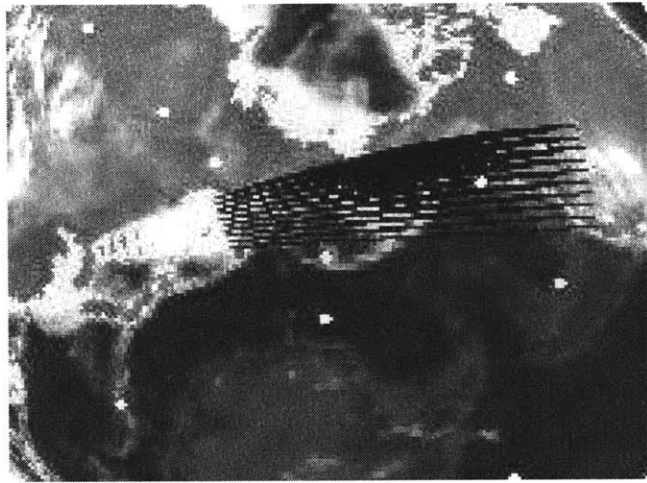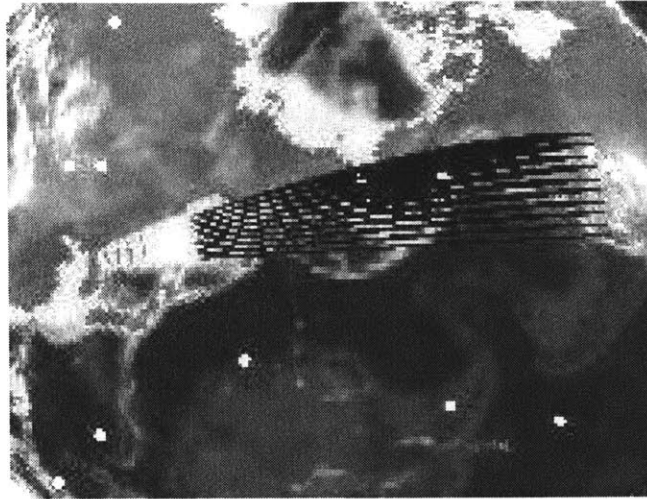
Figure 8.3: 5, 10, and 14-Minute Frames of Simulation Animation

ICBMs are starting to be intercepted

Few ICBMs remain
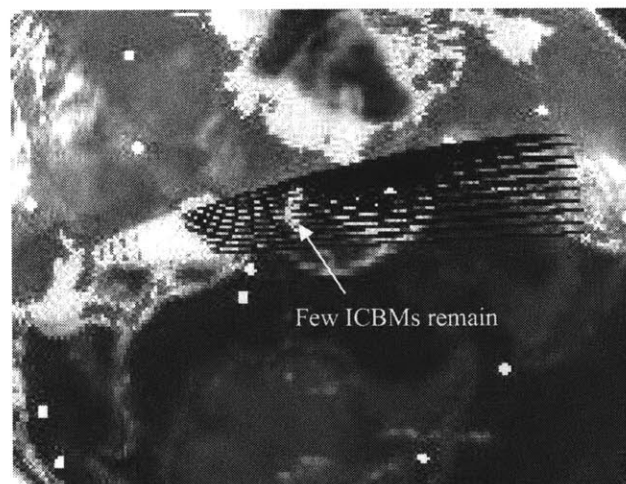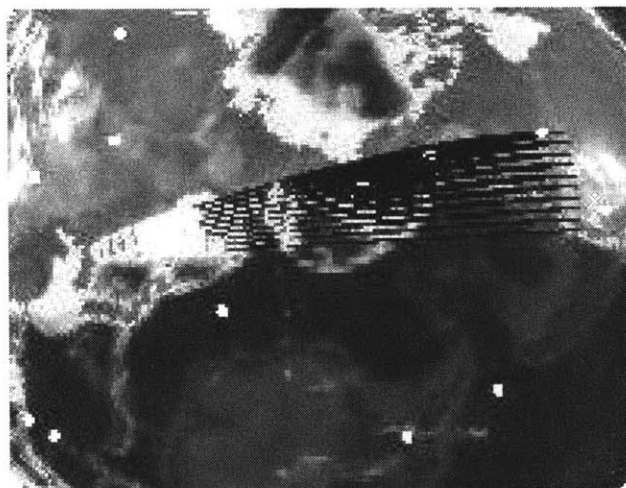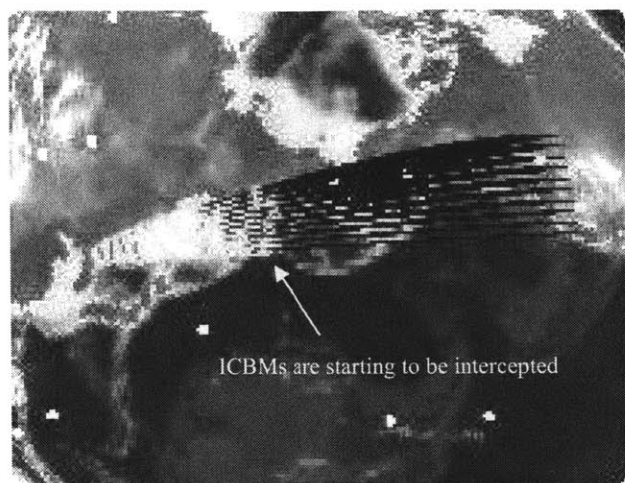
Figure 8.4: 15, 16, and 17-Minute Frames of Simulation Animation

183
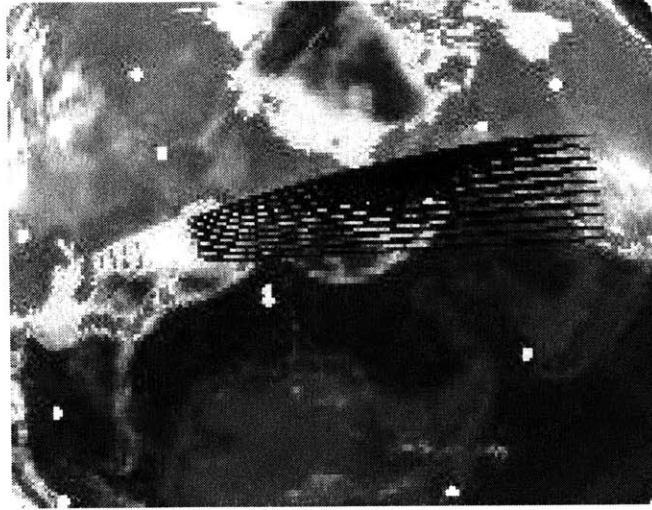
Figure 8.5: 18th-Minute Frame of Simulation Animation

8.2.4 Design Space Results

Due to exceptional volumetric coverage performance, an additional parametric exploration of the delta pattern configurations was completed. Smaller constellation configurations are optimized to maximize the new coverage definition. No a priori constellation design estimates were developed for this new coverage definition. For optimization of smaller configurations, the inclination, inter-plane phasing parameter, and semi-major axis were initially set to the average optimized fence coverage results. The following parameters were used to start each optimization: a semi-major axis of the optimized fixed Earth result (7470.3535 km), an inclination of 62.25 degrees (69-satellite configuration inclination), and an F of 2.4 (average delta pattern result). Once again the semi-major axis was optimized first for the constellation type. The remaining two parameters were optimized per configuration. The configurations in this scenario included the number of planes, P, and the total number of satellites, T. The total number of planes for this analysis was allowed to vary from 1 to 27 planes. The total number of satellites per plane was explored over a range from 1 to 25 satellites. In this manner, the volumetric constellation design space will encompass both delta pattern and single satellite-per-plane designs. Results of this section will include more delta pattern results than all of the previous fence coverage analysis.

184

Applying the volumetric coverage optimization scheme, the best constellation type was again the one satellite-per-plane constellation. With the new coverage definition, only a 21-satellite configuration is needed for 100% coverage. This configuration required an inclination of 62.26 degrees and an F parameter value of 2.335. This is a large decrease in the total number of satellites required for threat specific missile defense from the 116 required for fence coverage. Characteristics of the terminal interceptor closing velocities and approach angles for this constellation can be found in Figure 4.4 and Figure 4.5. Smaller configurations created here share the constellation symmetry of larger constellation and are capable of providing nearly zonal coverage over the latitude bounds of the missile corridor.

While this constellation is capable of 100% coverage with the fewest total number of satellites, it may not be the most desirable due to the fact that some ICBMs nearly reach their target. Any malfunction or misfiring could lead to an impact. This can be seen in the histogram, Figure 8.6, which shows a distribution of intercepts near the terminating tubule locations. The potential for failing to intercept a target increases greatly due to real world effects at the terminal point. These effects are the large capture and flight times used for terminal point intercepts, compounded with the buildup of propagation errors from estimated trajectories of the missile. For this reason, configurations with more satellites may be more desirable. Comparing this figure with the 69-satellite configuration, it can be seen that more satellites provide additional intercept opportunities. A design trade, of which 100% configuration to use, would explore the cost of more satellites versus the additional lethality that they would provide. It is left to the constellation designer and/or user to decide which is more important.
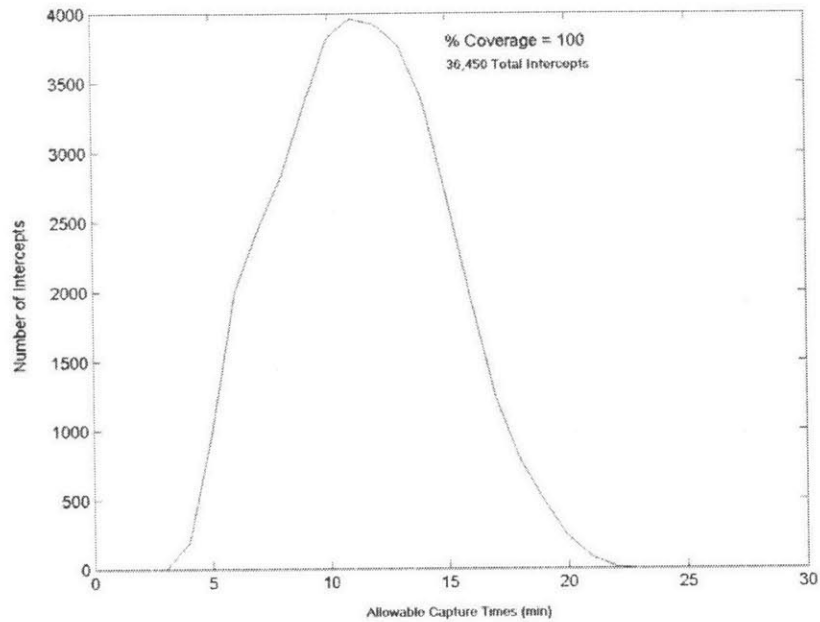
Figure 8.6: Histogram of Intercepts for a 21-Satellite Constellation

Volumetric coverage results for the entire delta pattern design space represent an array of possible design configurations. The percent coverage results from a full parametric exploration of the delta configurations are given in Figure 8.7. These results show that many configurations meet the 100% coverage requirement. The choice of a specific constellation that provides 100% coverage can be weighed against other design factors. The smallest configuration is identified on the figure along with several other 100% configurations. Note that the entire design space of the previous analysis, given in Figure 6.7, is contained in the 100% coverage region of this figure.
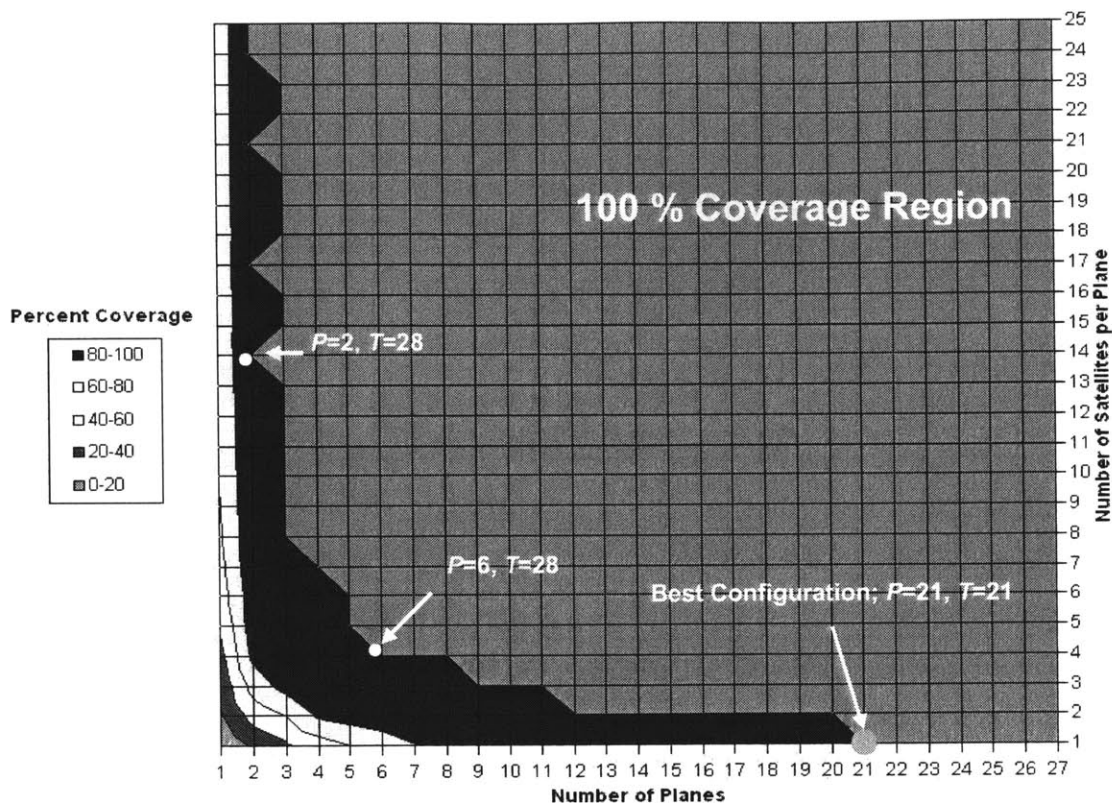
Figure 8.7: Volumetric Coverage Design Space Results for Delta Patterns

8.2.5 *Multiple Intercept Opportunities*

As mentioned with the 69-satellite configuration, there may be many opportunities for a missile to be intercepted during its flight. Either the same satellite platform or additional satellites may be capable of intercepting an ICBM over several time periods. When the ICBM's location is allowed to progress through a simulation after being intercepted, data on additional interception times may be gathered by the same bookkeeping functions. The ability of a constellation configuration to intercept an ICBM multiple times is defined as its lethality. In ballistic missile defense, increased defense comes with more lethal constellations.

The constellations constructed above can be explored in this manner to determine their lethality. The smallest effective configuration, with 21-satellites, was analyzed as a demonstration of the lethality. The histogram of intercepts is modified to show the

187

number of intercepts per location in the tubule along with the number of times a particular missile has been intercepted. Another histogram can be created from this data stating the total number of intercepts for each fold of coverage. With this data one can determine if 100% coverage can be maintained by only looking at the second, third, and so on opportunities for intercept. Using the optimum 21-satellite configuration, a lethality analysis shows that some ICBMs can be intercepted 24 times. This means that those ICBMs have 24-fold coverage. A bar graph of the total percent coverage per number of possible intercepts of an ICBM is shown in Figure 8.8. The bar representing 1-fold coverage signifies all ICBM are intercepted for 100% coverage. This figure shows that the 21-satellite constellation is capable of intercepting 90% of the ICBM's 6 times. Additionally, 50% of the ICBM's can be intercepted 11 times. The ability to intercept missiles additional times drops significantly after this point. Figure 8.9 represents the same results seen in Figure 8.6 with lines signifying the distribution of the intercept locations for each fold of ICBM coverage. The data from 1 to 17-fold coverage is given in the figure to show the trend in the intercept distributions. The number representing the fold of coverage is identified near the peak of each individual histogram line. The peaks of these curves tend to move back towards the terminating locations. The peaks also appear to grow and then decrease as the available room for intercepting multiple times decreases. These results also show that the lethality capability inherent in volumetric coverage could not be exploited using only the fence coverage definition.
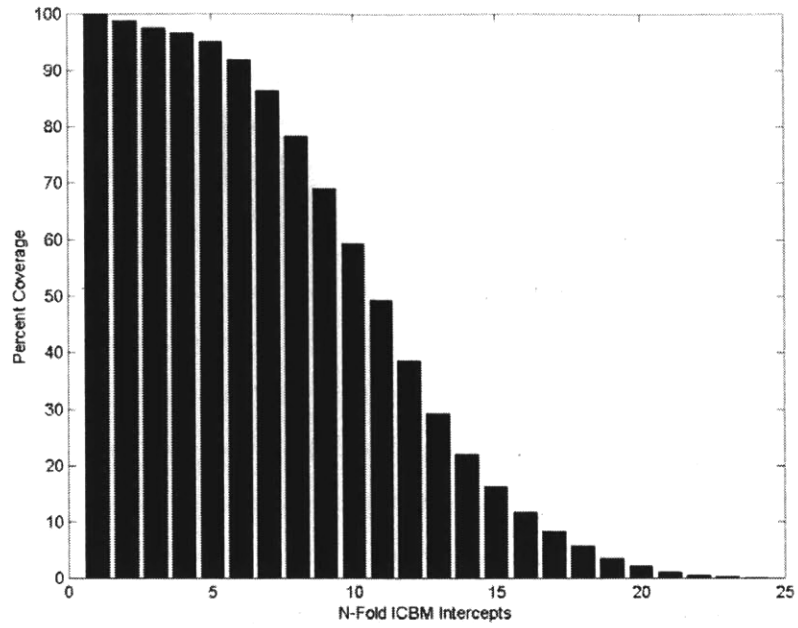
Figure 8.8: 21-Satellite Percent Coverage per N-Fold ICBM Intercepts
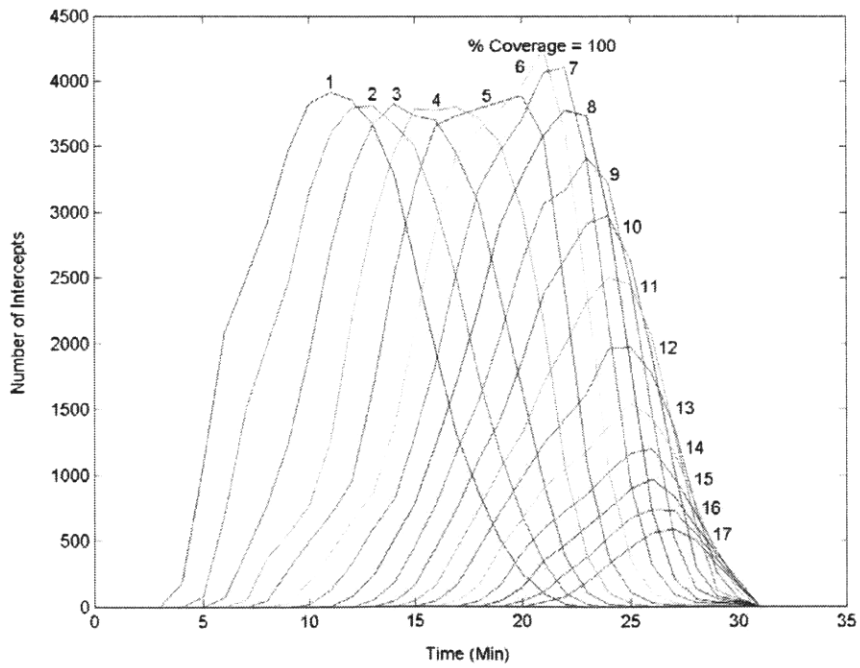
Figure 8.9: Lethality Histogram of Intercepts for 21-Satellites

189

8.2.6 Alternative Constellation Development

No constellations in this chapter were designed solely from abstracted classical methods as was possible with the fence coverage. The constellations developed here are the result of volumetric coverage optimization around an estimation of the a priori design. Fence coverage results were used to establish this a priori estimate. A question may arise at this point pertaining to how good was the initial approximation of fence coverage for designing optimal volumetric coverage constellations. To understand the differences between the coverage from configurations developed around different optimizing goals, the 21-satellite configuration was also optimized for fence coverage. Optimizing 21 satellites for fence coverage, it was found that the constellation was capable of 32.21% fence coverage. This 21-satellite constellation only provided 99.79% volumetric coverage. The histogram of volumetric coverage results for this constellation is given in Figure 8.10. This figure is very similar to the intercept histogram given in Figure 8.6. However, the figure now shows more intercepts occurring near the terminal points of the tubules. This result shows that fence coverage optimization is insufficient to create optimum volumetric coverage constellations. The volumetric simulation is necessary to tweak the design parameters properly for the best coverage results. However, the fence coverage results did provide good constellation design estimates that could be optimized for volumetric coverage.
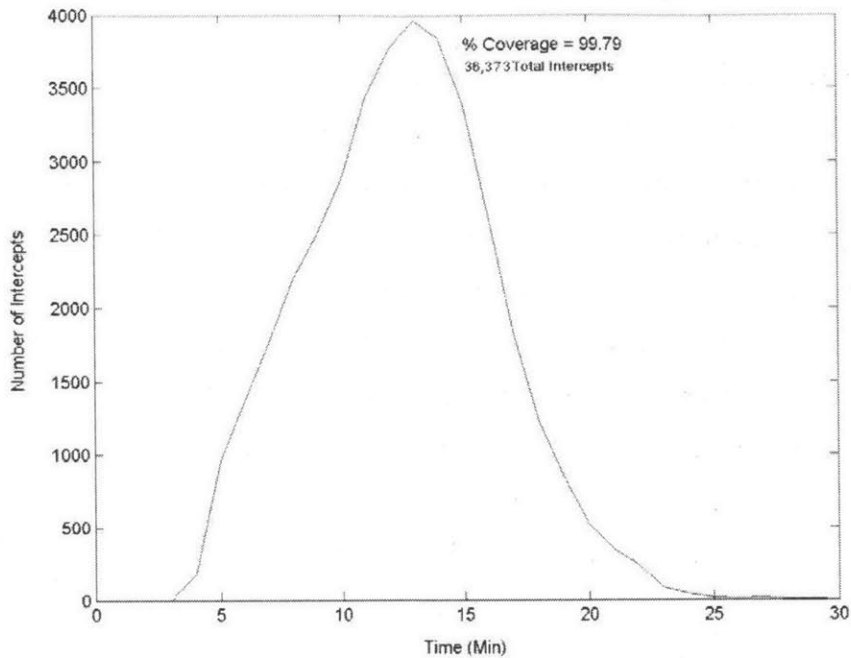
Figure 8.10: Fence Coverage Optimized, 21-Satellite, Intercept Histogram

8.3 Variability of Design Space

This section will attempt to open up the design space to possible changes in the fixed interceptor ΔV and in the singular nature of the threat. The algorithms and functions described throughout this work are capable of handling such changes. From a system design standpoint, it is desirable to determine the effects in constellation design for different available ΔV intensities. Constellations capable of 100% defense from additional threats beyond North Korean are more desirable. Constellations with the excess deniability are especially important when attempting missile defense from global threats for CONUS protection. There are many other possibilities for refining the constellation design trade-space. The design possibilities and results explored here serve as two such metrics for trade-space refinement.

8.3.1 Interceptor Capability

The interceptor's ΔV value was determined from the abilities of existing interceptors. This value was assumed to be a conservative 1.3 km/sec. It was for a fixed impulsive burn corresponding to a chemical rocket firing. Realistically, any type of rocket ΔV or directed energy technology could be used as the interceptor. Interceptors capable of continuous thrust and directed energy concepts require a slight modification to the coverage determination mathematics.

This section will explore the use of an increased ΔV. The ΔV will be more than doubled to 2.8 km/sec for this analysis. When this is applied and volumetric coverage determined, it can be seen that missile intercept becomes an easier task. This increase more than doubles the size of the interceptor reachability envelope. The intercept histogram of the 69-satellite configuration is given in Figure 8.11. This figure shows that all of the first opportunity intercepts now take place well before the previous fence barrier location (about 12 minutes.) When increased ΔV is applied to the 21-satellite configuration, the results look very much like the original volumetric results for the 69-satellite constellation. The 21-satellite configuration results are shown in Figure 8.12. The full design space of delta pattern configurations was not explored with this increased capability. Doing so may produce a smaller configuration capable of 100% missile defense. The figures given here can be compared with their respective intercept histograms given in Figure 8.2 and Figure 8.6 earlier. Decreasing the ΔV has the reverse effects.

192

% Coverage = 100
36,450 Total Intercepts
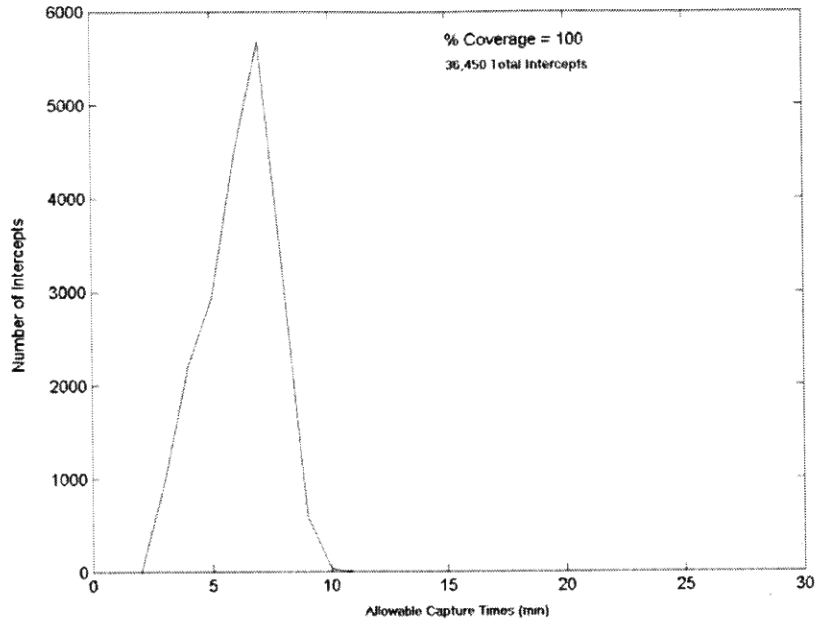
Figure 8.11: Intercept Histogram, 69-Satellites with a 2.8 Km/sec ΔV

% Coverage = 100
36,450 Total Intercepts
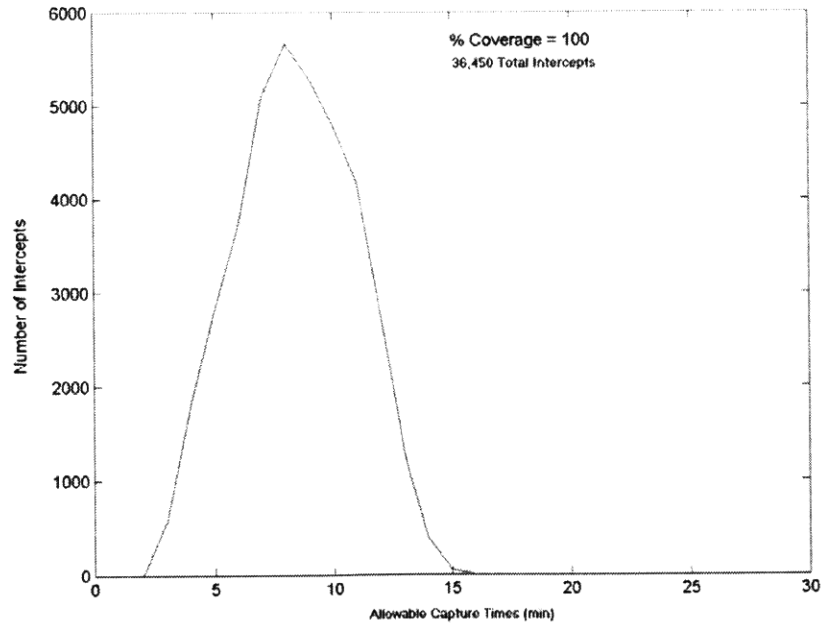
Figure 8.12: Intercept Histogram, 21-Satellites with a 2.8 Km/sec ΔV

193

8.3.2 Additional Threat Deniability

Constellations up to this point were designed for defense against a simulated missile launch from North Korea. The notion of expanding the list of threatening countries and available targets was discussed in detail in Chapter 7. A larger threat corridor (set of ICBM tubules) was created and can be identified in Figure 7.6. Several, previously optimized, constellation configurations were tested against this new threat corridor. No additional optimization was performed on the design parameters of these constellations. A missile defense constellation would be much more valuable if it were capable of defending the whole CONUS against multiple threats.

The scope of the defense capability of volumetric coverage constellations first focused on an enhanced North Korean range capability. This capability is illustrated in the graphic of Figure 7.4. This figure illustrates the threat corridor of ICBMs if North Korea had the ability to hit any point in the CONUS. A simulation was developed substituting the previous missile tubules for those used in a launch from North Korea to all of the target cities in Table 7-1. These tubules are not a dense set but they will give a good estimation of the true defense capability.

The 21-satellite configuration, described earlier as the smallest configuration capable of complete coverage, was tested in this simulation. The resulting coverage heuristics of the six-hour simulation are given in Figure 8.13. As illustrated in the figure, tubules against the CONUS have flight times slightly greater than those previously examined, ranging from 21-39 minutes in length. It was found that the 21-satllite configuration is still capable of 100% missile defense for the whole CONUS. This is an interesting result given that the constellation was not designed for such an expanded threat corridor. The histogram of intercept locations illustrates that a majority of the intercepts occur in two regions of the tubules, one region near the beginning and one near the terminal point in the tubules. This is not a favorable result despite the continued 100% coverage. This is because most of the intercepts in the later region take place near the terminal points of the tubules leaving no room for error. It was observed in simulation animations that ICBMs, in tubules in or near the original threat region, were intercepted

more frequently near the corridor beginning. Missiles in tubules outside of the original corridor, i.e. those over the polar region, were more difficult to intercept. Note that this constellation type was designed to provide zonal latitude coverage bounded by the latitudes of the original corridor. The delta patterns designed earlier cannot intercept ICBMs when those missiles are over pole.
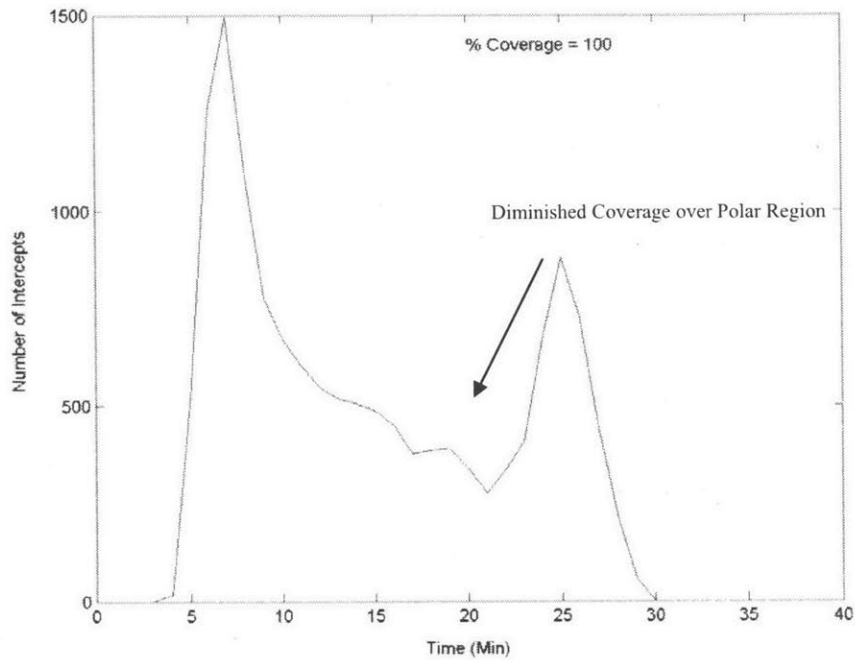
Figure 8.13: Intercept Histogram of 21-Satellite Configuration for CONUS Defense

The additional launch threats from across the globe is a natural extension of this analysis. The threat corridors can be seen in the illustrations of Figure 7.6. The first analysis will once again explore the capability of the 21-satellite configuration designed to defend against only a North Korean ICMB launch. Results of a six hour simulation show that the constellation is only capable of 98.1624% coverage from the global threats. Figure 8.14 depicts the intercept histogram for this simulation. The figure clearly illustrates that there are again two primary regions for intercepting ICBMs: before and after they traverse the polar region. Star patterns or higher-inclination delta patterns may provide better coverage against this global threat, and could be the subject of future work.

Trajectories from Libya, India, and Pakistan to the Western United States were the primary contributors of missiles escaping intercept. It is more difficult for the constellation to intercept these retrograde orbits. Missiles in these trajectories are in retrograde to polar orbits at slightly higher than normal altitudes, due to the relative positions of the launch and target locations.
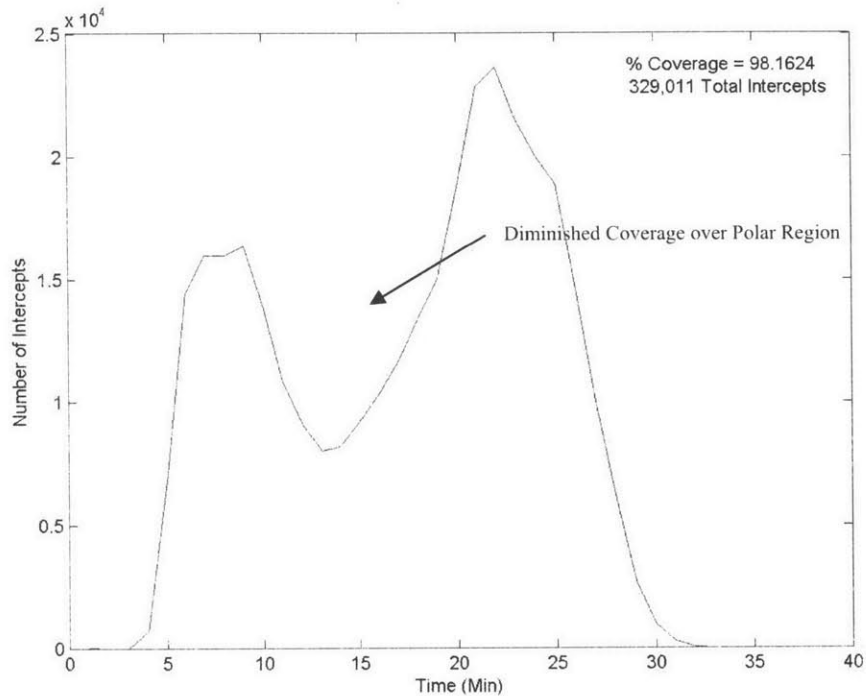
Figure 8.14: Intercept Histogram of 21-Satellites for Global CONUS Defense

This simulation was also run with both the 69-satellite fence coverage optimized constellation, and the 21-satellite volumetric coverage optimized constellation with an increased, 2.8 km/sec, interceptor ΔV. Since the threat trajectories are not based on current, but rather the future missile technological capability of each launching nation. Simulation results from each constellation are shown in the intercept histograms below. Figure 8.15 illustrates the intercept capability of the 69-satellite constellation. This constellation was able to obtain 100% defense of the CONUS from a global array of launch threats (with only a 1.3 km/sec interceptor ΔV!) The figure shows two large and distinct regions where more intercepts occur due to the delta pattern design of this

constellation. Figure 8.16 illustrates the results of the 21-satellite constellation with an increased interceptor ΔV. This constellation is capable of 99.87% coverage. In this figure, the relative sizes of the two distinct coverage regions are flipped from those of Figure 8.14. Increased ΔV allows for more intercepts earlier in the tubules. The only misses were missiles launched from Libya. These results show that existing constellation designs for a singular threat region have extended threat deniability capabilities beyond their original designs. With simple modifications and/or the addition of a small number of satellites, space-based mid-course missile defense from a global threat environment can be a realistic possibility.
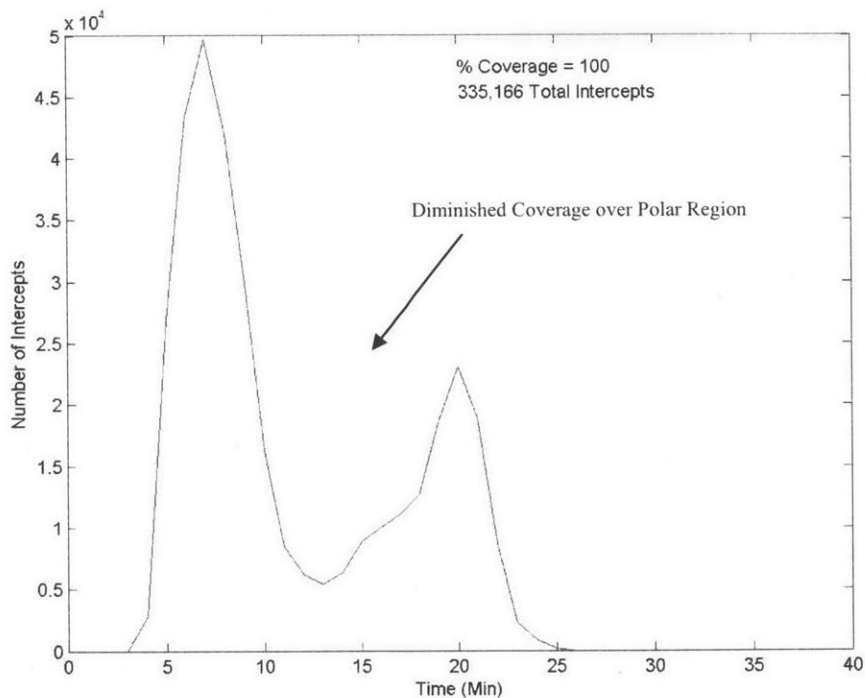
Figure 8.15: Histogram of 69-Satellites, 1.3 km/sec ΔV, for Global Defense
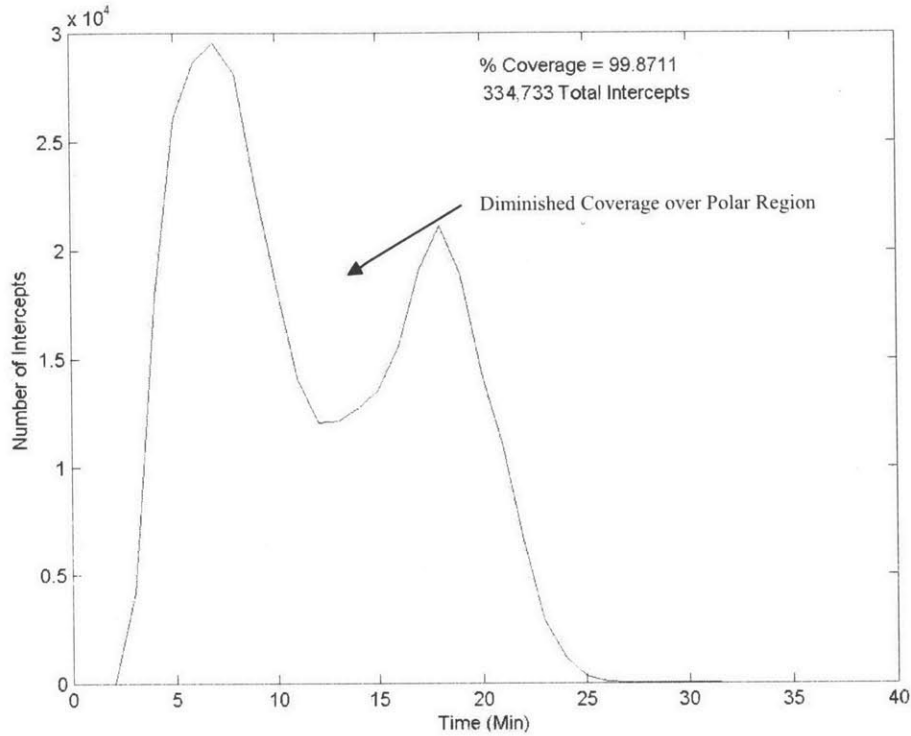
Figure 8.16: Histogram of 21-Satellties, 2.8 km/sec ΔV, for Global Defense

8.4 Summary of Volumetric Coverage Results

Volumetric coverage applied to the optimized results of Chapter 6 showed that all of the previous constellation designs were capable of 100% missile intercept. While the fence coverage definition was not the best approach for constellation design, it was a tractable design method that allowed for a priori estimates of volumetric constellation design methods. Volumetric design optimization reduced the number of satellites needed for defense against the Taepodong threat from 116 to 21. A 21-satellite delta pattern is much more cost effective to launch than a 116-satellite configuration. The multiple intercept capability of the 21-satelite case illustrates the potential for additional intercepts if a first-opportunity intercept failed. Other volumetric heuristics were provided, such as the location statistics of each intercept. Table 8-1 illustrates a summary of the volumetric coverage analysis.

Table 8-1: Minimum Satellite Configuration Summery

Constellation Analysis	Total Number of Satellites	Important Parameters	Key Design Advantages
Regular Delta Pattern	21	P=21 F=2.335 i=62.25° a=7470.3535 km	This 100% configuration has the smallest total number of satellites of any developed in this research. Volumetric coverage serves to enhance the capability of constellations of satellite-base interceptors
Multiple Intercept Capability	21	27 Fold Coverage for some ICBMs	Nearly 100% capability for multiple folds of coverage. Greater safety through redundant intercept solutions
Increased Interceptor ΔV	21 & 69	2.8 km/sec	Increasing interceptor ΔV has the effect of shifting the location of intercepts to the tubule beginnings. Greatly improves constellation capabilities.
Increase Threat Deniability Region	21	North Korea Vs. CONUS & Global Threats Vs. CONUS	21-Satellite constellation can defend the CONUS from North Korea. However, it is only 98% effective at protection from global threats. Increasing the number of satellites or the ΔV allows for increased CONUS protection from global threats.

The extensive delta pattern design space results, given in Figure 8.7, illustrate the range of available configurations capable of 100% defense. Allowing for more satellites in a constellation gives a designer greater freedom in choosing which configuration to use, among all those that are 100% effective. Constellations with fewer planes could potentially be launched entirely on a few launch vehicles. Additional intercept capabilities of a constellation can be explored within the 100% coverage region to help refine this design space. Inspection of a constellation's threat deniability allows a designer to choose a configuration that provides more defense power with the same number of satellites.

199

[This Page Intentionally Left Blank]

Chapter 9

Conclusions and Future Work

The objective of this thesis is to present several approaches to the development of constellations for mid-course ballistic missile intercept. Satellite-based missile defense could potentially add a capable defensive layer to existing and future missile defense programs. Satellite-based ICBM intercept requires a new formulation of satellite coverage based on a fixed-impulse ΔV and time limited intercept capability. Interceptor coverage is determined through an iterative mathematical process that computes the exact ignition time necessary for missile intercept. This new coverage paradigm is adopted in the development of constellations to ensure mid-course missile defense from a postulated North Korean threat.

The satellite constellation design concepts developed here are adapted from classical design methods. Several constellation design techniques are applied to the missile intercept problem, ranging from an abstracted streets-of-coverage method for creating symmetric circular-orbit constellations, to constellations designed from the optimized placement of coverage timelines. Several methods, that modify existing constellation types to improve their ability to provide mid-course defense, are also developed.

Applying new coverage definitions, classical constellation design methods, and optimization tools, standard constellation types are optimized to maximize missile defense coverage. Results of the design and optimization process show that there are many constellation types and individual configurations capable of achieving complete missile defense from North Korea. The constellation type with the fewest total number of satellites, found to accomplish 100% coverage, was a single satellite-per-plane pattern with 21 satellites. Additional coverage capabilities of the constellation design space are

explored to understand the full protection and deniability of pre-designed constellations. This chapter will highlight the important conclusions reached throughout this research. Additionally, constellation design issues and applications of this research are discussed. The chapter concludes with the author's recommendations on future work applications.

9.1 Conclusion Summary

Current missile defense programs have some boost phase, mid-course phase, and terminal phase capabilities. Nearly all of these capabilities are ground-based. Ground and space-based sensors systems are currently on-line and capable of detecting enemy missile launches. One additional measure of protection could potentially be space-based interceptors. A constellation of satellite-based interceptors could provide an additional layer of defensive capability. Space-based mid-course missile defense has been shown, through this research, to be achievable with a small number of space-based interceptors.

This thesis explored the development of a constellation for the defense against a postulated North Korean missile launch. This is one example of a rogue nation with potential ICBM capabilities seeking nuclear weapons. A launch from such a nation could be difficult if not impossible to defend against with current defensive systems. The constellations designed here will be applied to the protection of the United States from this threat. The constellation design approach can be adapted to other threats as needed. Constellations designed to protect against the North Korean threat are also capable of protecting the CONUS from additional global threats.

9.1.1 Interceptor Coverage Development

The postulated capability of the North Korean Taepodong ICBM directly threatens a large portion of the western United States. This research explored the protection from any launch capable of hitting the Western Hemisphere over a range from Anchorage, AK to Los Angeles, CA. The threaten region extends over an azimuth from Los Angeles to Bismarck, ND. The collection of missile trajectories capable of hitting this threatened area is considered the missile corridor. Complete missile defense is only

achieved by not allowing any missiles to travel completely through the missile corridor. The trajectories in this corridor are based on the minimum energy flight path. Considering non-minimum energy trajectories, like those used for lobbing or suppressing a flight path, could extend this corridor roughly 200 km vertically. However, this is not a concern because interceptor reachability envelopes usually extend a couple thousand kilometers above the corridor.

Satellite based interception of a ballistic missile requires placing an interceptor at the same physical location and at the same time as the incoming missile. Terminal stage conditions, such as closing speed and terminal approach angle, were not considered in the constellation design process, but statistics of these results were collected. For the 21-satellite volumetric constellation, the relative closing speeds are usually between 3 to 9.5 km/sec. Orbital analysis of the interceptor's firing time, direction, and transfer orbit are calculated through an iterative use of the hyperbolic locus of velocity vectors connecting any two points in an orbit. The transfer orbit is formed about a two-body mathematical relationship. The interceptor reachability manifold is defined as the swath of space that a fixed impulse interceptor can reach within a bounded flight time. This manifold describes all potential intercept locations.

9.1.2 Fence Coverage Constellation Design

Using interceptor reachability to intercept a missile at a fence in the threat corridor provides a constrained coverage definition. The fence barrier is a vertical slice through the missile corridor at a specific location over the Earth. Fence coverage simplifies the intercept problem by specifying the intercept location. Coverage of the fence at all times ensures 100% missile defense. The fence location was intuitively chosen and may not be the optimal placement for such a barrier.

Many methods of classical constellation design were adapted for missile defense. Additionally, new schemes were developed to fill in coverage gaps, and add eccentricity to symmetric constellations. The design goal of this thesis is to create constellations with the fewest total number of satellites capable of 100% missile defense.

9.1.3 Fence Coverage Design Results

A priori constellation designs are obtained from an abstraction of classical methods which do not provide optimal fence coverage. Constellation design parameters were optimized to obtain maximum missile defense capability, using either a gradient-based nonlinear programming package (SNOPT) or a genetic algorithm package. The nonlinear programming package was computationally faster, but could result in locally optimal results (instead of globally optimal results.) The genetic algorithm allowed for more freedom in the design process and more likelihood of achieving a globally optimal answer. However, the genetic algorithm process was slow and cumbersome.

The smallest constellation found to provide 100% fence coverage was a 116-satellite configuration from the single satellite-per-plane constellation type. A great many configurations were explored within each constellation type. It was found that the circular-orbit symmetric constellations tended to provide better coverage results with fewer numbers of satellites per plane. However, asymmetric constellation types, or those with too much symmetry, tended to have diminished coverage results.

Additional modifications to constellations developed for fence coverage included the use of eccentric orbits and constellation gap filling. Constellation gap filling is motivated by the need to correct outages in symmetric constellation coverage with asymmetric orbit placement. This is done in an effort to reduce the total number of satellites, but was found to have only limited benefits in the few test cases considered. An additional modification was applied through the use of slightly eccentric orbits. A small bit of eccentricity was added to existing constellations in an effort to further maximize coverage. Several constellations benefited from the addition of small amounts of eccentricity. Coverage from symmetric constellations benefited the most from eccentric orbits. However, these modifications were not successful in achieving large improvements in coverage.

9.1.4 Volumetric Coverage Constellation Design

Limiting the intercept of any missile to a single location on the fence barrier is a significant constraint. While tractable for classical design adaptations, the fence coverage definition is too restrictive. Allowing an intercept to take place at any location in the corridor adds back a degree of intercept freedom at a cost of increased computation time. Volumetric coverage is an expansion of fence coverage. It allows for missile intercept at any point in the mid-course flight. Volumetric coverage is more complex, and as such an a priori constellation cannot easily be abstracted from classical design concepts. Constellation types that fared the best with fence coverage were measured and optimized using the more robust volumetric coverage.

Constellations producing 100% coverage can also be judged on a number of other intercept metrics, such as the lethality of the constellation, the protective capability, and the global threat deniability. Volumetric coverage provides a means for such additional intercept analyses.

9.1.5 Volumetric Coverage Results

All previously optimized fence coverage constellations, applied to the volumetric definition, produce 100% volumetric coverage. Additional constellations were created to determine the smallest configuration capable of 100% volumetric coverage. The smallest configuration, of the single satellite-per-plane constellation type, contained 21 total satellites. A large number of additional configurations were also capable of obtaining 100% missile defense coverage from the North Korean threat. It was found that the 21-satellite constellation also provided nearly four-fold 100% coverage. Increasing the interceptor velocity allowed for interceptions at earlier points in the corridor. The 21-satellite constellation was also capable of 100% defense for the whole United States from any future North Korean missile capability.

9.2 Constellation Design and Maintenance Costs

Constellations with the fewest total number of satellites might not be the best choice for every constellation application. The parametric expanse of configurations presented here, allows a designer to look at other criteria, when choosing which 100% configuration to use. Some real-world design criteria for constellation designs are described below.

9.2.1 Launch Costs

Launch costs are some of the most applicable real-world design factors for selecting a constellation. Constellations with hundreds of satellites are unreasonable to launch and setup, unless the satellites are very small. Constellations with more satellites per orbital plane, and fewer planes, are less expensive to launch. Each set of satellites in a unique orbital plane require either their own separate launch vehicle, or fuel to establish themselves in their orbital plane. If multiple satellites can be launched on a vehicle, then less fuel would be required to properly space several satellites with the same orbital inclination. It is much easier to change orbital planes and spacing within those planes if all the planes have the same inclination. An entire symmetric constellation with the same inclination could potentially be launched using very few individual launch vehicles. Ad-hoc and asymmetric constellations are more difficult and costly to launch for these same reasons.

9.2.2 Maintenance Costs Due to Perturbations

Any constellation of satellites will require some amount of fuel to ensure proper placement within the constellation and maintenance of the configuration. All of the constellations discussed in this work are in relatively low Earth orbit at altitudes of roughly 1000 km. Satellites in lower orbits experience significant drag effects and thus have shorter usable lifespan, without orbit adjusting maneuvers. For the orbits considered here, drag is not a major issue for constellation maintenance. Higher orbits would require additional launch capability and thus higher launch costs. At higher altitudes,

206

perturbations like solar radiation pressure and third-body gravitation will have a larger relative impact on the orbit. The orbital effects of the zonal J_2 geo-potential perturbation have the largest impact on the orbit by several orders of magnitude over all other perturbations for this altitude[58]. For this reason, only the J_2 perturbation was used in this research. In symmetric commonly inclined constellations, all of the orbits feel the same zonal perturbations. In such constellations no fuel is required to make-up for J_2 perturbations. However, third-body perturbations will pull even symmetric constellations apart by affecting each orbit individually. The largest maintenance costs will be imparted by negating the effects of such perturbing forces in orbit. Designers, wishing to create missile defense constellations, must consider such issues when choosing their constellation.

9.3 Future Work Recommendations

Constellations developed for missile intercept purposes were designed with only one coverage goal: defense against a Taepodong missile attack from North Korea. Additional design constraints and objectives can be explored. The methods employed to solve the constellation design for the space-based mid-course intercept problem can be applied to other applications where sensor payloads have time, range, and/or velocity constraints.

9.3.1 Additional Constellation Design Factors

There are many additional areas in which the constellations can be evaluated when developing a design. Issues such as the number of planes and their placement affect the launch costs as previously mentioned. However, these issues also affect the ground operations involved with the constellations. Constellations with erratic plane placement and large numbers of planes are usually harder to monitor and maintain. If very few satellites are required per orbital plane, sparing additional satellites, in the event of an on-orbit failure, becomes a more difficult task. One aspect of future work could incorporate launch and operation issues of a constellation into the design criteria.

207

The development and optimization of constellations for global deniability and complete protection of the United States represents an area of future work. This problem has been considered briefly in this thesis, by measuring the effectiveness of a regionally designed constellation against a more global threat. From these initial results, it is apparent that effective global defense could be established with higher inclination constellations and more analysis. The design techniques, and software tools, documented in this thesis are readily applicable to this larger problem.

Another area of future work is the bounds of the missile threat corridor. The starting and terminating points of the allowable intercept region per trajectory are variable. These values were constrained to a common point in the fence coverage analysis. However, the terminating point can be constrained not to allow missile over-flight of the CONUS or other allied countries. Constellation design could then be focused on maximizing coverage in these smaller corridor volumes.

Interceptors in this analysis were based on the capability of a chemical rocket. Throttlable and highly maneuverable interceptors could lead to quicker and more accurate intercept geometries. The terminal stage of the intercept was not a constraint in this work. Future work should include defensive strategies and additional requirements on the terminal stages of intercept. Head-to-head closing geometries and relative closing speeds are examples of such terminal state restrictions. As a research note, the terminal conditions for a head-to-head closing geometry were explored by inverting the 21-satellite configuration (from volumetric analysis) into a retrograde orbit with an inclination of 117.7371 degrees. Figure 9.1 and Figure 9.2 illustrate histograms of the number of intercepts to the relative terminal interceptor closing-speed and the terminal approach angles (zero degrees represents a tail chase) respectively. The terminal intercept conditions for the nominal 21-satellite constellation were explored earlier in the development of the intercept problem. This constellation nearly achieved 100% coverage from the standard North Korean threat without any optimization of its design parameters. Varying the inclination of the constellation will greatly impact the terminal intercept conditions. If higher closing speeds and head-to-head geometries are desired, then a mix

of retrograde and prograde constellations, i.e. a 42-satellite constellation, would allow a range of terminal velocities and approach angles to select from for each intercept.
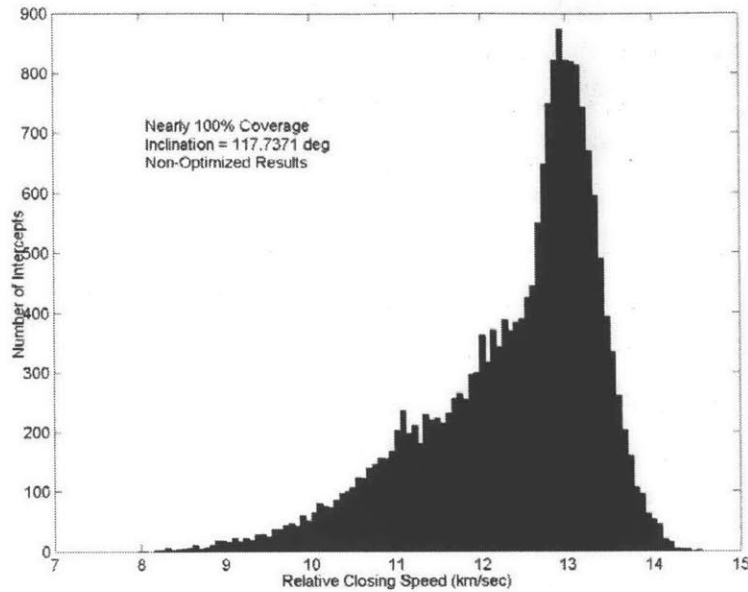

Figure 9.1: Histogram of Retrograde 21-Satellite Relative Closing Speeds
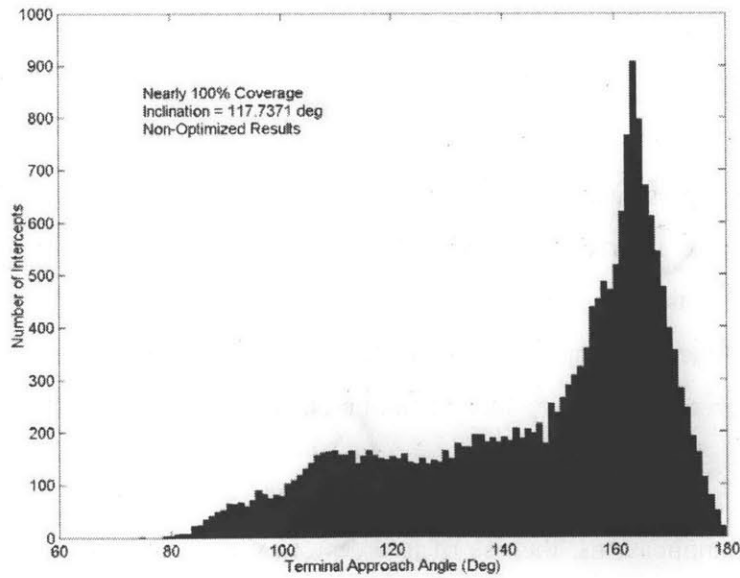

Figure 9.2: Histogram of Retrograde 21-Satellite Approach Angles

When determining the intercept histogram for volumetric coverage, an interesting statistic is the number of intercepts per remaining ICBM time to target. This slightly different view of the data would give a more accurate picture of how close to the threatened area ICBMs get before interception.

Another design metric is the lethality index of a constellation. This index is essentially the number of times an ICBM can be intercepted by space-based assets. By adding a lethality index to the constellation design, future configurations could be optimized for greater than 100% coverage.

Currently, there is not an analytic method available for determining when a constellation will precisely repeat some initial state. An exact determination of this repeat cycle would allow for a more complete analysis of existing constellations, and possibly the creation of other constellation types.

Constellation types involving highly eccentric orbits and/or highly asymmetric arrangements were not considered in this work, but have been shown to produce interesting coverage results in other applications. Constellation design methods, types, and configurations discussed in this research are merely a small selection of a much greater design space.

9.3.2 Additional Application of Design Methods

The work presented throughout this thesis has been a conceptual exercise of space-based missile intercept and constellation design. The constellation designs and coverage definitions developed here can be applied to additional satellite-based applications[10]. One such application is the use of satellites for space-based anti-satellite engagement or protection. The principles and methods could be easily adapted to engage or protect existing satellite assets.

In other applications, the use of interceptors with conventional rockets could be replaced with directed energy concepts. In particular, any application that lends itself to a range and/or power limited reachability envelope can be explored with these methods, i.e.

210

satellites with laser, radar, or telecommunication payloads. Constellations for electronic jamming or eavesdropping could use the same localized coverage techniques for constellation design. Constellations with enhanced coverage over one region and limited range capability, like those discussed for missile intercept, could be applied to high powered communication or imaging constellation purposes. As these examples illustrate there are a great number of satellite-based applications where sensor or payload capability is limited by range, velocity, and/or time. The research conducted here could have a potential benefit to the design of constellations for such applications.

[This Page Intentionally Left Blank]

Appendix 1

Optimization Applications

This appendix is an aid to readers unfamiliar with optimization and/or the optimization software used throughout this research. The first section will explain basic concepts of optimization. The following sections will discuss the software optimization packages and their implementation within in this thesis. The focus of this work is the design of constellations for the purpose of space-based ballistic missile intercept. Optimization was used as a means by which to tweak constellation design parameters, of a specific configuration, to obtain maximum coverage. Therefore this thesis used optimization only as a tool for enhancing results. Some additional optimization concepts were developed to enhance the computation time of simulations. The methods and implementation of such concepts are discussed below.

A1.1 Optimization Basics

Optimization is the process in which a set of variables, belonging to an objective function, are chosen to provide a maximum or minimum value of that function. The objective function can be any mathematical expression of a desired goal. In this research, the objective function is the percent coverage a satellite constellation can obtain over some time period. Maximizing this function involves picking the best combination of constellation design parameters. In basic calculus, optimization of a function, $f(x)$, involves determining the value of x that will make the derivative of the function, $f'(x)$, equal to zero. If x has the highest objective value in a surrounding region, it is a local maximum. Likewise, if x has the lowest value in a region it is a local minimum. The second derivative of the objective function at x is another method for determining maxima and minima. If the local maximum or minimum value is the highest or lowest for all other values of x in the function, then that x is the global maximum or minimum.

The coverage objective function in this thesis is a non-linear multi-variable function. Optimization using derivative information from multiple variables involves an analysis of the final value to ensure a saddle point has not been reached. Saddle points are points where the partial derivatives of the function have zero value, but objective function value is not the local maxima or minima.

Constraints are used to limit the scope of certain variables or linear functions of those variables. One analytic approach to dealing with multi-variable constrained optimization problems is the use of Lagrange Multipliers, λ. Using this process, a tailored n-variable objective function, $J(x_1,x_2,..., x_n,\lambda_1,...,\lambda_m)$, is created by adding m constraint functions, $g(x_1,x_2,...x_n)$ and their corresponding Lagrange Multipliers[6],[49]. The functional setup is illustrated in Equation (0.1). Lagrange multipliers represent the negative rate of change of an objective function with respect to the constraint functions. This expression is illustrated in vector form in Equation (0.2). Optimization of the tailored objective function with Lagrange multipliers is identical to classical calculus optimization. The optimum value of tailored objective function is reached when the $(x_1,x_2,..., x_n,\lambda_1,...,\lambda_m)$ values generate a zero functional derivative. This method is graphically represented in Figure 0.1. In the figure, dotted circles represent lines of increasing equipotential-value of the two-variable objective function. A constraint function is also denoted on the figure. If one wishes to find the maximum unconstrained value, the optimum point would be the point (A, C). The constraint, $g(x_1,x_2)$, is an inequality constraint, meaning that the answer must line on one side of the constraint line. The optimum tailored objective function value occurs when the gradient, of the original objective function, aligns with the gradient of the constraint. Both of these functional gradients are denoted on the graph as $\dot{f}(x_1,x_2)$ and $\dot{g}(x_1,x_2)$. When the functional gradients coincide, these values can be scaled by λ and subtracted from each other to obtain a zero value for the tailored objective function derivative[49]. The optimum constrained optimization point on this figure is the point (B, D).

$$J(x_1,x_2,...,x_n,\lambda_1,\lambda_2,...,\lambda_m) = f(x_1,x_2,...,x_n)$$
$$+\lambda_1 g_1(x_1,x_2,...,x_n)+\lambda_2 g_2(x_1,x_2,...,x_n)+...+\lambda_m g_m(x_1,x_2,...,x_n)$$

(0.1)

$$\frac{\partial J(x_1, x_2, ..., x_n)}{\partial \overline{g}(x_1, x_2, ..., x_n)} = -\overline{\lambda}^T \qquad (0.2)$$
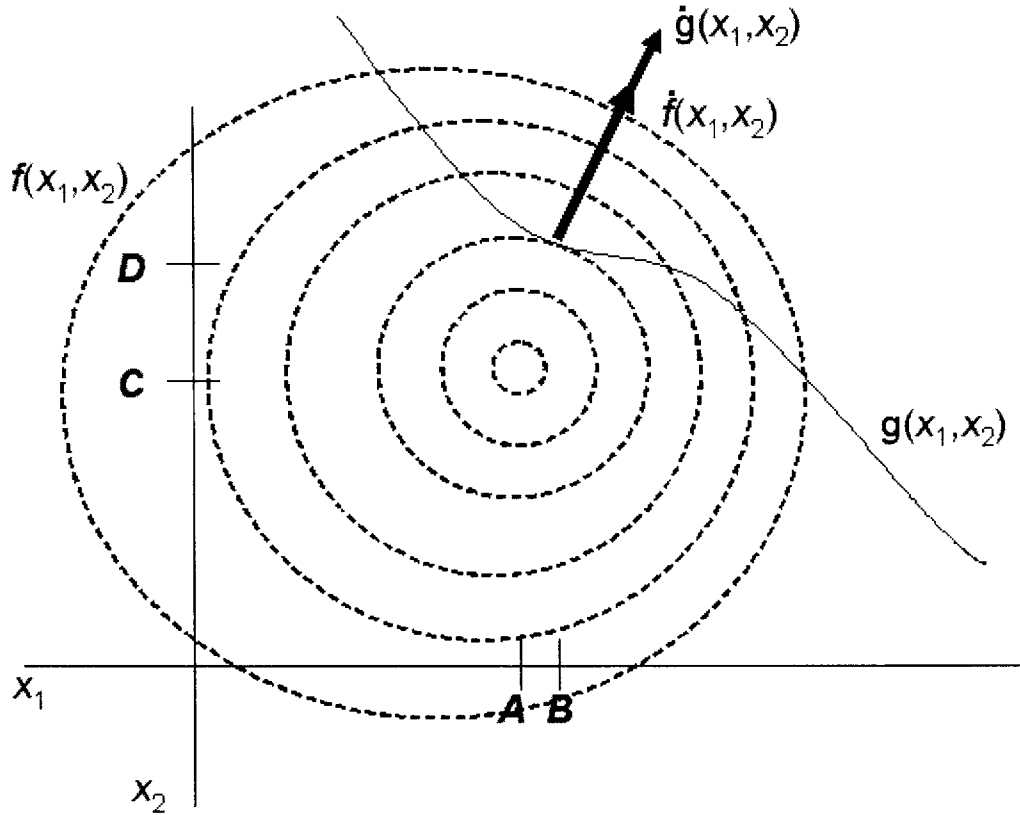
Figure 0.1: Example of a Multi-Variable Constrained Optimization Problem

Unfortunately, the objective function and constraint functions of this thesis are non-linear. In a nonlinear problem, minimums and maximums can be found through the same analytic processes, but there is no simple guarantee on the nature of the global solution. For this reason, several numerical iteration techniques and tools have been developed to search for global optima. The following sections are devoted to describing the development and implementation of some of these methods. There are additional optimization methods beyond those discussed or used in this work. One is encouraged to use the optimization technique of their choice in future analysis.

A1.1.1 Bisection Algorithm

One numerical search technique developed for optimization purposes is the bisection technique. This technique is not designed to find minima or maxima values, but is used to find zero crossings of a function. In this process, a function is evaluated at some x. If the resulting value is greater than zero this point becomes the maximum range limit (MAX). Likewise if the value is less than zero this point becomes the minimum range limit (MIN). The function is evaluated at a large step size in x on either side of this point to establish the other bound. Once both a MIN and a MAX have been identified, the interval between these points is calculated. If this interval is less than some tolerance the algorithm stops, and the zero point is approximated at the center of the interval. If the interval is above the tolerance, the mid-point is established and its objective value calculated. If the x value is less than the MAX, and the x value is greater than zero, the x value becomes the new MAX. Likewise, if the x value is less than zero, but greater than the MIN, the x value becomes the new MIN. If the point is exactly zero, the algorithm breaks and the zero crossing value of x has been found, otherwise the algorithm returns to the point where the interval between MIN and MAX is established. This algorithm is very efficient at honing in on the zero crossing. However, this algorithm is not sensitive enough to catch multiple zero crossings in an interval. For this reason, the initial starting interval must be established with only one known zero crossing. The modification of this approach to finding the exact ignition time in the coverage determination algorithm can be seen in Figure 4.10 of this work.

A1.1.2 Greedy Algorithm

Greedy algorithms are a means of simple optimization based on choosing the value which provides the best objective function gain towards an optimal value. Greedy algorithms look only at the next possible values and choose the one that will provide the largest objective function gain that next step. No information on the globally optimal solution path is considered for this analysis. Greedy algorithms will not always provide the best optimal solution. When used in this thesis, the algorithm was applied to selecting the best of available orbits for coverage purposes. No consideration was given to the

total coverage combination from several sets of satellites. In this way, there is the potential for sub-optimal results. An example of a greedy algorithm approach can be seen in Figure 0.2. The dots in this figure represent the available orbits to add to a constellation. The values on the lines represent a hypothetical coverage gain from each orbit. The greedy algorithm would choose to add Satellite B first and then choose satellite E for a total constellation coverage of 80% (path A-B-E.) The greedy algorithm did not choose the most optimal path, A-D-E, to maximize coverage. While the greedy algorithm is not the most accurate optimization scheme, it is a relatively efficient way to get an approximate solution.
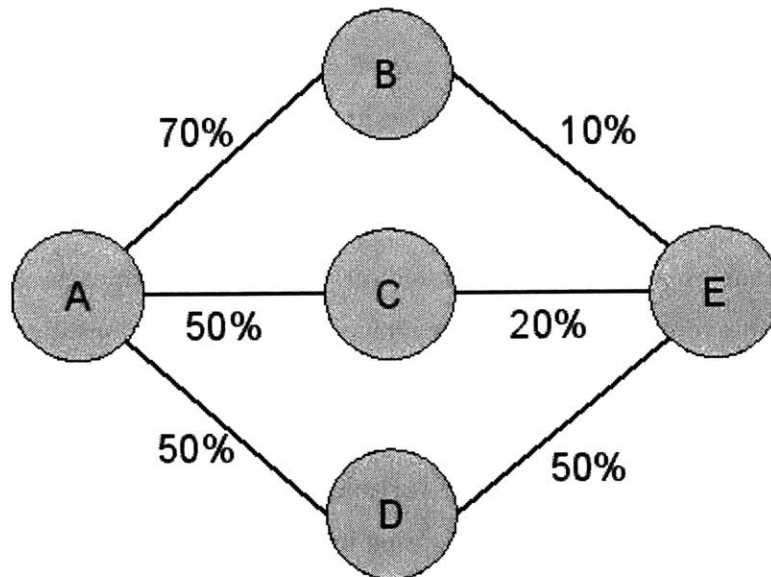
Greedy Plan = A – B – E; Total Percent Coverage = 80%
Optimal Plan = A – D – E; Total Percent Coverage = 100%

Figure 0.2: Example reedy Algorithm Optimization Strategy

A1.2 SNOPT Toolbox

The SNOPT toolbox is a Fortran based nonlinear programming package. SNOPT is designed to handle both linear problems and nonlinear problems containing thousands of variables and constraints. A Sequential Quadratic Programming (SQP) is used to optimize an objective function to a specified minimum or maximum condition. The

results of the SNOPT analysis provide a local optimum. However, the program takes steps to ensure an answer is as globally optimal as possible. This program was designed to work with smooth continuous objective and constraint functions. The software analysis is able to handle small amounts of discontinuities. If no information on the functional gradients is given, SNOPT is capable of approximating gradients with finite differencing[20]. The package itself is a very robust software tool for optimizing any nonlinear problem.

A1.2.1 Enabling Concepts

SQP is the mathematical workhorse behind the SNOPT toolbox. SNOPT will take a stated nonlinear problem and determine a feasible solution through a major and minor step process. The major step involves finding points that satisfy the first order optimality conditions from the objective Jacobian matrix[6]. This process involves introducing slack variables, like Lagrange Multipliers, into the constraints to create a general-form nonlinear programming problem. Quadratic sub-problems are used at each search point to search all variable directions. These quadratic sub-problems constitute the minor iterations of the search process. This process solves for values that decrease the reduced gradients in each direction below a set tolerance. Partial differencing is completed by taking finite steps in the direction of each variable. The objective function is evaluated, and this linear derivative approximation, is used in place of unknown Hessian values. A line search of an augmented Lagrangian merit function, based on the gradient values, is used to determine estimated solution values for the nonlinear program variables[20]. This quasi-Newtonian process is continued until no additional gain can be achieved in the objective function value.

A1.2.2 Program Implementation

SNOPT is designed for large-scale nonlinear programming type problems. A Matlab® driver program was used to interface user created functions with the SNOPT Fortran code. The basic functional layout for the SNOPT implementation into this research is found in Figure 6.2 and Figure 8.1. A user defined function was created to

initialize the SNOPT toolbox. Gradient and objective value tolerances, function description, constraints, and variable limits were established in this function. The SNOPT Fortran code calls a user defined Matlab® sub-function. This function determines the coverage given: constellation design parameters, a configuration, and the desired coverage definition. The constellation design process is a nonlinear mix-integer program. For design parameter optimization, linear approximations to partial derivatives were computed by SNOPT. In this manner, the integer nature of the constellation coverage function was smoothed out. This is not the most efficient implementation; however the design process worked quite well for its intended purpose.
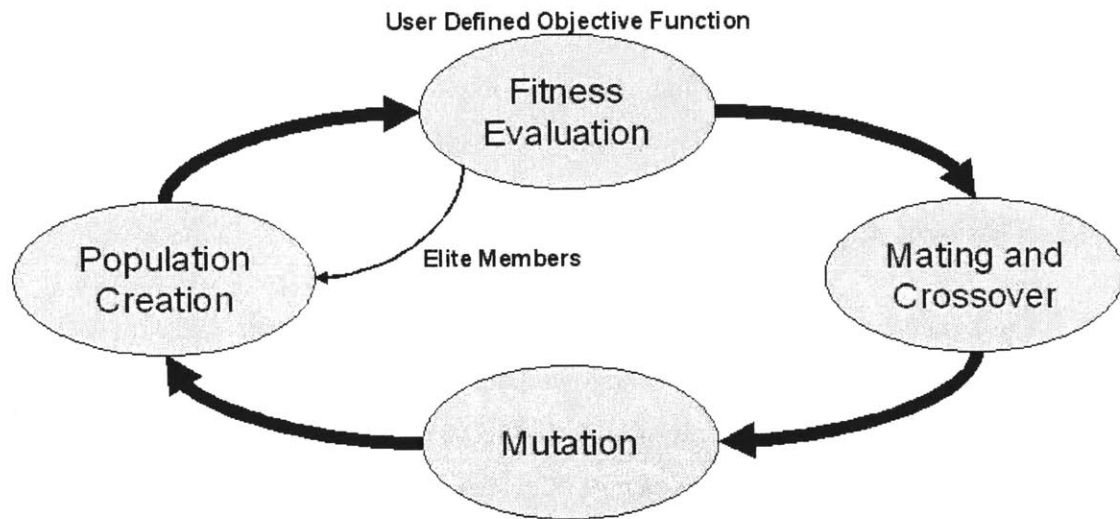
A1.3 Genetic Algorithm Toolbox

The Genetic Algorithm toolbox used for this research is a complete Matlab® set of functions using the stochastic global search methods of a standard genetic algorithm[18]. In this section the toolbox will only be referred to in the sense of the general genetic algorithm (GA) concepts. The GA is one of a few stochastic search algorithms designed for nonlinear problems. The GA is also uniquely designed to handle both integer and continuous functions and variables. It is designed around the evolutionary aspect of living genetic processes. Since the process uses a pseudo random search technique, there is no guarantee of optimality in the final solution. At the same time, this process allows the GA to avoid pitfalls of locally optimal points. One drawback that was found in this research, and also noted by other constellation designers, is the extensive computation and time requirements of the algorithm[16],[17],[19].

A1.3.1 Enabling Concepts

The genetic algorithm process mimics the natural evolutionary process. A population of potential solutions competes in a "survival of the fittest" test to determine the most optimal member. The cyclic exploration process of the genetic algorithm is better understood through Figure 0.3. Individuals are coded into the algorithm usually as binary strings. These strings are called chromosomes, and each chromosome is composed of a set of individual decision variables. In biological terms, these variables are known as

219

genotypes. A set portion of the chromosome, or the phenotype, is devoted to expressing a value of the genotype. Decoding an individual chromosome results in a set list of variables each with an assigned value. When these variables are applied to the objective function a fitness value is obtained. The fitness value determines how good an individual chromosome is compared to the entire population[18],[22].

Figure 0.3: Genetic Algorithm Functional Flow Diagram

Comparing the fitness values for each member of the population, a list of the most fit individuals is created. Through a weighted-random selection process two members of the population are chosen to mate. The most fit members have a higher probability of mating each time. During mating the binary strings of the parent chromosomes are each split at a random crossover point, without regard for the phenotype designations, and flipped. Multiple crossover points may exist for each mating. In this manner, two children are created from the partial binary strings of each parent. The mating process for a two-point crossover is shown in Figure 0.4. These children continue on to the next phase of the genetic process. In this phase, a small mutation is added by randomly flipping one bit in the child's binary string. Mutation occurs with a very low probability within each child. The mutation process is shown in the example of Figure 0.5. From this point a new population is created from the children of each mating pair. In an elitists scheme, the most fit chromosomes continue to the next fitness determination unchanged.

Once the entire population is filled with the same number of chromosomes in which it started, the fitness determination process starts again. The genetic cycle continues in this fashion until a generation limit is reached. The probability of finding the global optimal solution increases with each generation[22].
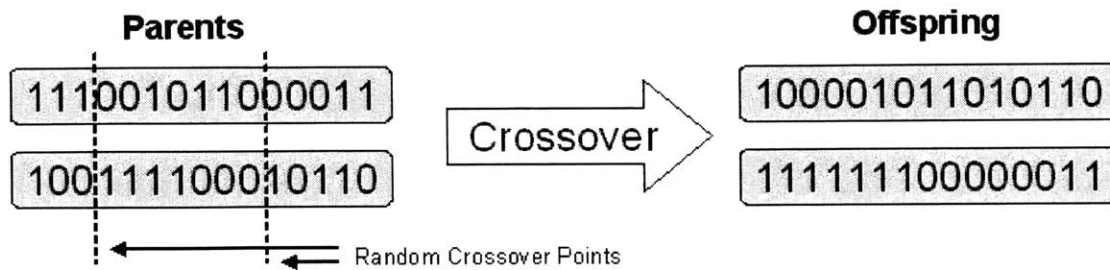
Parents   **Offspring**

1111001011000011   Crossover >   100001011010110

1001111000010110   111111100000011

← Random Crossover Points

Figure 0.4: Example of Two-Point Crossover

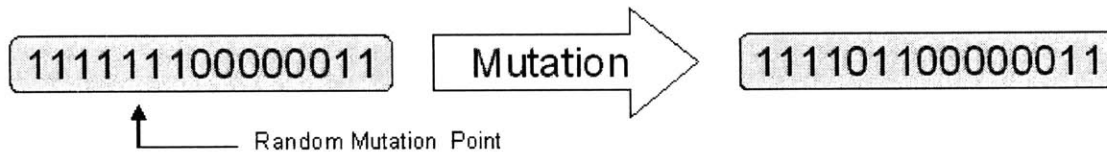111111100000011   Mutation >   111101100000011

↑ Random Mutation Point

Figure 0.5: Example of Mutation Process

A1.3.2 Program Implementation

The Genetic Algorithm toolbox developed used for this research was developed entirely with Matlab® functions[18]. This made for simple implementation with existing user defined functions. The functional layout for the genetic algorithm package usage is shown in Figure 6.3. The genetic algorithm package allowed the user several different variable parameters corresponding to the elitism, mutation, and crossover rates as well as additional functions for the fitness selection, mutation, and cross over schemes. Only the basics of the process were developed here. Additional information on the particulars to this package can be found in the noted reference[18]. The genetic algorithm was successfully implemented into this research. The individual members of the populations corresponded to a specific constellation. The design variables for each satellite in the constellation defined the genotype. A common 20 bit phenotype representation was used

to represent each variable. The design process of this thesis was not focused around perfecting the tool to the application of constellation design. As with all of the optimization schemes described in this appendix, the goal was to use developed optimization packages to maximize the coverage of missile intercept constellations.

References

[1] Astrodynamics I & II Course Notes. 2002-2003. Prof. R.H. Battin.

[2] Ballard, A.H. "Rosette Constellations of Earth Satellites," *IEEE Transactions on Aerospace and Electronic Systems*, Vol. AES-16, No. 5, pp/ 656-673, September 1980.

[3] Barker, L., Stoen, J. "Sirius Satellite Design: The Challenges of the Tundra Orbit in Commercial Spacecraft Design," Paper No. AAS 01-071.

[4] Bate, R., Mueller, D., White, J. "Fundamentals of Astrodynamics," New York, New York: Dover Publications, Inc., 1971.

[5] Battin, R.H. "An Introduction to the Mathematics and Methods of Astrodynamics," New York, New York: American Institute of Aeronautics and Astronautics, 1987.

[6] Bertsimas, D. and J Tsitsiklis. *Introduction to Linear Optimization.* Athena Scientific, Belmont, MA, 1998.

[7] Beste, D.C. "Design of Satellite Constellations for Optimal Continuous Coverage," *IEEE Transactions on Aerospace and Electronic Systems*, Vol. AES-14, No. 3, May 1978 pp. 466-473.

[8] Baucom, Dr. D.R., "Ballistic Missile Defense: A Brief History," http://www.acq.osd.mil/bmdo/bmdolink/html/briefhis.html

[9] Baucom, Dr. D.R., "The Origins of SDI, 1944-1983", University Press of Kansas, Lawrence, Kansas, 1992.

[10] Budianto, I.A., Gerencser, D., McDaniel, P.J. "Design and Analysis of a Small Constellation of Satellites for Mid-Course Tracking," Paper No. AAS 03-634, AAS/AIAA Astrodynamics Specialist Conference, August 2003.

[11] DiDomenico, P.B. "A Phased-Based Approach to Satellite Constellation Analysis and Design," Master of Science Thesis, Massachusetts Institute of Technology, June 1991.

[12]   Draim, J.E. "Three- and Four-Satellite Continuous Coverage Constellations," *Journal of Guidance, Control, and Dynamics,* Vol. 8, No. 6, November-December 1985, pp. 725-730.

[13]   Draim, J.E. "A Common-Period Four SatelliteContinuous Global Coverage Constellation," *Journal of Guidance, Control, and Dynamics,* Vol. 10, No. 5, September-October 1987, pp.492-499

[14]   Draim, J.E. "Continuous Global N-Tuple Coverage with (2N+2) Satellites," Journal of Guidance, Control, and Dynamics, January-February 1991.

[15]   Easton, R.L., Brescia, R. "Continuously Visible Satellite Constellations," NRL Report 6896, April, 1996.

[16]   Ely, T.A., Crossley, W.A., Williams, E.A. "Satellite Constellation Design for Zonal Coverage Using Genetic Algorithms," Journal of the Astronautical Sciences, Vol. 47, No. 3, July 1999, pp. 207-228.

[17]   Frayssinhes, E. "Investigating New Satellite Constellation Geometries with Genetic Algorithms," Paper AIAA-96-3636, AIAA/AAS Astrodynamics Specialist Conference, San Diego, California, 29-31 July 1996.

[18]   "Genetic Algorithms Toolbox," Evolutionary Computation Research Group, Automatic Control & Systems Engineering Dept., University of Sheffield, UK. http://www.shef.ac.uk/~gaipp/ga-toolbox/.

[19]   George, E. "Optimization of Satellite Constellations for Discontinuous Global Coverage via Genetic Algorithms," Paper No. AAS 97-621, AAS/AIAA Astrodynamics Specialist Conference, August 1997.

[20]   Gill, P.E., Murray, W., Saunders, M.A., "User's Guide for Snopt Version 6, A Fortran Package for Large-Scale Nonlinear Programming," Dept. of Mathematics, University of California, December 2002

[21]   Gobetz, F.W. "Satellite Networks for Global Coverage," *Advances in the Astronautical Sciences,* Vol. 9 AAS, 1963 pp. 134-156.

[22]   Goldberg, D.E. "Genetic Algorithms in Search, Optimization, and Machine Learning," Reading, Massachusetts: Addison-Wesley Publishing Company, Inc., 1989.

[23] Hanson, J.M., Evans, M.J., Turner, R.E., "Designing Good Partial Coverage Satellite Constellations," *The Journal of the Astronautical Sciences*, Vol. 40, No. 2, April-June 1992, pp. 215-239.

[24] Hays, E. "An Algorithm for the Computation of Coverage Area by Earth Observing Satellites," Paper AIAA 86-2067, Proceedings of the AIAA/AAS Astrodynamics Specialist Conference, August 1986.

[25] Kantsiper, B. "A Systematic Approach to Station-Keeping of Constellations of Satellites," PhD. Thesis, Massachusetts Institute of Technology, Department of Aeronautics and Astronautics, March 1998.

[26] Kantsiper, B., Weiss, S. "An Analytic Approach to Calculating Earth Coverage," AAS Paper 97-620, AAS/AIAA Astrodynamics Specialist Conference, August 1997.

[27] Lang, T.J., Hanson, J.M. "Orbital Constellations Which Minimize Revisit Time," Paper AAS 83-402

[28] Lang, T.J. "A Parametric Examination of Satellite Constellations To Minimize Revisit Time for Low Earth Orbits Using a Genetic Algorithm," Paper AAS 01-345.

[29] Lang, T.J. "Symmetric Circular Orbit Satellite Constellations for Continuous Global Coverage," Paper AAS 87-499, AAS/AIAA Astrodynamics Specialist Conference, August, 1987

[30] Lang, T.J. "Optimal Low Earth Orbit Constellations for Continuous Global Coverage," Paper AAS 93-597, AAS/AIAA Astrodynamics Specialist Conference, August, 1993

[31] Lang, T.J. "Low Earth Orbit Satellite Constellations for Continuous Coverage of the Mid-Latitudes," Paper AIAA-96-3638, AIAA/AAS Astrodynamics Specialist Conference, July, 1996.

[32] Lang, T.J., Adams, W.S. "A Comparison of Satellite Constellations for Continuous Global Coverage," Paper1.4, IAF International Workshop on Mission Design and Implementation of Satellite Constellations, France, November, 1997

[33] Lang, T.J. "Walker Constellations to Minimize Revisit Time in Low Earth Orbit," Paper AAS 03-178, AAS/AIAA Space Flight Mechanics Meeting, February, 2003.

[34] Luders, R.D. "Satellite Networks for Continuous Zonal Coverage," *American Rocket Society Journal*, Vol. 31, February 1961, pp. 179-184.

[35] Luders, R.D., Ginsberg, L.J. "Continuous Zonal Coverage—A Generalized Analysis," AIAA Mechanics and Control of Flight Conference, AIAA Paper No. 74-842, August, 1974.

[36] Lo M.W. "Applications of the Ergodic Theory to Coverage Analysis," Paper No. AAS 03-638, AAS/AIAA Astrodynamics Specialist Conference, August 2003.

[37] Ma, D.-M. Hsu, W.-C. "Exact Design of Partial Coverage Satellite Constellations Over Oblate Earth," Paper AIAA-94-3721, AIAA/AAS Astrodynamics Conference, August 1994.

[38] Missile Defense Agency. "MDA Link". Public Web site:
http://www.acq.osd.mil/bmdo/bmdolink/html/bmdolink.html

[39] Mozhaev, G.V., "The Problem of Continuous Earth Coverage and Kinematically Regular Satellite Networks, II," *Kosmicheskie Issledovaniay*, Vol. 11, No. 1, January-February 1973, pp. 59-69. Translated in *Cosmic Research*, Vol. 11, No. 1, January-Febuary 1973, pp. 52-61.

[40] Proulx, R., Smith, J.E., Draim, J.E., Cefola, P.J. "Ellipso™ Gear Array: Coordinated Elliptical/Circular Constellations," Paper 98-4383, AIAA/AAS Astrodynamics Specialist Conference, August 1998.

[41] Raytheon's Missile Defense Mission Areas Website "Missile Defense" April 2004, http://raytheonmissiledefense.com/.

[42] "Report of the American Physical Society Study Group on Boost-Phase Intercept Systems for National Missile Defense," Scientific and Technical Issues, July 2003. http://www.aps.org/public_affairs/popa/reports/nmdexec.pdf

[43] "Report of the commission to Assess United States National Security Space Management and Organization," The Commission to Assess United States National Security Space Management and Organization, established pursuant to Public Law 106-65, the National Defense Authorization Act, Fiscal Year 2000, Online Copy available at: http://www.defenselink.mil/pubs/space20010111.html

[44] Rider, L. "Analytic Design of Satellite Constellations for Zonal Earth Coverage Using Inclined Circular Orbits," *The Journal of the Astronautical Sciences*, Vol. 34, No. 1, January-March 1986, pp. 31-64.

[45]   Rider, L. "Optimized Polar Orbit Constellations for redundant Earth Coverage," *The Journal of the Astronautical Sciences*, Vol. 33, No. 2, 1985, pp. 147-161.

[46]   Sellers, J.J. "Understanding Space: An Introduction to Astronautics," New York: McGraw-Hill, Inc., 1994.

[47]   Soccorsi, F.M., Palmerini, G.B., "Design of Satellite Constellations for Regional Coverage," Paper 96-208, AIAA/AAS Astrodynamics Specialist Conference, 1996.

[48]   Vallado, D.A., "Fundamentals of Astrodynamics and Applications," New York, New York: McGraw-Hill, Inc., 1997.

[49]   Vander Velde, W., Prof., "Principles of Optimal Control", Lecture Notes, M.I.T. Fall 2003.

[50]   Vargo, L.G. "Orbital Patterns for Satellite Systems," *Advances in the Astronautical Sciences*, Vol. 6, 1960, pp. 709-725.

[51]   Walker, J.G. "Circular Orbit Patterns Providing Continuous Whole Earth Coverage," *Royal Aircraft Establishment Technical Report* 70211, November 1970.

[52]   Walker, J.G. "Continuous Whole-Earth Coverage by Circular-Orbit Satellite Patterns," *Royal Aircraft Establishment Technical Report* 77044, March 1977.

[53]   Walker, J.G. "Satellite Patterns for Continuous Multiple Whole-Earth Coverage," *Maritime and Aeronautical Satellite Communication and Navigation*, IEEE Conference Publication 160, March 1978 pp. 119-122.

[54]   Walker, J.G. "Satellite Constellations," *Journal of the British Interplanetary Society*, Vol. 37. 1984, pp. 559-572.

[55]   Walker, J.G. "The Geometry of Satellite Clusters," *Journal of the British Interplanetary Society*, Vol. 35. 1982, pp. 345-354.

[56]   Walker, J.G. "Some Circular Orbit Patterns Providing Continuous Whole Earth Coverage," *Journal of the British Interplanetary Society*, Vol. 24. 1971, pp. 369-384.

[57]   Wertz, J.R. "Mission Geometry: Orbit and Constellation Design and Management," Kluwer Academic Publishers, Microcosm, Inc., 2001.

[58]   Wertz, J.R., Larson, W.J. "Space Mission Analysis and Design," Torrance, California: Microcosm, Inc., 1992.

[59]   Williams, E.A., Crossley, W.A., Lang, T.J. "Average and Maximum Revisit Time Trade Studies for Satellite Constellations Using a Multiobjective Genetic Algorithm,"

The Journal of Astronautical Sciences, Vol. 49, No. 3, July-September 2001, pp. 385-400.

[60]   Zarchan, Paul. "Tactical and Strategic Missile Guidance," 3rd Edition, Vol. 176, Progress in Astronautics and Aeronautics, AIAA, 1997.